Visual response characteristics of neuronal clusters in the caudate nucleus of behaving cats

Doctoral Thesis

Dr. Tamás Nagypál

Supervisor:

Attila Nagy, MS, PhD

Department of Physiology

Faculty of Medicine, University of Szeged

Szeged

2015

List of publications related to the subject of the thesis

I. Nagypál T, Gombkötő P, Utassy G, Averkin RG, Benedek G, Nagy A (2014) A new, behaving, head restrained, eye movement-controlled feline model for chronic visual electrophysiological recordings. J Neurosci Methods 221:1-7.
doi: 10.1016/j.jneumeth.2013.09.004

II. Nagypál T, Gombkötő P, Barkóczi B, Benedek G, Nagy A (2015) Activity of Caudate Nucleus Neurons in a Visual Fixation Paradigm in Behaving Cats. PLoS ONE 10(11): e0142526. doi:10.1371/journal.pone.0142526

Further publication

Gombkötő P, Berényi A, Nagypál T, Benedek G, Braunitzer G, Nagy A (2013) Co-oscillation and synchronization between the posterior thalamus and the caudate nucleus during visual stimulation. Neuroscience 242:21-27.
doi: 10.1016/j.neuroscience.2013.03.028

Table of contents

List of abbreviations

ANOVA - analysis of variance
CCK – cholecystokinin
cd - candella
CN - caudate nucleus
CR – calretinin
CRT – cathode ray tube
DAPI - 4',6-diamidino-2-phenylindole
EGFP - enhanced green fluorescent protein
FFN – fast-firing neuron
GABA - gamma-aminobutyric acid
HFN – high-firing neuron
ISI- interspike interval
MAC - minimum alveolar anesthetic concentration
MSN - medium spiny neuron
NADPH - nicotinamide adenine dinucleotide phosphate
NGF – neurogliaform
NOS - nitric oxide synthase
NPY - neuropeptide Y
VIP - vasoactive intestinal polypeptide
PAN- phasically active neuron
PLTS - persistent and low-threshold spike or plateau depolarization–low threshold spike
PropISI - proportion of interspike-intervals
PSTH – peristimulus time histograms
PV - parvalbumin
RT-PCR - reverse transcription polymerase chain reaction
SD – standard deviation
SOM – somatostatin
TAN- tonically active neuron
TFN – tonically-firing neuron
TH - tyrosine hydroxylase

1 Introduction

The caudate nucleus (CN), which is the main input structure of the basal ganglia, is one of the most researched structures in neuroscience. Electrophysiological studies of the CN in the last 50 years have confirmed its central role in the regulation of motor processes as well as cognitive processes such as goal-directed action, memory functions, learning methods, sleep, emotion and language (Elliott et al., 2003; McGaugh, 2004; Villablanca, 2004; Aron et al., 2005; Seger and Cincotta, 2005; Crinion et al., 2006; Kaufmann et al., 2006; Newberg et al., 2006; Obeso et al., 2008; Grahn et al., 2009; Kumar et al., 2009; White, 2009; Hannan et al., 2010; Villablanca, 2010; Ishizu and Zeki, 2011).

Furthermore, the basal ganglia are strongly involved in sensorimotor functions (Zhou et al., 2002; Schmitzer-Torbert and Redish, 2004; Barnes et al., 2005; Hikosaka et al., 2006; Tang et al., 2007; Kimchi and Laubach, 2009; Kubota et al., 2009; Yin et al., 2009; Thorn et al., 2010). It is also assumed that for the eliciting of the normal motor behavior, sensory input to the basal ganglia is essential. Thus, it follows logically that visual information is represented in the CN.

The origin of this visual input has not yet been fully clarified. The corticostriatal pathways send sensory information to the CN (Webster, 1965; Hollander et al., 1979; Norita et al., 1991). At the same time, evidence is accumulating in support of the role of extrageniculate pathways of tectal origin in the sensorimotor integration processes of the basal ganglia (Nagy et al., 2003; Nagy et al., 2008; Hoshino et al., 2009). The dorsolateral part of the caudate body in the cat can receive its visual afferentation from the tectum via the suprageniculate nucleus of the thalamus (Harting et al., 2001; Nagy et al., 2003; Rokszin et al., 2011).

1.1 Visual information processing in the caudate nucleus

Sedgwick and Williams (1967) were the first who suggested the existence of visual sensitivity in the feline CN. From the 1980s to the present, a number of studies have been carried out to clarify the role of CN in visual information processing. It is known that CN neurons are sensitive to various modalities of visual stimulation, i.e. both static and dynamic visual components are represented here (Pouderoux and Freton, 1979; Rolls et al., 1983; Strecker et

al., 1985; Hikosaka et al., 1989; Kolomiets, 1993; Brown et al., 1995; Chudler et al., 1995; Nagy et al., 2003; Nagy et al., 2008; Gombkoto et al., 2011; Rokszin et al., 2011; Vicente et al., 2012). Thus the CN seems to belong to those brain structures that have the capacity to sample and evaluate a wide variety of changes in the visual environment.

Beside the characterization of classical visual receptive field properties of the CN neurons (Pouderoux and Freton, 1979; Nagy et al., 2003), their responsiveness to extended visual stimuli was also investigated (Nagy et al., 2008; Nagy et al., 2010). By the application of drifting grating stimulation, it was possible to determine specific response characteristics of the CN neurons. They were strongly sensitive to very low spatial, intermediate to very high temporal frequencies, and exhibited narrow temporal and spatial frequency tuning. Neurons with these spatio-temporal visual response properties have all the capacities to perceive optic flow and are good candidates for tasks involved in the perception of motion and probably in the perception of changes in the visual environment during self-motion (Morrone et al., 1986; Brosseau-Lachaine et al., 2001; Nagy et al., 2008). From this emerges the question whether an optic flow stimulus can directly activate the CN neurons and what neuronal responses it elicits.

1.2 Neuronal groups of the caudate nucleus

Since the 1960s, neurons of the NC were classified in two big groups based on their firing patterns: phasically active neurons (PANs) and tonically active neurons (TANs) (Albe-Fessard et al., 1960; Connor, 1970; Feltz and Albe-Fessard, 1972; Anderson and Yoshida, 1977; Wilson and Groves, 1981; Kimura et al., 1984; Alexander and DeLong, 1985; Kimura, 1986). Wilson and Groves (1981) observed that one type of cell in the striatum is often silent for seconds, but fires in brief episodes. These cells are commonly called PANs. This group may correspond to the medium spiny projection neurons of the striatum. The other cell type, which was named tonically active, shows variable discharge rates, and they do not show long, discharge-free periods. This group may correspond to the cholinergic interneurons of the CN. In the middle of the 1990s, new evidence came to light on a third distinct subtype of striatal neurons, the GABAergic interneurons that could be further divided in different subpopulations on the basis of their neurochemical properties. The different subpopulations

are characterized by their parvalbumin (PV), calretinin (CR), somatostatin (SOM), neuropeptide Y (NPY), and nitric oxide synthase (NOS) content (Vincent and Johansson, 1983; Chesselet and Graybiel, 1986; Cowan et al., 1990; Kita et al., 1990; Bennett and Bolam, 1993; Kawaguchi, 1993; Kubota and Kawaguchi, 1993, 1994; Kawaguchi et al., 1995). Altogether, CN interneurons can be classified based on their morphology, neurochemistry and physiology at least in one cholinergic and at least three distinct subtypes of GABAergic types.

1.2.1 Medium spiny projection neurons

The large majority of the striatal neurons (77–97% in different mammalian species) belong to the group of GABAergic medium spiny projection neurons (MSN). Striatal projection neurons comprise up to 97% of the rodent striatum but this proportion is significantly lower in higher vertebrates, especially in primates (Kemp and Powell, 1971; Graveland et al., 1985; Wise et al., 1996; Luk and Sadikot, 2001; Rymar et al., 2004; Yarom and Cohen, 2011). In awake animals, MSNs are activated in brief episodes, which are separated from each other by longer periods of quiescence (Schultz and Romo, 1988; Kimura et al., 1990). Medium-sized spiny projection neurons were characterized low or very low spontaneous activity (<10 Hz), mostly under 2 Hz (Apicella, 2002; Lau and Glimcher, 2007). In the light of morphological and electrophysiological studies, which were performed in the last 25 years, it is widely accepted that the electrophysiologically classified PANs are same to the anatomical classified MSNs (Wilson et al., 1990; Wilson, 1993; Apicella, 2002; Mallet et al., 2005; Berke, 2008; Deffains et al., 2010; Inokawa et al., 2010; Adler et al., 2013). The remaining small minority of the CN neurons are cholinergic and GABAergic interneurons (Kawaguchi, 1993; Kawaguchi et al., 1995; Wu and Parent, 2000; Zhou et al., 2002; Tepper and Bolam, 2004; Ibanez-Sandoval et al., 2010; Tepper et al., 2010).

1.2.2 GABAergic interneurons

There are at least three subtypes of GABAergic interneurons in the neostriatum, which can be classified based on their neurochemical properties. One group expresses the peptides somatostatin and neuropeptide Y (NPY), as well as the enzymes NADPH diaphorase and

nitric oxide synthase. The other two groups express the calcium binding proteins parvalbumin or calretinin (Kawaguchi et al., 1995). The GABAergic interneurons add up to about 2-3% of the neostriatal cells in rodents and to 23% of CN neurons in primates (Graveland et al., 1985; Rymar et al., 2004; Tepper and Bolam, 2004; Tepper et al., 2010).

1.2.2.1 Parvalbumin-containing interneurons

Parvalbumin-immunoreactive striatal neurons were first reported by Gerfen et al. (1985), who demonstrated the existence of medium-sized, aspiny interneurons. This is the only striatal neuron group which is characterized by gap junctions (Humphries et al., 2010; Tepper et al., 2010). On the basis of their electrophysiological properties, these neurons seem to correspond to the neurophysiologically characterized high firing neurons (HFN, (Kita et al., 1990; Chang and Kita, 1992; Kawaguchi, 1993; Koos and Tepper, 1999; Berke, 2008; Tepper et al., 2010; Fino and Venance, 2011; Do et al., 2012; English et al., 2012; Isomura et al., 2013). They comprise roughly 1-20% of the striatal neurons (Luk and Sadikot, 2001). These neurons are characterized by high spontaneous discharge rates, typically 10–30 Hz in behaving animals (Plenz and Kitai, 1998; Berke, 2008).

1.2.2.2 Neuropeptide Y, nitric oxide synthase and somatostatin-containing interneurons

The second neostriatal GABAergic interneuron group can be characterized by the absence of parvalbumin, but at the same time the presence of NPY, somatostatin, nitric oxide synthase and NADPH diaphorase (Vincent and Johansson, 1983; Smith and Parent, 1986). These neurons comprise 0.8% of the neostriatal cells in rats (Rymar et al., 2004). These cells can be characterized electrophysiologically by low threshold calcium spikes and a prolonged calcium-dependent plateau potential. They have therefore been termed persistent and low-threshold spike (PLTS) neurons (Kawaguchi, 1993; Kawaguchi et al., 1995). Recently Ibanez-Sandoval et al. (2011) suggested that there are two electrophysiologically, morphologically, and neurochemically distinct subtypes of NPY interneurons, one of which had not been previously described. English and his colleagues (2012) demonstrated the

existence of a group of neuropeptide Y-expressing interneurons in the neostriatum, the NPY neurogliaform cells (NPY-NGF interneurons), which can be both morphologically and electrophysiologically separated from the NPY-expressing plateau depolarization–low threshold spike (NPY-PLTS) interneurons.

1.2.2.3 Calretinin-containing interneurons

The third GABAergic interneuron group of the CN can be characterized by the co-localization of a calcium binding protein, calretinin. These neurons add up to 0.5% of the neostriatal neurons in rats (Rymar et al., 2004). Our knowledge about these interneurons is limited. Morphological observations in immunostained material were made, but the electrophysiological properties have not been studied. It is also known that in primates, including humans, the proportion of CR positive neurons is much greater than in rodents (Wu and Parent, 2000; Tepper and Bolam, 2004; Tepper et al., 2010).

1.2.2.4 Striatal tyrosine hydroxylase immunpositive interneurons

Dubach et al. (1987) were the first to describe tyrosine hydroxylase (TH) immunoreactive neurons in the CN of three normal monkeys. The vast majority of these neurons was actually outside of the borders of the CN and putamen, and were located in the white matter ventral to the striatal neuropil. The neurons which were actually within the striatum, were restricted to a narrow band in the dorsomedial periphery of the CN. Subsequently, several studies from different laboratories confirmed the existence of neurons that could be immunostained with different monoclonal or polyclonal antibodies directed against for tyrosine hydroxylase in mice, rats, monkeys and humans. Recently Tepper et al. (2010) could visualize striatal tyrosine hydroxylase positive neurons in brain slices by using genetically modified mice. Whole cell patch clamp recording and biocytin labeling allowed the study of the electrophysiological and anatomical properties of striatal TH positive neurons. Four distinct groups have been described so far (Ibanez-Sandoval et al., 2010).

1.2.2.5 Cholecystokinin and vasoactive intestinal polypeptide immunpositive interneurons

Beside the already mentioned CN neuronal groups a small number of vasoactive intestinal polypeptide (VIP) immunpositive spiny neurons were described in the striatum of the rat (Takagi et al., 1984; Theriault and Landis, 1987; Hokfelt et al., 1988). Furthermore cholecystokinin (CCK) immunpositive neurons were found in the feline CN (Adams and Fisher, 1990). In contrast with the sparsely distributed VIP neurons, which can be found in all areas of the striatum (Theriault and Landis, 1987) the information about the very small population of CCK immunpositive neurons is not satisfactory in the sense that there were reported only in cats but these finding can not be confirmed in rodents and primates (Gilles et al., 1983; Schiffmann et al., 1989; Adams and Fisher, 1990). Preliminary single cell RT-PCR analysis of a small number of TH interneurons suggest that some of these neurons may express CCK and/or VIP implying a possible overlap among these types of interneurons. Genetic reporting and/or targeting methods as well as gene expression assays will be essential to clarify the existence and possible roles these neurons in the striatum (Tepper et al., 2010).

1.2.3 Cholinergic interneurons

Cholinergic interneurons were first identified as giant interneurons by Koelliker (1896). Nowadays, the long-known and researched large aspiny interneurons, which release acetylcholine, are generally agreed to correspond to the tonically active neurons in the striatum (Bolam et al., 1984; Kimura et al., 1984; Wilson et al., 1990; Aosaki et al., 1994; Kawaguchi et al., 1995; Bennett and Wilson, 1999; Apicella, 2002; Tepper and Bolam, 2004; Tepper et al., 2004; Mallet et al., 2005; Pisani et al., 2007; Berke, 2008; Inokawa et al., 2010; Berke, 2011; Schulz et al., 2011; Yarom and Cohen, 2011; Beatty et al., 2012). Although these cells are only 1–3% (~10% in primates (Fino and Venance, 2011), ~2% in cats (Phelps et al., 1985)) of all striatal neurons, they can show different endogenous firing patterns (regular, irregular and bursting), which can modulate the information processing in the striatum (Bennett and Wilson, 1999; Goldberg and Reynolds, 2011). The spontaneous discharge rate of the cholinergic CN interneurons is between 3-10 Hz in primates (Bolam et

al., 1984; Aosaki et al., 1994; Goldberg and Reynolds, 2011; Adler et al., 2013; Schulz and Reynolds, 2013).

In summary, the conclusion can be drawn that there is strong overlap between the anatomical and electrophysiological clustering of the CN neurons. PANs overlap strongly with the medium spiny projection neurons, HFNs overlap with parvalbumin immunpositive GABAergic interneurons and the TANs seem to comprise the same cluster as the cholinergic interneurons. Being a research group traditionally working with feline models, it was natural that the fact that the question as to whether a similar classification is possible in the feline brain has not been investigated before, could not escape our attention.

1.3 Evolution of the behaving feline research models

The domestic cat is a classical mammalian model organism in visual neurophysiology and neuroanatomy. Several high-impact discoveries have been based on the feline model, of which the most well-known may be those of the Nobel laureates Hubel and Wiesel (1961, 1962). In the last few decades, animal research has seen a clear tendency toward the use of awake, behaving animals, instead of the previously used anesthetized, paralyzed models.

Behaving feline models have gone through several stages of development. Since the beginning of the second half of the 20th century, mostly anesthetized, paralyzed cats were used in the investigation of the primary visual (striate) cortex, but in the first years some experiments were performed with behaving, unrestrained cats, too (Hubel, 1959; Griffith and Horn, 1963). Later, behaving cats were placed in a restraining box and they could put out their head through a small hole. The cats were in this position during the experiments. The head- and eye- movements were not controlled (Berkley, 1970; Blake et al., 1974; Franklin et al., 1975). Strecker et al. (1985) used freely moving cats, which were placed in a sound-attenuated behavioral chamber, however, also without eye control. Stryker and Blakemore (1972) took a step further, fixated the body and head of the cat with a canvas bag on a platform, and the eye movements were under video surveillance. For some time, scleral magnetic search coils developed for primates were utilized (Robinson, 1963; Fuchs and Robinson, 1966; Judge et al., 1980), but later they were adapted to cats (Pigarev and

Rodionova, 1998; Populin and Yin, 1998, 2002; Huxlin and Pasternak, 2004; Tollin et al., 2005; Pigarev and Levichkina, 2011). Nowadays, behaving animal models are often used in primate visual experiments, but they have rarely been utilized in cats, due to technical difficulties. Only a few research groups can perform visual experiments with behaving cats. The animals have to learn the behavioral visual fixation task. In order to exclude the effects of eye movements, they have to maintain fixation during the electrophysiological recordings and the eye position of the animal has to be controlled continuously (Robinson, 1963; Fuchs and Robinson, 1966; Judge et al., 1980). Pigarev and his colleagues investigated the visual cortical areas (Pigarev and Rodionova, 1998; Pigarev and Levichkina, 2011). Populin and Yin performed mainly auditory and auditory-visual experiments in the superior and inferior colliculi (Populin and Yin, 1998, 2002; Tollin et al., 2005). Huxlin and Pasternak (2004) investigated the training-induced recovery of visual motion perception after extrastriate cortical damage in adult cats. In each case, the head of the animal was fixed and its body was put either in a box or on a trolley, which could move along a 3-m long railway.

In our laboratory we investigate the sensory properties of the basal ganglia and the connected ascending tectofugal visual system. We have hitherto performed our experiments on anaesthetized and paralyzed cats (Nagy et al., 2006; Nagy et al., 2008; Gombkoto et al., 2013). One of the main goals of my thesis work was to introduce a feline model that could be suitable for chronic visual and multisensory electrophysiological recordings in the awake, behaving cat.

2 Aims of the study

The specific aims of the research work serving as the basis of the present thesis were the following:

1. To establish a new, behaving, head-restrained and eye movement- controlled feline model for chronic visual experiments.
2. To classify the CN neurons in the feline brain according to their electrophysiological properties.
3. To describe the visual response characteristics of the CN neurons to static and dynamic visual stimuli.
4. To compare the response characteristics of the CN neurons.

The thesis undertakes to describe the results of the work aimed at reaching these ends.

3 Materials and Methods

Experiments were performed on two adult domestic cats (2.6 kg and 3.25 kg). All experimental procedures were carried out to minimize the number and the discomfort of the animals involved, and followed the European Communities Council Directive of 24 November 1986 (86 609 EEC) and the National Institutes of Health guidelines for the care and use of animals for experimental procedures. The experimental protocol has been accepted and approved by the Ethics Committee for Animal Research of the University of Szeged (No: I-74-24/2012).

3.1 Animal preparation and surgery

The animals were initially anesthetized with ketamine hydrochloride (Calypsol (Gedeon Richter®), 30 mg/kg i.m). To reduce salivation and bronchial secretion, a subcutaneous injection of 0.2 ml 0.1% atropine sulphate was administered preoperatively. A cannula was inserted in the femoral vein and after intubation of the trachea the animals were placed in a stereotaxic headholder. All wounds and pressure points were treated regularly with local anesthetic (1%, procaine hydrochloride). Throughout the surgery, the anesthesia was maintained with 1.5% halothane in a 2:1 mixture of N_2O and oxygen. The depth of anesthesia was monitored by continuously checking the end-tidal halothane concentration and heart rate (electrocardiogram). The minimum alveolar anesthetic concentration (MAC) values calculated from the end-tidal halothane readings were kept in the range recommended by Villeneuve and Casanova (2003). The end-tidal halothane concentration, MAC values and the peak expired CO_2 concentrations were monitored with a capnometer (CapnomacUltima, Datex-Ohmeda, ICN). The O_2 saturation of the capillary blood was monitored by pulse oxymetry. The peak expired CO_2 concentration was kept within the range 3.8-4.2% by adjustment of the respiratory rate or volume. The body temperature of the animal was maintained at 37^{o}C by a computer-controlled, warm-water heating blanket. Craniotomy was performed with a dental drill to allow a vertical approach to the target structures. The dura mater was preserved, and the skull hole was covered with a 4% solution of 38^{o}C agar dissolved in Ringer's solution. Then a reclosable plastic recording chamber (internal diameter: 22.5 mm) was mounted on the skull. Following this, the eight electrodes were

implanted in the brain with the help of an adjustable microdrive system (a modified Harper-McGinty microdrive for the first animal, see McKown and Schadt (2006), and a modified Korshunov microdrive for the second animal (Averkin et al., 2009)). The implanted chamber and microdriver system allowed a stable recording background for two years in the first and second cat. In order to monitor the eye movements of the animals, a scleral search coil was implanted into one eye. Although this method was originally developed for primates (Robinson, 1963; Fuchs and Robinson, 1966; Judge et al., 1980), it was later adapted to cats, too (Pigarev and Rodionova, 1998; Populin and Yin, 1998, 2002; Huxlin and Pasternak, 2004; Tollin et al., 2005; Pigarev and Levichkina, 2011). Additionally, a stainless steel headholder was cemented to the skull for head fixation purposes. All surgical procedures were carried out under aseptic conditions. Before the surgical procedure, a preventive dose of antibiotic was given (1000 mg ceftriaxon, i.m., Rocephin 500 mg (Roche®)). The first five postoperative days 50 mg/kg antibiotic was provided intramuscularly. Nalbuphin and non-steroidal anti-inflammatory drugs were administered until the seventh postoperative day.

3.2 Behavioral training of the animals

The experimental animals were selected with distinguished care, in a one-year process, during which the animals were adapted to the laboratory environment and their temper was also observed. It was only after this selection and training process that the insertion of the recording electrodes took place. Water deprivation was not used. Cooperative behavior and adaptation to the laboratory environment was formed by a feeding routine. Independently of behavioral training or recording, the animals received food only in the laboratory (150-250 gram/day). During the weekends, the animals had access to food in their cage ad libitum, without any weight control. Once the cat got accustomed to the laboratory environment, it was carefully clothed into the canvas harness. This harness leaves the head, tail and legs free. Initially, the cat spent only a few minutes in the harness, which was extended to two hours. It was also during this period that we gradually shifted to pulpy food provided through a plastic tube. The next step in training, which is a novelty of our model, was the suspension of the animal. Cats, by nature, like to lie in a hammock; therefore, it is relatively easy to get them accustomed to the canvas harness in a suspended position. In this specific case, it was done as follows: first, we lifted the animal manually only a few centimeters from the floor in the

canvas harness, while it was being fed. When the animal got used to being suspended this way, it was gradually introduced to the experimental stand (Figure 1). The experimental stand is a cubical structure with each side open, in which the suspension harness is fastened at two points in by a rope pulley block. Before the implantation of the electrodes, it took approximately three months to adapt the cat to these circumstances. In the following step, the head of the suspended cat was fixed to the stereotaxic frame by the implanted steel headholder with two stainless steel bars (see Figure 1B). In this paradigm, the stereotaxic device is placed within an electromagnetic field, which is generated by metal coils, installed into the wall of the stand. Once in the stereotaxic device, the animals were fed only with pulpy food (now as reward for successful trials, see below) through a plastic tube, dosed by a computer-driven hydraulic pump installed outside the magnetic field.

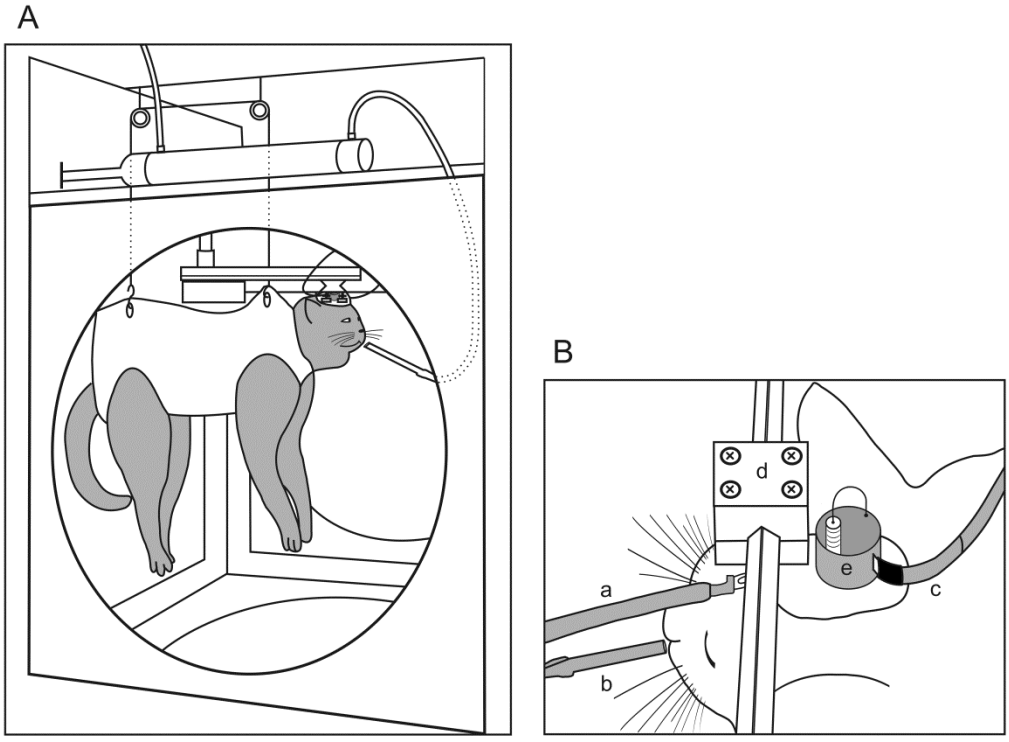

Figure 1. Schematic drawing of the experimental setup. Figure 1A: the suspended cat in the canvas harness in the experimental stand. The head of the suspended cat is restrained in the stereotaxic frame. The cat is inside an electromagnetic field, generated by metal coils, installed in the four walls of the stand. Above (outside the magnetic field) is a hydraulic pump, which doses the food reward. Figure 1B: the schematic drawing of the head of the cat

with the accessories for chronic recordings. The head of the cat is restrained via the implanted steel headholder (d) with two stainless steel bars, which are attached to the stereotaxic frame. The recording chamber with adjustable microdrive, which moves the eight recording wire-electrodes (e) and the recording cable with preamplifier (c) are placed behind the headholder. On the other side of the headholder, the adapter of the eye movements recording cable (a) can be seen. The cat receives the food reward through a plastic tube (b).

That is, in our model, the cats have to tolerate a canvas bag around their body, being in a suspended position, head restraint and also a scleral search coil. The suspended position is a further novelty as compared to earlier feline models. It must be added that we experimented with the lying position too, but the animals either tolerated this poorly for longer periods, or simply fell asleep. We found the suspended position superior both in terms of its tolerability for the animals and handling.

3.3 Behavioral paradigm and visual stimulation

Having established the physical circumstances, the animals had to be taught the behavioral paradigm. A standard 17- inch CRT monitor (at 100 Hz refresh rate) was placed in front of the animal, at a distance of 57 cm. The initial part of behavioral training concentrates on fixation. The fixation point is projected on the centre of the CRT monitor within an acceptance window of changeable size. The size of the fixation point is constant, 0.8^{o} in diameter. If the cat holds fixation for a pre-set duration within the acceptance window, it receives food reward. During the fixation training, the fixation time was gradually increased from 100 ms to 1500 ms. Square fixation windows were used. The size of the initial fixation window was $\pm 10^{o}$ for both cats. During the training period, it was reduced to $\pm 2.5^{o}$ in $\pm 2.5^{o}$ steps, which took two months. The $\pm 2.5^{o}$ was the final size of the fixation window in case of both cats. After the fixation training, either random dots (static) or optic flow (dynamic) stimuli were applied, while the animal maintained fixation. The size of the dots was 0.1^{o} in diameter and their speed increased 0 to 7^{o}/sec toward the periphery. Summarized, if the animal started the task (put practically its eye within the fixation acceptance window and held there until 500 ms) visual stimulation was performed. Firstly random dots (stationary visual

stimulus) and then optic flow (dynamic visual stimulus) stimuli were applied. The size of the whole stimulus screen was 40.5^{o} by 30.5^{o}.

A trial consisted of the following stages (Figure 2):

1. Fixation phase: a central green fixation point appears on the center. The cat has to see the fixation point and has to hold its eye within the given fixation acceptance window up to 500 ms.

2. Stationary visual stimulation phase: if the fixation is held up to 500 ms static random dots (4000 dots) appeared in the visual field (random dots pattern) for 200-500 ms.

3. Dynamic visual stimulation phase: after 200-500 ms stationary stimulation, the static dots started moving together radially building an optic flow stimulus. The duration of the optic flow stimulus was 1000 ms. The dots moved either toward the periphery of the screen (center out optic flow) or toward the center of the screen (center in optic flow).

4. Reward phase (500 ms post stimulation): after successful completion of a trial, the animal got some drops of pulpy food reward.

The recordings took place in a dark laboratory room (background luminance: 0.5 cd/m^2). The luminance of the stimulus was 5 cd/m^2 (Mavolux 5032C, GOSSEN Foto- und Lichtmesstechnik GmbH). The computer-controlled trials (either with center out or center on optic flow) were presented in a random order. In each recording the cat had to perform at least 30 correct trials to center out and also to center in optic flow stimuli.

To exclude the influence of eye movements on neuronal activity, the trial was aborted immediately if the animal broke fixation. In such cases, no reward was given either. The intertrial interval was between 4000 and 10000 ms. Recording sessions began when the cats reached a stable 80% efficiency at the task.

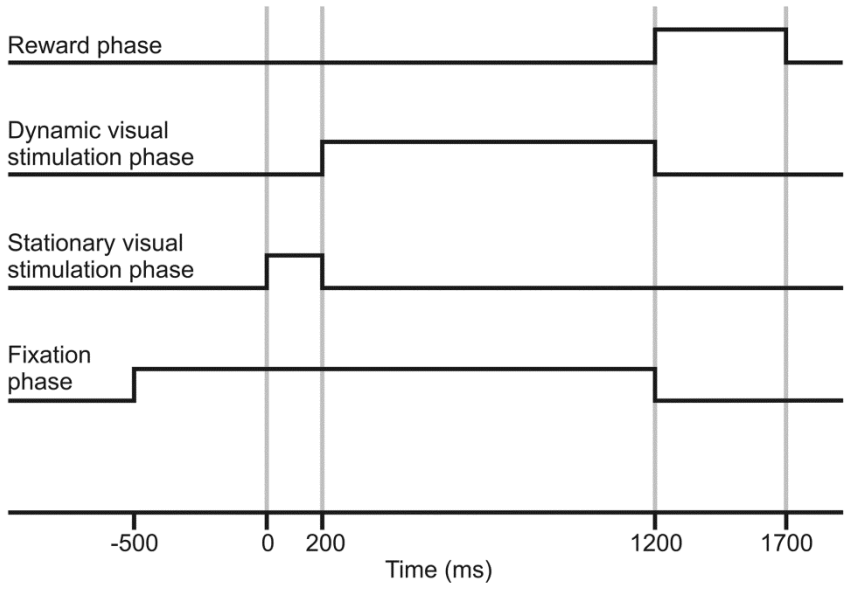

Figure 2. Schematic drawing of the behavioral visual fixation paradigm. At the beginning of the trial the cat has to move its eye in a green fixation point projected in the center of a CRT monitor (refresh rate 100 Hz). The cat has then to maintain the fixation within a given fixation acceptance window up to 500 ms (fixation phase). After 500 ms fixation, static random dots appeared (0 ms represents the appearance of it) on the monitor for 200-500 ms (stationary visual stimulation phase). After this period the static dots started moving radially together either in ‘center in’ or ‘center out’ direction and built in this way flow field (optic flow) with a duration of 1000 ms (dynamic visual stimulation phase). As can be seen on the figure the animal had to hold the fixation during the whole static and dynamic stimulation phase of paradigm. If a trial was completed the animal get some drops of mashed cat food (reward phase).

Both the aforementioned training phases and the recordings took place in a dark laboratory room. Sessions (either training or recording) lasted 1–2 hours a day, four to five times a week. The weight of the animals was checked regularly and was kept at least 90% of the initial value.

At the end of the experiments, the first animal was deeply anesthetized with pentobarbital (200 mg/kg i.v.) and perfused transcardially with 4% paraformaldehyde solution. The brain was removed and cut into coronal sections of 40 μm, and the sections were stained with DAPI (4',6-diamidino-2-phenylindole, Sigma-Aldrich Co., USA). Recording sites were localized on the basis of the marks of the electrode penetrations.

3.4 Recording and data analysis

Extracellular multielectrode recordings were made with eight implanted parylene isolated platinum-iridium wire-electrodes (diameter: 25 μm) from the first cat and with eight implanted formvare insulated Nickel-Chrome wire-electrodes (diameter: 50 μm) from the CN of the second cat. The implantation of the electrodes was made according to the Horsley-Clarke system (anterior 12-14 mm, lateral 4.5-6.5 mm at stereotaxic depths between 9 and 13.5 mm).

Amplified neuronal activities were band-pass filtered (300 to 5000 Hz) in order to analyze single cell and multiunit activity. The raw data were first processed by NeuroScope, NDManager, KlustaKwik and then broken down into single unit signals by the use of Klusters (Harris et al., 2000; Hazan et al., 2006) under manual control. The KlustaKwik extracted spikes from the filtered data automatically adjusted amplitude thresholding, and clustered based on the automatically calculated characteristic parameters of the extracted spike waveforms (peak and trough amplitude and timing, 1st and 2nd principal components). We used the same parameters for all signals to avoid manipulation of the manually adjusted amplitude thresholding. The quality of the sorted units was tested by analyzing autocorrelograms and overlays of spike waveforms.

The neuronal firing rates during different epochs of the behavioral paradigm (fixation, stationary, dynamic and reward periods) were compared to the background activity (average firing rate of the last 3000 ms period of the intertrial interval from each trial, during which the animal saw a black screen) using the Mann-Whitney rank-sum test. In the dynamic period we investigated the neuronal responses during the total lenght of the dynamic visual stimulus (1000 ms). Similarly, the comparison between the discharge rate of the single neurons in response to center in and center out optic flow stimuli was performed using the Mann-Whitney test. We also calculated the net firing rate of each unit by substracting the spontaneous activity from the whole firing of the neurons. The gross and net firing rates of different CN neuron subpopulations (PAN, HFN and TFN) in different epochs of the paradigm were compared by one-way analysis of variance (ANOVA). All statistical analyses were performed in Matlab® (MathWorks Inc., Natick, MA).

Eye movements were recorded via a search coil system (DNI Instruments, Newark, DE, USA) with a sampling rate of 250 Hz, and these were also processed by Matlab®. The experiment was controlled by a custom-made software, including eye movement-recording, stimulus presentation, reward delivery and data collection via National Instruments DAQ®. The stimuli were generated by the Psychophysics Toolbox of Matlab®.

3.5 Classification of the CN neurons

Although the description of the electrophysiological properties of the CN started in the early 1960s the turning point in the electrophysiological clustering of the CN units was only in the middle of 2000s (Schmitzer-Torbert and Redish, 2004; Barnes et al., 2005; Schmitzer-Torbert et al., 2005). Schmitzer-Torbert provided the detalied electrophysiological analysis of the rodent striatum. To separate phasically and non-phasically active neurons and to distinguish the FFNs from the TFNs, the proportion of long interspike-intervals to all spike intervals was introduced ($PropISI_{>xsec}$). Post-spike suppression[1] was also calculated. Based on these properties, the striatal neurons were separated into three categories: PFNs, TFNs, and HFNs. The classifications of PFNs and HFNs were highly stable, 98.9% for PFNs and 95.3% for HFNs (Schmitzer-Torbert and Redish, 2004; Schmitzer-Torbert et al., 2005). Barnes et al. (2005) have classified the recorded rodent striatal cells putative projection neurons, putative fast-firing neurons and putative tonically-firing neurons. For each unit two autocorrelograms (with ±100 msec and with ±1 sec windows), an interspike interval (ISI) plot and average firing rates were calculated. Putative projection neurons were characterized by the occurrence of long (> 2 sec) ISIs in addition to phasic activity with short ISIs, putative fast-firing neurons by their high average firing rates and a lack of ISIs > 1 sec, and putative tonically-firing neurons by wide central valleys in the autocorrelograms and spiking at 2-10 Hz. Later, several studies on rodents and primates applied the above categorization criteria (Schmitzer-Torbert and Redish, 2008; Kubota et al., 2009; Gage et al., 2010; Thorn et al., 2010; Barnes et al., 2011; Stalnaker et al., 2012). However, such electrophysiological characterization of the CN units in the feline brain is still missing. We have therefore intended to classify and, if it is

[1]Post-spike suppression: It was calculated for each cell by measuring the length of time that a cell's firing rate was suppressed following an action potential.

possible, to clusterize the neurons of the feline CN in the light of their electrophysiological properties in different functional groups.

4 Results

4.1 The new behaving, head-restrained and eye movement-controlled feline model

As part of the work providing the basis of this study, we developed a new chronic feline model, which is suitable for electrophysiological recordings from visual brain structures. The most noteworthy features of the extended recording time (minimum two hours per day, and several years in total), the continuous eye control, and the use of head restraint, which makes this model ideal also for classic visual electrophysiological experiments.

In order to exclude the effect of eye movements on the recordings of neuronal activities, the head-restrained cats had to be able to maintain their fixation. In the pilot study of the new model, the animals could be trained to fixate quite accurately (within a ±2.5 degree fixation acceptance window), even during dynamic visual stimulation.

A continuous control of eye movements was an essential part of our experiments. By the eye-tracker method, it became possible to follow and exactly reconstruct (visualize) the eye movements of the animals. This also enabled us to detect failed fixation, which was a rejection criterion (Figure 3).

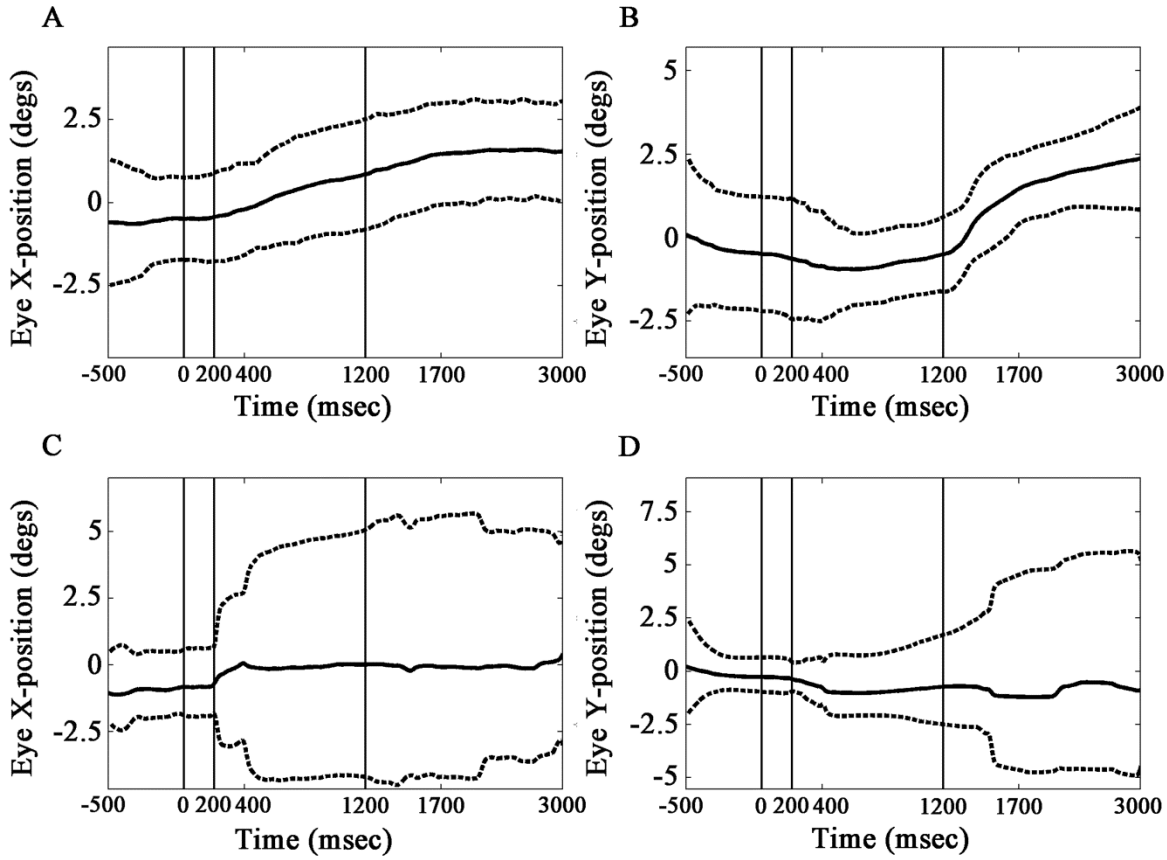

Figure 3. Eye movements of the cat during the visual fixation paradigm. Top (A,B): successful fixation, bottom (C,D): failed fixation. 3A,C: horizontal eye positions. 3B,D: vertical eye positions (assuming a $\pm 2.5^{o}$ acceptance window). The bold black line shows the mean of eye movements, and the dotted lines denote standard deviations. Time is marked on the abscissa, and the ordinates show the horizontal (X) or the vertical (Y) positions of the eye. The vertical black lines indicate the phase limits: fixation period (-500 to 0 ms), random static dot stimulation (0 to 200 ms), optic flow (200 to 1200 ms) and reward (1200 to 1700 ms). Failed fixation is indicated by a sudden and marked increase of SD in the horizontal (C), but not in the vertical (D) plane.

4.2 Classification of the CN neurons

In the applied behavioral visual fixation paradigm (see Materials and Methods) altogether 346 neurons were recorded from the dorsolateral part of the CN.

The CN units were classified by their spontaneous discharge rate, ISI plot, $propISI_{>2sec}$ and the shape of the autocorrelogram at different time resolutions (100ms, 1000 ms). It is known from rat and primate studies that spontaneous activity, $propISI_{>2sec}$ and the shape of the autocorrelogram at different time resolutions (100 ms, 1000 ms) can be used to classify the CN neurons (Schmitzer-Torbert and Redish, 2004; Barnes et al., 2005). We estimated the spontaneous discharge rate of each neuron in the last 3000 ms period of the intertrial intervals. The above mentioned electrophysiological parameters of each recorded CN unit were calculated. Based on the above mentioned properties the recorded neurons were divided in three groups: phasically active (n=221), high-firing (n=88) and tonically active (n=28) neurons.

PANs are characterized by peaky autocorrelogram and ISI values over 2 seconds. The $propISI_{>2sec}$ was usually higher than 0.5, and the spontaneous discharge rate was low, in most cases under 3 spikes/sec. The HFNs have autocorrelograms with a blunt peak, the $propISI_{>2sec}$ is lower than 0.5, and the spontaneous discharge rate is higher than 5 spikes/sec. Finally, TANs are characterized by a deep gap in the autocorrelogram, the $propISI_{>2sec}$ is lower than 0.5, and the spontaneous discharge rate is between 2 and 12 spikes/sec (Figure 4).

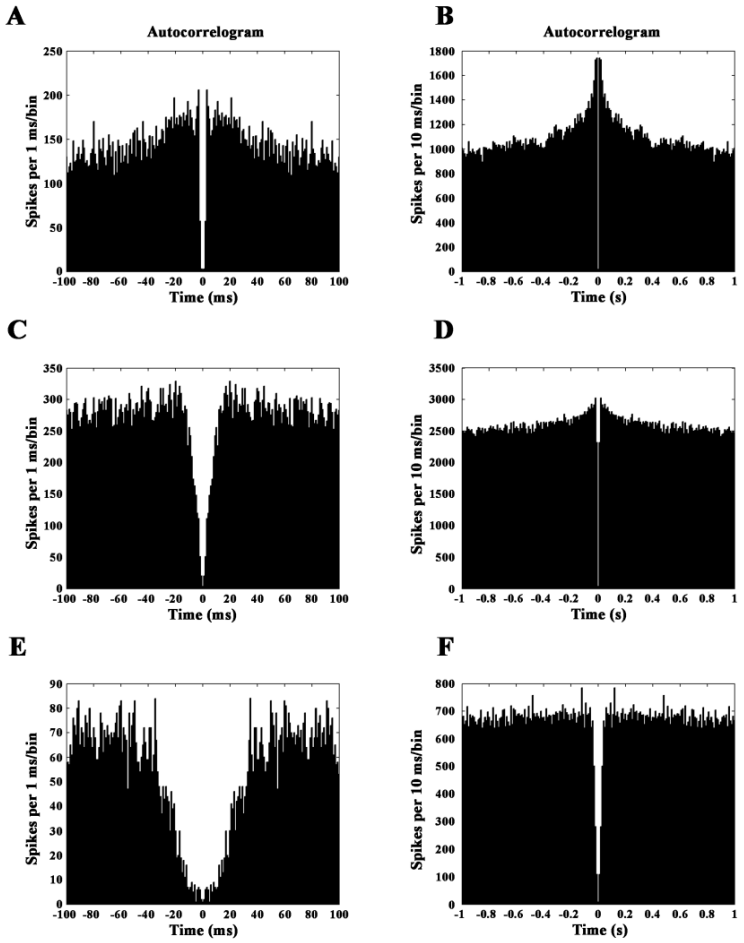

Figure 4. Autocorrelograms of the CN neurons. Neurons were classified on the basis of the shape of their autocorrelograms (at 100 ms and 1000 ms time resolutions), prop$ISI_{>2sec}$ and the background discharge rate in three big groups (PAN, HFN, TAN). Neurons belonging to each group have characteristic autocorrelogram. PANs are usually characterized by peaky autocorrelogram (A,B). HFNs have autocorrelograms with a blunt peak (C,D) and TANs are characterized by a deep gap in the autocorrelogram (E,F).

Because of the very low spontaneous discharge rate (below 1 spike/second), we excluded 135 phasically active putative projection CN neurons from the analysis. Further nine CN neurons were excluded from the analysis as we were unable to classify them in any of the above mentioned three major groups.

4.3 Visual responses of the neuronal subtypes in the CN

The responsive CN neurons showed mainly increased firing rate, while in some cases decreased activity was also found. Significant changes in the activity of the CN neurons were recorded not only during stationary and dynamic visual stimulation. In line with earlier results (Schultz, 1998), reward-related neuronal responses were also recorded shortly before and during the reward period after the correct completion of the task. Table 1 summarizes the responsiveness of the different CN neuron clusters.

	Stationary	Optic flow		Stimulus off	Reward
		center out	center in		
Phasically active neuron					
increased activity	26	17	16	1	27
decreased activity	24	2	6	0	6
High-firing neuron					
increased activity	18	16	20	7	30
decreased activity	18	9	8	1	0
Tonically-firing neuron					
increased activity	11	3	5	0	6
decreased activity	2	1	1	1	0

Table 1. denotes the number of responsive CN neurons in the different phases of the applied visual fixation paradigm.

In the following, the stimulus-related response characteristics of the functional clusters are described.

4.3.1 Response characteristics of the PANs

After the exclusion of the neurons which showed spontaneous activity lower than 1 spike/s, 86 phasically active neurons were analyzed during the fixation paradigm. The mean spontaneous discharge rate was 2.93 spikes/sec (SD: ±2.18 spikes/sec). Overall, the visual responses of the PANs were moderate or weak (Table 2). During stationary visual stimulation 50 neurons showed significant change in their activity. In 26 cases this meant a significant increase, and in 24 cases a significant decrease was seen. Figures 5A and B show the responses of a PAN CN neuron to stationary visual stimulation.

Twenty-nine neurons showed activity change during dynamic visual stimulation. During the ‘center out’ optic flow 17 of them and during ‘center in’ optic flow 16 of them showed increased activity. On the other hand, 8 of the PANs showed decreased responses to optic flow. Figure 6A and B show the peristimulus time histograms (PSTHs) of one representative example of the decreased activity.

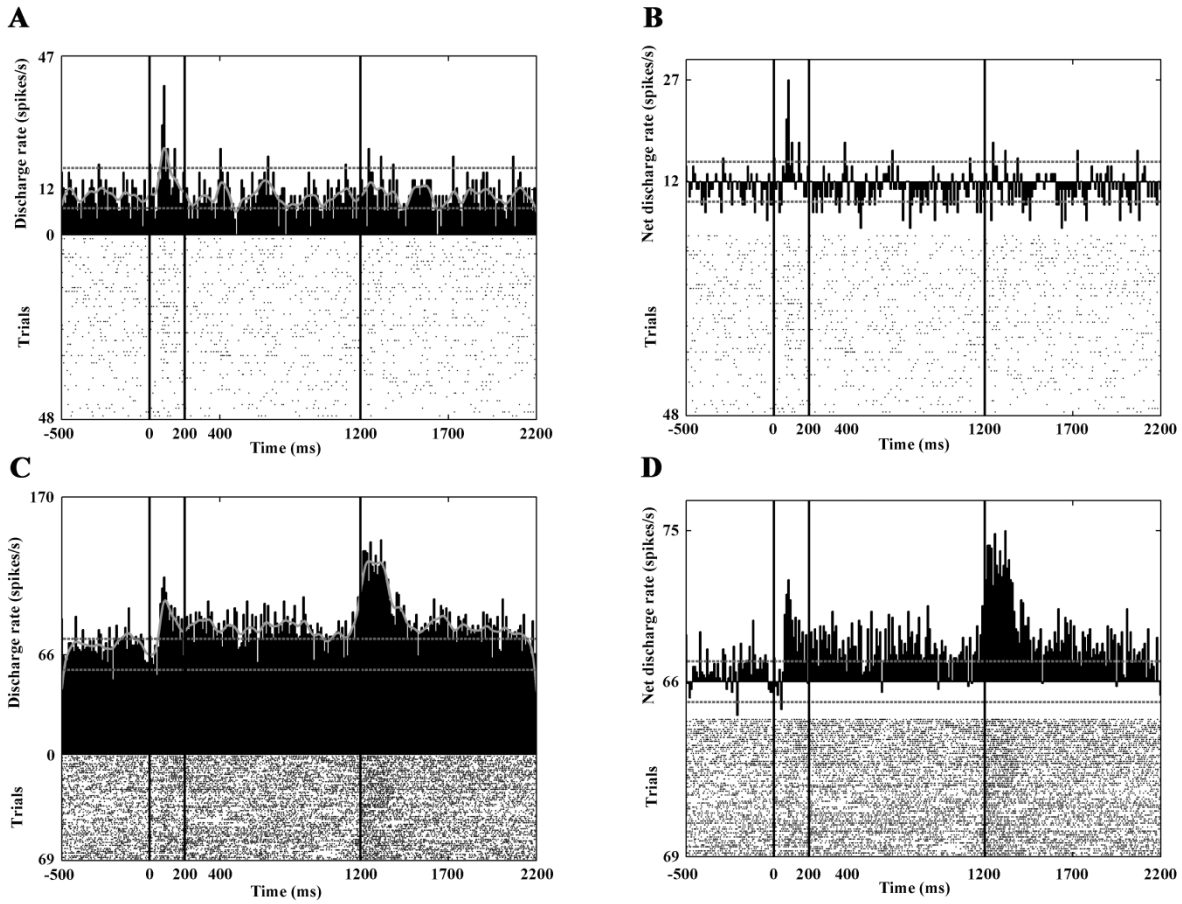

Figure 5. Response characteristics of CN neurons to stationary visual stimulation. Each panel of the figure contains a PSTH (top) and a raster plot (bottom) to represent the activity of a neuron. Panels A and B show the activity of a PAN, panels C and D show the firing pattern of a HFN. A and C show the gross activities, B and D show the net activity change after the subtraction of the background activity. The vertical black lines denote the boundaries between the different phases of the paradigm: fixation phase (-500 to 0 ms), static visual stimulation (0 to 200 ms), dynamic visual stimulation (200 to 1200 ms), reward phase (1200 to 1700 ms). Note the phasic response of the PAN to static stimulation (A,B). The activity pattern of the presented HFN (C,D) is more complex: increased activity can be observed not only to random

dot patterns, but also to optic flow and during the reward phase. The abscissa denotes time in milliseconds. Along the ordinate, the following values are shown (from the bottom to the top): the number of successful trials, the average discharge rate (spikes/sec) and a calibration value (spikes/sec) to help magnitude approximation along the plot. Zero marks the 0 spikes/sec reference line (no activity). The continuous grey curve is a smoothed curve of the activity, and the dashed grey lines indicate ±2 SD of the average discharge rate in the whole recording.

In the reward phase, 27 neurons showed significantly increased activity and six of them decreased their discharge rate. The question arises whether this activity is purely reward-related and/or related to the offset of the stimulus. In order to check this, we analyzed the aborted trials too, where the animal had broken the fixation. In this case the stimulus disappeared immediately and the animal got no reward. While the animal has broken the fixation the appearing eye movements could also elicited changes in the neuronal activity. In order to exclude the effects of eye movement- related activity in this case, the correlation between the interspike intervals and the normalized amplitude of the eye movements recorded during the experiment was computed. Figure 7D denotes the result of the linear regression analysis. This clearly shows the lack of connection (ρ^2: 0.02, $p>0.05$) and in this way the absence of eye movement- related activity. Whether the change in activity is reward-related can be told by a simple examination of the PSTHs in relation to the offset of the stimulus: if the response is reward-related, no peak in the PSTH can be observed. If there is a peak in these histograms, the activity is likely to be related to the stimulus offset. Figure 7 denotes the activity of a PAN, which responded with increased discharges to the offset of the stimulus.

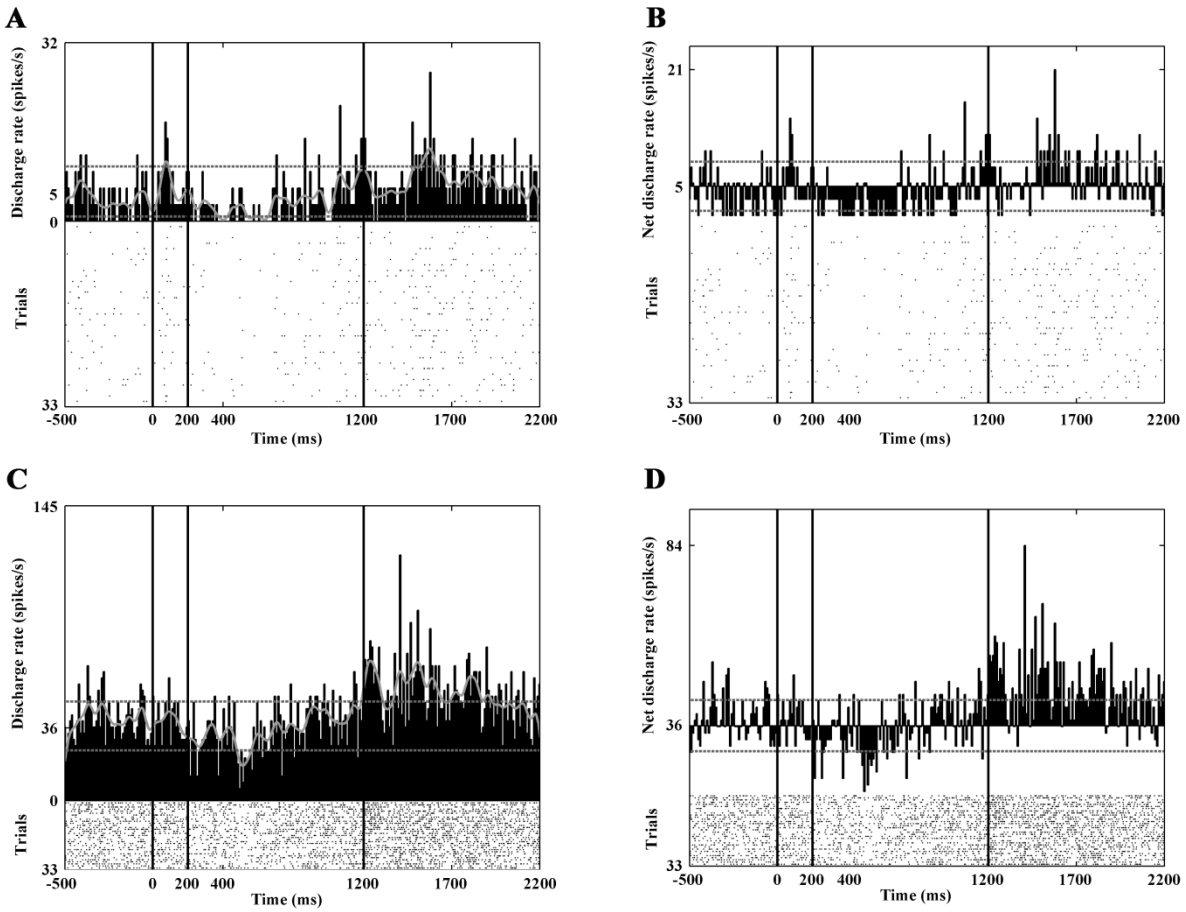

Figure 6. Decreased responses to optic flow stimulation. Panels A and B show the activity of a PAN, while panels C and D show the firing pattern of a HFN (top: PSTH, bottom: raster plot). The activity decrement during optic flow stimulation is notable. The conventions are the same as on Figure 5.

4.3.2 Response characteristics of the HFNs

In the paradigm 88 high-firing neurons were analyzed. The mean spontaneous discharge rate was 14.45 spikes/sec (SD: ±6.81 spikes/sec). During the stationary phase of the paradigm 18 neurons increased and 18 neurons decreased their activity significantly (Figure 5 C,D). Thirty-seven high-firing CN neurons responded to the optic flow stimulus. During the 'center out' optic flow stimulation, 16 neurons increased their activity, and during 'center in' 20 of them responded the same way. The visual responses of this group are much clearer and stronger than those of the PAN and TANs (Table 2). Figure 8 shows the responses of two HFNs to optic flow.

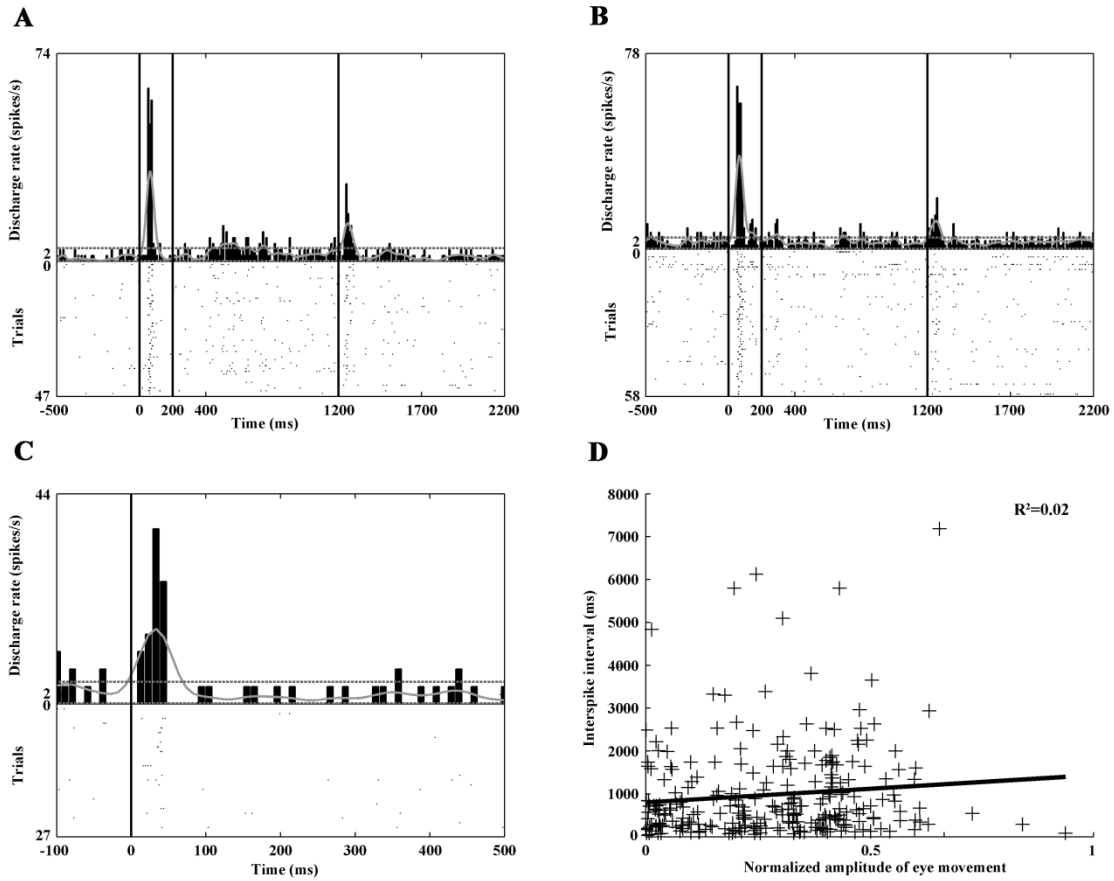

Figure 7. Stimulation-related response of a PAN. The PSTHs in panels A and B show the activity of the neuron in response to stimulation. A: response to center-out optic flow. B: response to center-in optic flow. The response to random dot patterns (A, B) and to center-out optic flow (A) is readily observable, but there is no remarkable response to center-in stimulation (B). The conventions are the same as in Figure 5. In order to decide whether the increased activity at the beginning of the reward phase is purely reward-related or related to stimulus offset, the aborted trials (where the cat had broken the fixation during visual stimulation and therefore got no reward) were also analyzed (C). Panel C is aligned to the time of the breaking of the fixation, which corresponded to the offset of the stimulus because the trial was immediately aborted upon fixation breaking. Note the PSTH peak, which indicates responsiveness to the offset of the stimulus. Furthermore, in order to control for the effects of saccadic activity, the correlation between the interspike intervals and the normalized amplitude of the eye movements recorded during the experiment was computed (D). The

linear regression analysis clearly shows the lack of connection (ρ^2: 0.02, $p>0.05$). This means the activity is of no saccadic origin.

During the reward phase of the paradigm, 30 neurons increased their activity and none of the high-firing neurons decreased their activity (Fig. 5 C, D and Fig. 9). The analysis of the responses to the disappearance of the stimulus revealed that 8 of the analyzed HFNs were active during the offset of the stimulus. Similarly to the PAN, which was sensitive to the offset of the stimulus the HFNs with offset-related responses showed no eye movement connected activity.

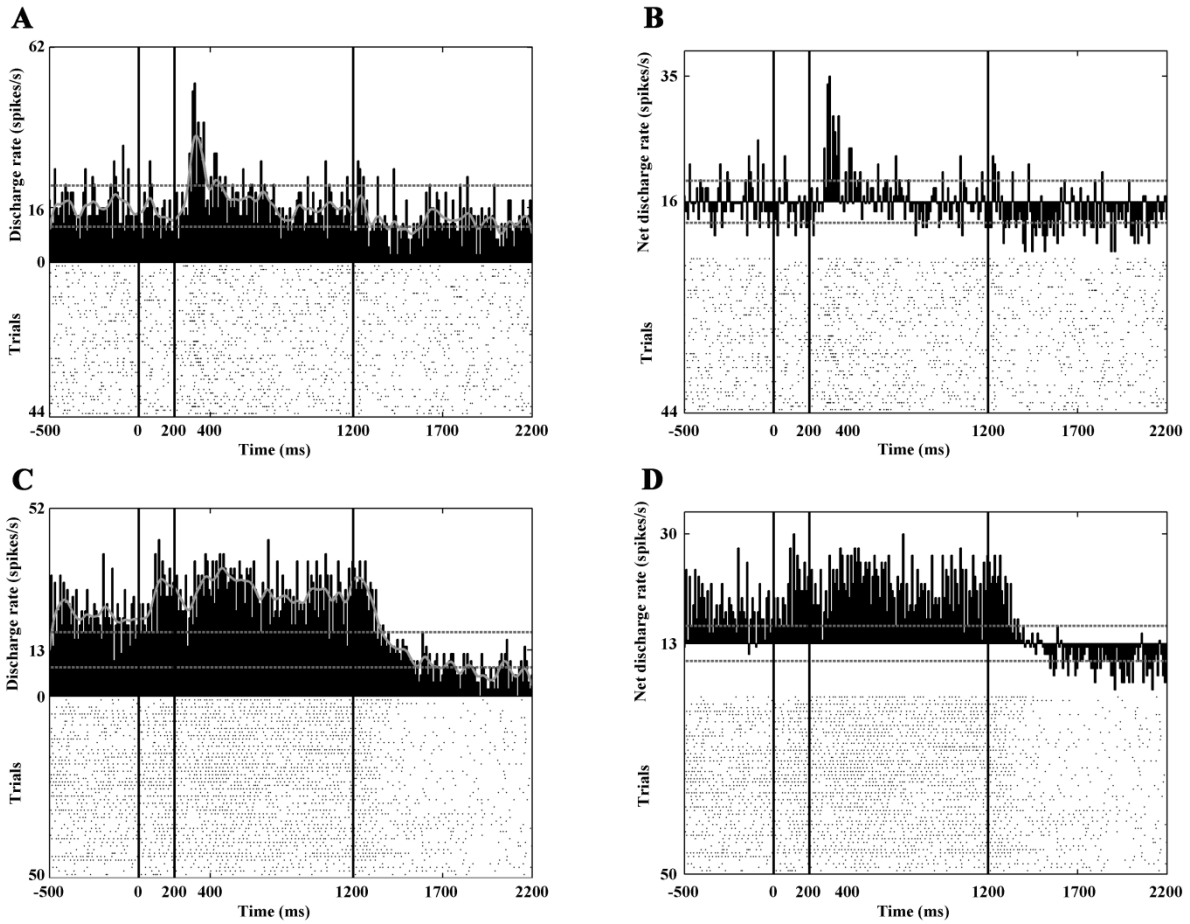

Figure 8. Increased responses to optic flow stimulation. In each panel of the figure, PSTHs (top) and raster plots (bottom) are presented to graphically represent the activity of the neuron. Panels A and B denote the activity of a HFN with a clear phasic response to the onset of the optic flow. Panels C and D show the responses of another HFN to static as well as to

optic flow stimulation. Note the strong responses of these units to optic flow stimulation. The conventions are the same as on Figure 5.

4.3.3 Response characteristics of the TANs

Beside the PANs and HFNs a low number of CN neurons (28) were classified in the TAN group. The mean spontaneous discharge rate was 5.24 spikes/sec (SD: ±2.37 spikes/sec). During static visual stimulation 11 neurons showed significantly increased, and 2 of them decreased activity. Seven of them responded with increased discharges to optic flow stimulus (3 to ‘center out’ and 5 ‘center in’ stimulus). The visual responses of the TANs were moderate or weak (Table 2). During the reward phase of the paradigm 6 neurons posessed increased activity. The offset of the stimulus modified the activity of one TAN. Similarly to the PAN and the HFNs, which were sensitive to the offset of the stimulus the TAN with offset-related response showed no eye movement connected activity.

4.3.4 Sensitivity to the direction of the optic flow

Altogether 74 (30 PANs, 36 HFNs and 8 TAN) of the 346 analyzed CN neurons showed significant activity change upon optic flow stimulation. In the majority of the analyzed neurons this change was not direction-dependent. Direction-dependent activity change was observed in twenty neurons (9 PAN, 8 HFN, 3 TAN). About half of the selective neurons (11 neurons) responded stronger to center-in stimulus while the second half of them (9 neurons) responded stronger to the center out optic flow. Figure 9 shows the PSTHs of a direction sensitive HFN.

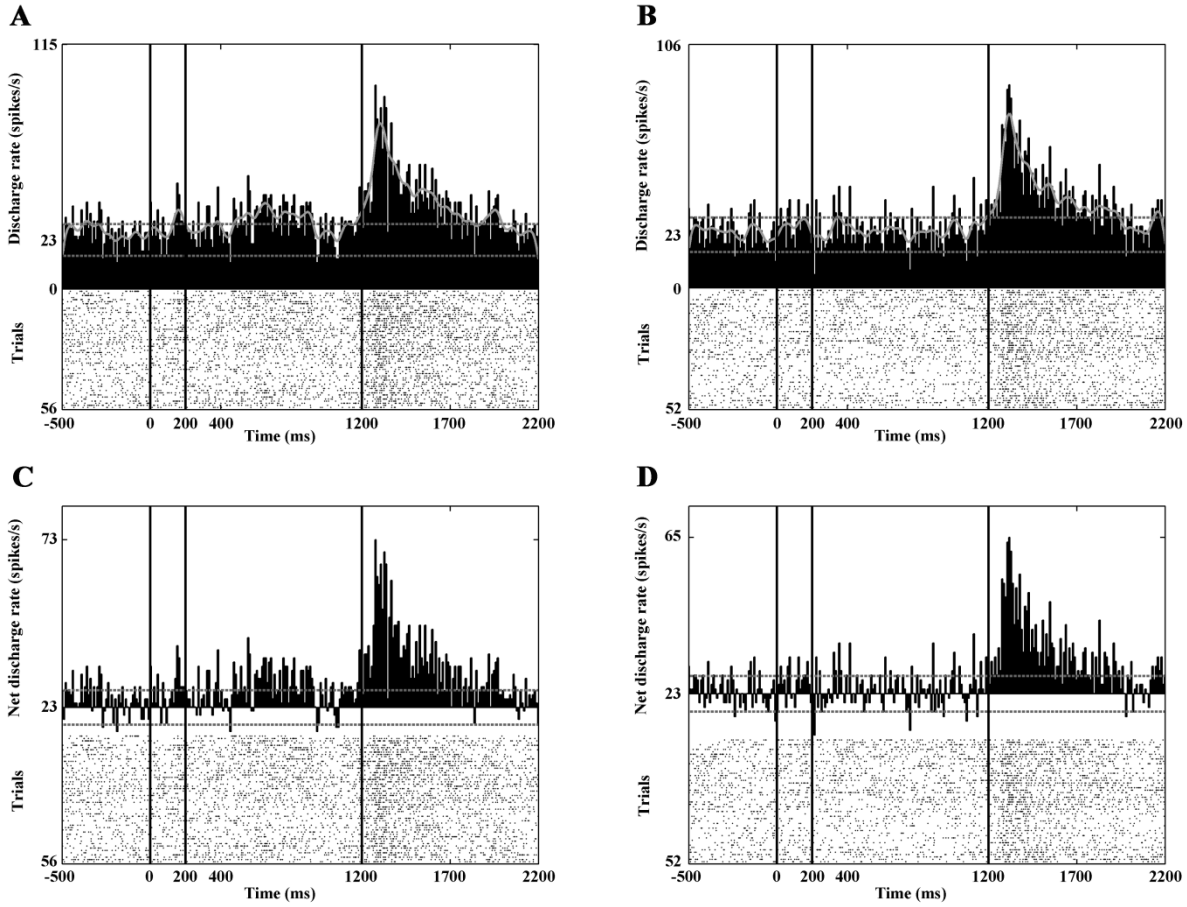

Figure 9. Selective responses to the direction of the optic flow. This figure demonstrates the activity of a HFN. Panels A (gross activity) and C (net activity) show the activities in response to center-out optic flow. Panels B (gross activity) and D (net activity) show the activities in response to center-in optic flow. Note that this neuron exhibits increased activity to center-out optic flow but no response to center-in optic flow. In other words, the neuron is selectively sensitive to the center-out direction. A strong reward-related activity can also be observed. The conventions are the same as in Figure 5.

At the population level there was no significant difference between the proportion of direction preferences within PANs, HFNs and TANs (χ-square test; $\chi^2(2)=1.001$, df=2, level of significance: 0.05). Thus the PANs, the HFNs and the TANs of the CN could code the direction of the optic flow to approximately the same extent.

4.3.5 Activity of neuron groups during different phases of the behavioral paradigm

Similarly to other studies (Plenz and Kitai, 1998; Berke et al., 2004), we found that the background activity of the HFNs was significantly higher ($p<0.001$) than that of the PANs and the TANs (Table 2). To exclude the effect of the background activities, we subtracted these from the gross activities and so calculated the net firing rates. For the further analyses, the absolute values of the net discharge rates were applied. Table 2 provides information about the net discharge rates of the PANs, HFNs and TANs by phase (i.e. static, dynamic, reward). A one-way ANOVA indicated significant variance ($p<0.01$). The subsequent post-hoc analysis (Tukey's HSD) revealed that the HFNs were both the most sensitive and exhibited the most vigorous responses throughout all the phases of the fixation paradigm. In summary, the activity of the HFNs differed significantly from the activity of both PANs and TANs, while the activities of the latter two did not differ significantly.

Phasically active neuron

	N	Mean	Median	SD	Min	Max
Background activity	86	2.93	2.34	2.18	0.97	8.88
Stationary						
increased activity	26	1.91	0.72	3.34	0.23	16.51
decreased activity	24	0.55	0.44	0.52	0.06	1.43
Optic flow-center out						
increased activity	17	0.94	0.87	0.48	0.38	1.92
decreased activity	2	0.37	0.37	0.13	0.28	0.46
Optic flow-center in						
increased activity	16	1.34	1.04	0.90	0.41	3.60
decreased activity	6	0.88	0.88	0.33	0.50	1.32
Reward						
increased activity	27	3.11	2.14	2.65	0.53	10.09
decreased activity	6	0.38	0.18	0.47	0.12	1.32

High-firing neuron

	N	Mean	Median	SD	Min	Max
Background activity	88	14.45	12.85	6.81	4.67	37.91
Stationary						
increased activity	18	8.51	7.92	4.51	1.80	19.52
decreased activity	18	3.18	1.88	3.75	0.45	15.91
Optic flow-center out						
increased activity	16	5.34	4.47	3.80	0.99	14.48
decreased activity	9	1.13	1.12	0.57	0.29	1.77
Optic flow-center in						
increased activity	20	4.56	3.51	3.63	0.30	12.84
decreased activity	8	0.79	0.85	0.38	0.24	1.33
Reward						
increased activity	30	9.57	7.06	7.05	1.82	32.65
decreased activity	0	-	-	-	-	-

	Tonically-firing neuron					
	N	Mean	Median	SD	Min	Max
Background activity	28	5.24	5.81	2.37	1.26	10.11
Stationary						
increased activity	11	1.69	1.20	1.49	0.43	4.83
decreased activity	2	0.23	0.23	0.23	0.06	0.39
Optic flow-center out						
increased activity	3	1.24	1.36	0.23	0.98	1.38
decreased activity	1	0.21	-	-	-	-
Optic flow-center in						
increased activity	5	0.97	0.98	0.59	0.32	1.85
decreased activity	1	0.81	-	-	-	-
Reward						
increased activity	6	2.89	1.86	3.79	0.24	9.91
decreased activity	0	-	-	-	-	-

Table 2. The net discharge rates (spikes/sec) of the PANs, HFNs and TANs by the different phases of the applied paradigm. Increased activities are given as net values after the subtraction of the background activity from the gross activity. Decreased activities are given as absolute values.

5 Discussion

During the work leading to this thesis we managed to provide a detailed description of the visual response profile of different CN neurons in the brain of behaving cats, after having classified them according to their electrophysiological characteristics. To our knowledge, such observations have not been made before. Not less important is the fact that these observations have been made on a feline model developed in our laboratory.

In the last few decades, behaving animal models have gradually gathered ground in neurophysiology, due to their advantages over anesthetized, paralyzed models. Behaving animals can be relatively easily used after brief behavioral training for several experimental purposes, but this is unfortunately not the case in visual and multisensory electrophysiological research. In visual electrophysiology, the investigated structures often exhibit visuomotor activity (e.g. saccades). This makes a continuous monitoring of eye movements indispensable. To minimize the influence of eye movements on the neuronal activities, the animal had to maintain fixation during the whole length of trials. In this way the eye movement- related components of the activity can be excluded. During the analysis of neuronal responses, which were correlated to stimulus offset (see in Results) the aborted trials were also analyzed where the animal has broken the fixation. In these cases because of the lack of fixation the effects of eye movements on the neuronal activities were also investigated. The correlation between the interspike intervals and the normalized amplitude of the eye movements recorded during the experiment revealed no eye movement- correlated activity among the CN neurons, which were sensitive to the offset of the visual stimuli.

In a recent study we gave a detailed description a new feline model for chronic visual electrophysiological recordings (Nagypal et al., 2014). This model yielded a relatively long recording time per day throughout several years from the same animal, with continuous eye movement control and stable head position. This model was also the basis of the present study.

Turning now to the discussion of the results, the most important achievement of this study may be the electrophysiological categorization of neurons in the feline CN. Similarly to earlier findings in rodents and primates (Schmitzer-Torbert and Redish, 2004; Schmitzer-Torbert and Redish, 2008; Kubota et al., 2009; Gage et al., 2010; Thorn et al., 2010; Barnes et al., 2011; Stalnaker et al., 2012) PANs, TANs and HFNs were found. The validity and

applicability of this classification is signified by the fact that over 97% of the recorded CN units fell into one of the three major categories, and it was only 3% that did not fit any of them. Earlier studies suggested a strong correspondence between the three biggest anatomical (medium spiny, cholinergic and parvalbumin immunpositive GABAergic interneurons) and electrophysiological (PAN, TAN, HFN) groups of the CN neurons. A growing body of evidence suggests that PAN neurons correspond to the medium spiny projection neurons, HFNs to the parvalbumin immunpositive GABAergic interneurons and the TFNs to the cholinergic interneurons (Wilson et al., 1990; Kawaguchi, 1993; Wilson, 1993; Kawaguchi et al., 1995; Apicella, 2002; Mallet et al., 2005; Berke, 2008; Tepper et al., 2010). As for the uncategorizable neurons (three percent in this study), these can belong to one of the numerous interneuron types of the caudate nucleus, such as the neuropeptide Y-, nitric oxide synthase- and somatostatin- containing (Vincent et al., 1983; Smith and Parent, 1986), calretinin immunpositive (Rymar et al., 2004), tyrosine hydroxylase immunpositive (Dubach et al., 1987; Tepper et al., 2010), cholecystokinin immunpositive (Adams and Fisher, 1990) and vasoactive intestinal polypeptide immunpositive (Takagi et al., 1984; Theriault and Landis, 1987; Hokfelt et al., 1988) interneurons - with no claim to being exhaustive. The low prevalence of these interneurons in the feline brain is in line with earlier findings in rodents and primates where the prevalence of each group of these interneurons is under 1%.

A further finding that fits with earlier studies in other species is that the majority of the CN units in the feline brain appear to be PAN (64% of the investigated units in this study). In other species 77–97% of the striatal projection neurons belong to this most probably GABAergic cluster. Striatal projection neurons comprise up to 97% of the rodent striatum, while this proportion is significantly lower in higher vertebrates, especially in primates (Kemp and Powell, 1971; Graveland et al., 1985; Wise et al., 1996; Luk and Sadikot, 2001; Rymar et al., 2004; Yarom and Cohen, 2011). It must be noted that PANs are often difficult to detect because of their extremely low background activity (Apicella, 2002; Lau and Glimcher, 2007), which means that the sixty-four percent finding may be an underestimation due to undersampling, which, in turn, can also have an effect on the estimations of the two other groups.

As for the two other major groups, our results suggest that they are much less prevalent than PAN (HFN 25% and TAN 8%). This is also in line with the results of earlier rodent and primate studies. The parvalbumin immunpositive GABAergic interneurons comprise roughly

1-20% of the striatal neurons of rats and primates (Luk and Sadikot, 2001), while the cholinergic group adds up to only about 10 percent of the CN neurons (up to 10% in primates (Fino and Venance, 2011), an 2% in cats (Phelps et al., 1985)).

Beyond the electrophysiological classification of the neurons in the feline CN, we also determined the visual response characteristics of the neurons belonging to the three major classes. The applied dynamic stimulus was quite new in this context, as hitherto optic flow has not been applied to investigate CN neurons. In our earlier studies we demonstrated that the CN neurons are strongly sensitive to very low spatial and high temporal frequency sinewave gratings and exhibit narrow temporal and spatial frequency tuning (Nagy et al., 2008, 2010). It has been hypothesized for some time that neurons with such spatio-temporal visual response characteristics could have a role in the processing of optic flow (Morrone et al., 1986; Brosseau-Lachaine et al., 2001). In the present study we revisited this hypothesis and provided the first piece of direct evidence on the processing of optic flow in the feline CN.

After the categorization of the CN units based on their electrophysiological properties, it was possible to investigate their visual response characteristics by group. Our results demonstrate that both the static and the dynamic components of the visual information are represented in the CN. The PANs and TANs were more sensitive to static than to dynamic visual stimulation, that is, they responded to the random dot patterns, but not to the optic flow. On the other hand, HFNs were almost equally sensitive to both static and dynamic stimulation (i.e. approximately the same proportion of these neurons responded to random dot pattern and to optic flow stimulation). The stimulus offset modulated the activity of a significant proportion of HFNs, which was not observed with PANs and TANs. This suggests that the PANs and TANs are primarily sensitive to static, continuous, unchanging visual stimuli. As mentioned before, the response characteristics of the HFNs are different: these neurons seem to be equally responsive to both static and dynamic stimulation (including stimulus offset). Furthermore, the net activity changes of the HFNs were significantly stronger than what was observed in PANs and TANs, regardless of the actual phase of the behavioral paradigm. These suggest that HFNs are the most sensitive units in the CN to visual stimuli.

We have also investigated whether the direction of the optic flow (center-in or center-out) is reflected in the activity of the CN neurons. The majority of the CN units showed no such sensitivity. About half of the direction sensitive units responded stronger to center in stimuli

and the second half of them were more sensitive to center out flow field. The sensitivity of the CN neurons to optic flow gives further support to the hypothesis that the CN neurons participate in motion perception, most probably in the perception of changes in the visual environment during self-motion (Morrone et al., 1986; Brosseau-Lachaine et al., 2001; Nagy et al., 2008).

In summary, we consider the following as the most important achievements of this study:

First, we managed to utilize our head-restrained, eye movement-controlled behaving feline model (Nagypal et al., 2014) in a visual electrophysiological study aimed at the analysis and classification of CN neurons in terms of their visual responsiveness.

Second, we described that different CN neuronal groups (PAN, TAN, HFN) are differently sensitive to static and dynamic visual stimulation. PAN and TAN neurons are primarily sensitive to static stimuli, while HFNs are primarily sensitive to changes in the visual environment of the animal. By this we also showed that visually sensitive neurons in the feline CN can be classified similarly to what had previously been found in other species.

Third, we managed to demonstrate optic flow processing in the feline CN, which emphasizes the role of this structure in the detection and processing of visual information related to motion.

6 Summary

Beside its motor functions, the caudate nucleus (CN), the main input structure of the basal ganglia, is also sensitive to various sensory modalities. The goal of our work was to investigate the effects of visual stimulation on the CN by using a behaving, head-restrained, eye movement-controlled feline model developed recently for this purpose in our laboratory. Extracellular multielectrode recordings were made from the CN in a visual fixation paradigm applying static and dynamic stimuli. The recorded neurons were classified in three groups according to their electrophysiological properties: phasically active (PAN), tonically active (TAN) and high-firing (HFN) neurons. The visual response characteristics were investigated according to this classification. The PAN and TAN neurons were sensitive primarily to static stimuli, while the HFN neurons responded primarily to changes in the visual environment i.e. to optic flow and the offset of the stimuli. The HFNs were the most sensitive to visual stimulation; their responses were stronger than those of the PANs and TANs. The majority of the recorded units were insensitive to the direction of the optic flow, regardless of group, but a small number of direction-sensitive neurons were also found. These demonstrate that both the static and the dynamic components of the visual information are represented in the CN. Furthermore, these results provide the first piece of evidence on optic flow processing in the CN, which, in more general terms, indicates the possible role of this structure in dynamic visual information processing.

7 Acknowledgements

I respectfully thank to Dr. Attila Nagy who was my mentor and supervisor during my PhD work. Special thanks to Professor Dr. György Benedek, for his helpful and instructive guidance. I express my gratitude to Professor Dr. Gábor Jancsó for allowing me to participate in the Neuroscience PhD Program. My special thanks go to Dr. Péter Gombkötő and Dr. Antal Berényi for their help in laboratory work and in data analysis and their friendship. I am also grateful to Dr. Gábor Braunitzer for his critical review of the drafts and the final version of this thesis. I would like to acknowledge the help of Györgyi Utassy, Robert Averkin, Tamás Puskás, Anett Nagy, Dr. Mihály Vöröslakos, Dr. Attila Őze, Dr. Balázs Barkóczi and Dr. Balázs Bodosi.

I express my most sincere gratitude to Gabriella Dósai for her valuable laboratory assistance. Many thanks go to Péter Liszli for his expert help in solving hardware and software problems. I would like to express my thanks to all of my colleagues and friends in the Department of Physiology for their support and kindness. It has been nice to work with them in this department.

My deepest thanks go to my parents for their continuous love and help in my life and scientific work.

I would like to express my extra gratitude to the Talentum Foundation of the Gedeon Richter Plc. for their financial support.

8 References

1. Adams CE, Fisher RS (1990) Sources of neostriatal cholecystokinin in the cat. J Comp Neurol 292:563-574.
2. Adler A, Katabi S, Finkes I, Prut Y, Bergman H (2013) Different correlation patterns of cholinergic and GABAergic interneurons with striatal projection neurons. Front Syst Neurosci 7:47.
3. Albe-Fessard D, Rocha-Miranda C, Oswaldo-Cruz E (1960) [Activity evoked in the caudate nucleus of the cat in response to various types of afferent stimulation. II. Microphysiological study]. Electroencephalogr Clin Neurophysiol 12:649-661.
4. Alexander GE, DeLong MR (1985) Microstimulation of the primate neostriatum. I. Physiological properties of striatal microexcitable zones. J Neurophysiol 53:1401-1416.
5. Anderson M, Yoshida M (1977) Electrophysiological evidence for branching nigral projections to the thalamus and the superior colliculus. Brain Res 137:361-364.
6. Aosaki T, Tsubokawa H, Ishida A, Watanabe K, Graybiel AM, Kimura M (1994) Responses of tonically active neurons in the primate's striatum undergo systematic changes during behavioral sensorimotor conditioning. J Neurosci 14:3969-3984.
7. Apicella P (2002) Tonically active neurons in the primate striatum and their role in the processing of information about motivationally relevant events. Eur J Neurosci 16:2017-2026.
8. Aron A, Fisher H, Mashek DJ, Strong G, Li H, Brown LL (2005) Reward, motivation, and emotion systems associated with early-stage intense romantic love. J Neurophysiol 94:327-337.
9. Averkin R, Korshunov V, Benedek G (2009) A microdrive assembly for chronic neuronal recording. In: 12th Meeting of the Hungarian Neuroscience Society. Budapest, Hungary: Front Syst Neurosci.
10. Barnes TD, Kubota Y, Hu D, Jin DZ, Graybiel AM (2005) Activity of striatal neurons reflects dynamic encoding and recoding of procedural memories. Nature 437:1158-1161.

11. Barnes TD, Mao JB, Hu D, Kubota Y, Dreyer AA, Stamoulis C, Brown EN, Graybiel AM (2011) Advance cueing produces enhanced action-boundary patterns of spike activity in the sensorimotor striatum. J Neurophysiol 105:1861-1878.
12. Beatty JA, Sullivan MA, Morikawa H, Wilson CJ (2012) Complex autonomous firing patterns of striatal low-threshold spike interneurons. J Neurophysiol 108:771-781.
13. Bennett BD, Bolam JP (1993) Characterization of calretinin-immunoreactive structures in the striatum of the rat. Brain Res 609:137-148.
14. Bennett BD, Wilson CJ (1999) Spontaneous activity of neostriatal cholinergic interneurons in vitro. J Neurosci 19:5586-5596.
15. Berke JD (2008) Uncoordinated firing rate changes of striatal fast-spiking interneurons during behavioral task performance. J Neurosci 28:10075-10080.
16. Berke JD (2011) Functional properties of striatal fast-spiking interneurons. Front Syst Neurosci 5:45.
17. Berke JD, Okatan M, Skurski J, Eichenbaum HB (2004) Oscillatory entrainment of striatal neurons in freely moving rats. Neuron 43:883-896.
18. Berkley MA (1970) Visual discrimination in the cat. In: Animal Psychophysics: the design and conduct of sensory experiments, 1970 Edition (Stebbins WC, ed). New York: AppletonCentury-Crofts.
19. Blake R, Cool SJ, Crawford ML (1974) Visual resolution in the cat. Vision Res 14:1211-1217.
20. Bolam JP, Wainer BH, Smith AD (1984) Characterization of cholinergic neurons in the rat neostriatum. A combination of choline acetyltransferase immunocytochemistry, Golgi-impregnation and electron microscopy. Neuroscience 12:711-718.
21. Brosseau-Lachaine O, Faubert J, Casanova C (2001) Functional sub-regions for optic flow processing in the posteromedial lateral suprasylvian cortex of the cat. Cereb cortex 11:989-1001.
22. Brown VJ, Desimone R, Mishkin M (1995) Responses of cells in the tail of the caudate nucleus during visual discrimination learning. J Neurophysiol 74:1083-1094.
23. Chang HT, Kita H (1992) Interneurons in the rat striatum: relationships between parvalbumin neurons and cholinergic neurons. Brain Res 574:307-311.

24. Chesselet MF, Graybiel AM (1986) Striatal neurons expressing somatostatin-like immunoreactivity: evidence for a peptidergic interneuronal system in the cat. Neuroscience 17:547-571.
25. Chudler EH, Sugiyama K, Dong WK (1995) Multisensory convergence and integration in the neostriatum and globus pallidus of the rat. Brain Res 674:33-45.
26. Connor JD (1970) Caudate nucleus neurones: correlation of the effects of substantia nigra stimulaton with iontophoretic dopamine. J Physiol 208:691-703.
27. Cowan RL, Wilson CJ, Emson PC, Heizmann CW (1990) Parvalbumin-containing GABAergic interneurons in the rat neostriatum. J Comp Neurol 302:197-205.
28. Crinion J, Turner R, Grogan A, Hanakawa T, Noppeney U, Devlin JT, Aso T, Urayama S, Fukuyama H, Stockton K, Usui K, Green DW, Price CJ (2006) Language control in the bilingual brain. Science 312:1537-1540.
29. Deffains M, Legallet E, Apicella P (2010) Modulation of neuronal activity in the monkey putamen associated with changes in the habitual order of sequential movements. J Neurophysiol 104:1355-1369.
30. Do J, Kim JI, Bakes J, Lee K, Kaang BK (2012) Functional roles of neurotransmitters and neuromodulators in the dorsal striatum. Learn Mem 20:21-28.
31. Dubach M, Schmidt R, Kunkel D, Bowden DM, Martin R, German DC (1987) Primate neostriatal neurons containing tyrosine hydroxylase: immunohistochemical evidence. Neurosci Lett 75:205-210.
32. Elliott R, Newman JL, Longe OA, Deakin JF (2003) Differential response patterns in the striatum and orbitofrontal cortex to financial reward in humans: a parametric functional magnetic resonance imaging study. J Neurosci 23:303-307.
33. English DF, Ibanez-Sandoval O, Stark E, Tecuapetla F, Buzsaki G, Deisseroth K, Tepper JM, Koos T (2012) GABAergic circuits mediate the reinforcement-related signals of striatal cholinergic interneurons. Nat Neurosci 15:123-130.
34. Feltz P, Albe-Fessard D (1972) A study of an ascending nigro-caudate pathway. Electroencephalogr Clin Neurophysiol 33:179-193.
35. Fino E, Venance L (2011) Spike-timing dependent plasticity in striatal interneurons. Neuropharmacology 60:780-788.
36. Franklin KB, Jacobson SG, McDonald WI (1975) Proceedings: The visual acuity of the cat. J Physiol 252:49P-50P.

37. Fuchs AF, Robinson DA (1966) A method for measuring horizontal and vertical eye movement chronically in the monkey. J Appl Physiol 21:1068-1070.
38. Gage GJ, Stoetzner CR, Wiltschko AB, Berke JD (2010) Selective activation of striatal fast-spiking interneurons during choice execution. Neuron 67:466-479.
39. Gerfen CR, Baimbridge KG, Miller JJ (1985) The neostriatal mosaic: compartmental distribution of calcium-binding protein and parvalbumin in the basal ganglia of the rat and monkey. Proc Natl Acad Sci U S A 82:8780-8784.
40. Gilles C, Lotstra F, Vanderhaeghen JJ (1983) CCK nerve terminals in the rat striatal and limbic areas originate partly in the brain stem and partly in telencephalic structures. Life Sci 32:1683-1690.
41. Goldberg JA, Reynolds JN (2011) Spontaneous firing and evoked pauses in the tonically active cholinergic interneurons of the striatum. Neuroscience 198:27-43.
42. Gombkoto P, Berenyi A, Nagypal T, Benedek G, Braunitzer G, Nagy A (2013) Co-oscillation and synchronization between the posterior thalamus and the caudate nucleus during visual stimulation. Neuroscience 242:21-27.
43. Gombkoto P, Rokszin A, Berenyi A, Braunitzer G, Utassy G, Benedek G, Nagy A (2011) Neuronal code of spatial visual information in the caudate nucleus. Neuroscience 182:225-231.
44. Grahn JA, Parkinson JA, Owen AM (2009) The role of the basal ganglia in learning and memory: neuropsychological studies. Behav Brain Res 199:53-60.
45. Graveland GA, Williams RS, DiFiglia M (1985) A Golgi study of the human neostriatum: neurons and afferent fibers. J Comp Neurol 234:317-333.
46. Griffith JS, Horn G (1963) Functional Coupling between Cells in the Visual Cortex of the Unrestrained Cat. Nature 199:876-895 PASSIM.
47. Hannan KL, Wood SJ, Yung AR, Velakoulis D, Phillips LJ, Soulsby B, Berger G, McGorry PD, Pantelis C (2010) Caudate nucleus volume in individuals at ultra-high risk of psychosis: a cross-sectional magnetic resonance imaging study. Psychiatry Res 182:223-230.
48. Harris KD, Henze DA, Csicsvari J, Hirase H, Buzsaki G (2000) Accuracy of tetrode spike separation as determined by simultaneous intracellular and extracellular measurements. J Neurophysiol 84:401-414.

49. Harting JK, Updyke BV, Van Lieshout DP (2001) The visual-oculomotor striatum of the cat: functional relationship to the superior colliculus. Exp Brain Res 136:138-142.
50. Hazan L, Zugaro M, Buzsaki G (2006) Klusters, NeuroScope, NDManager: a free software suite for neurophysiological data processing and visualization. J Neurosci Methods 155:207-216.
51. Hikosaka O, Sakamoto M, Usui S (1989) Functional properties of monkey caudate neurons. II. Visual and auditory responses. J Neurophysiol 61:799-813.
52. Hikosaka O, Nakamura K, Nakahara H (2006) Basal ganglia orient eyes to reward. J Neurophysiol 95:567-584.
53. Hokfelt T, Herrera-Marschitz M, Seroogy K, Ju G, Staines WA, Holets V, Schalling M, Ungerstedt U, Post C, Rehfeld JF, et al. (1988) Immunohistochemical studies on cholecystokinin (CCK)-immunoreactive neurons in the rat using sequence specific antisera and with special reference to the caudate nucleus and primary sensory neurons. J Chem Neuroanat 1:11-51.
54. Hollander H, Tietze J, Distel H (1979) An autoradiographic study of the subcortical projections of the rabbit striate cortex in the adult and during postnatal development. J Comp Neurol 184:783-794.
55. Hoshino K, Eordegh G, Nagy A, Benedek G, Norita M (2009) Overlap of nigrothalamic terminals and thalamostriatal neurons in the feline lateralis medialis-suprageniculate nucleus. Acta Physiol Hung 96:203-211.
56. Hubel DH (1959) Single unit activity in striate cortex of unrestrained cats. J Physiol 147:226-238.
57. Hubel DH, Wiesel TN (1961) Integrative action in the cat's lateral geniculate body. J Physiol 155:385-398.
58. Hubel DH, Wiesel TN (1962) Receptive fields, binocular interaction and functional architecture in the cat's visual cortex. J Physiol 160:106-154.
59. Humphries MD, Wood R, Gurney K (2010) Reconstructing the three-dimensional GABAergic microcircuit of the striatum. PLoS Comput Biol 6:e1001011.
60. Huxlin KR, Pasternak T (2004) Training-induced recovery of visual motion perception after extrastriate cortical damage in the adult cat. Cereb cortex 14:81-90.
61. Ibanez-Sandoval O, Tecuapetla F, Unal B, Shah F, Koos T, Tepper JM (2010) Electrophysiological and morphological characteristics and synaptic connectivity of

tyrosine hydroxylase-expressing neurons in adult mouse striatum. J Neurosci 30:6999-7016.

62. Ibanez-Sandoval O, Tecuapetla F, Unal B, Shah F, Koos T, Tepper JM (2011) A novel functionally distinct subtype of striatal neuropeptide Y interneuron. J Neurosci 31:16757-16769.
63. Inokawa H, Yamada H, Matsumoto N, Muranishi M, Kimura M (2010) Juxtacellular labeling of tonically active neurons and phasically active neurons in the rat striatum. Neuroscience 168:395-404.
64. Ishizu T, Zeki S (2011) Toward a brain-based theory of beauty. PloS One 6:e21852.
65. Isomura Y, Takekawa T, Harukuni R, Handa T, Aizawa H, Takada M, Fukai T (2013) Reward-modulated motor information in identified striatum neurons. J Neurosci 33:10209-10220.
66. Judge SJ, Richmond BJ, Chu FC (1980) Implantation of magnetic search coils for measurement of eye position: an improved method. Vision Res 20:535-538.
67. Kaufmann C, Wehrle R, Wetter TC, Holsboer F, Auer DP, Pollmacher T, Czisch M (2006) Brain activation and hypothalamic functional connectivity during human non-rapid eye movement sleep: an EEG/fMRI study. Brain 129:655-667.
68. Kawaguchi Y (1993) Physiological, morphological, and histochemical characterization of three classes of interneurons in rat neostriatum. J Neurosci 13:4908-4923.
69. Kawaguchi Y, Wilson CJ, Augood SJ, Emson PC (1995) Striatal interneurones: chemical, physiological and morphological characterization. Trends Neurosci 18:527-535.
70. Kemp JM, Powell TP (1971) The structure of the caudate nucleus of the cat: light and electron microscopy. Philos Trans R Soc Lond B Biol Sci 262:383-401.
71. Kimchi EY, Laubach M (2009) Dynamic encoding of action selection by the medial striatum. J Neurosci 29:3148-3159.
72. Kimura M (1986) The role of primate putamen neurons in the association of sensory stimuli with movement. Neurosci Res 3:436-443.
73. Kimura M, Rajkowski J, Evarts E (1984) Tonically discharging putamen neurons exhibit set-dependent responses. Proc Natl Acad Sci U S A 81:4998-5001.

74. Kimura M, Kato M, Shimazaki H (1990) Physiological properties of projection neurons in the monkey striatum to the globus pallidus. Exp Brain Res 82:672-676.
75. Kita H, Kosaka T, Heizmann CW (1990) Parvalbumin-immunoreactive neurons in the rat neostriatum: a light and electron microscopic study. Brain Res 536:1-15.
76. Koelliker A (1896) Handbuch der Gewebelehre des Menschen, 6th Edition. Leipzig: W. Engelmann.
77. Kolomiets B (1993) A possible visual pathway to the cat caudate nucleus involving the pulvinar. Exp Brain Res 97:317-324.
78. Koos T, Tepper JM (1999) Inhibitory control of neostriatal projection neurons by GABAergic interneurons. Nat Neurosci 2:467-472.
79. Kubota Y, Kawaguchi Y (1993) Spatial distributions of chemically identified intrinsic neurons in relation to patch and matrix compartments of rat neostriatum. J Comp Neurol 332:499-513.
80. Kubota Y, Kawaguchi Y (1994) Three classes of GABAergic interneurons in neocortex and neostriatum. Jpn J Physiol 44 Suppl 2:S145-148.
81. Kubota Y, Liu J, Hu D, DeCoteau WE, Eden UT, Smith AC, Graybiel AM (2009) Stable encoding of task structure coexists with flexible coding of task events in sensorimotor striatum. J Neurophysiol 102:2142-2160.
82. Kumar R, Ahdout R, Macey PM, Woo MA, Avedissian C, Thompson PM, Harper RM (2009) Reduced caudate nuclei volumes in patients with congenital central hypoventilation syndrome. Neuroscience 163:1373-1379.
83. Lau B, Glimcher PW (2007) Action and outcome encoding in the primate caudate nucleus. J Neurosci 27:14502-14514.
84. Luk KC, Sadikot AF (2001) GABA promotes survival but not proliferation of parvalbumin-immunoreactive interneurons in rodent neostriatum: an in vivo study with stereology. Neuroscience 104:93-103.
85. Mallet N, Le Moine C, Charpier S, Gonon F (2005) Feedforward inhibition of projection neurons by fast-spiking GABA interneurons in the rat striatum in vivo. J Neurosci 25:3857-3869.
86. McGaugh JL (2004) The amygdala modulates the consolidation of memories of emotionally arousing experiences. Annu Rev Neurosci 27:1-28.

87. McKown MD, Schadt JC (2006) A modification of the Harper-McGinty microdrive for use in chronically prepared rabbits. J Neurosci Methods 153:239-242.
88. Morrone MC, Di Stefano M, Burr DC (1986) Spatial and temporal properties of neurons of the lateral suprasylvian cortex of the cat. J Neurophysiol 56:969-986.
89. Nagy A, Eordegh G, Norita M, Benedek G (2003) Visual receptive field properties of neurons in the caudate nucleus. Eur J Neurosci 18:449-452.
90. Nagy A, Eordegh G, Paroczy Z, Markus Z, Benedek G (2006) Multisensory integration in the basal ganglia. Eur J Neurosci 24:917-924.
91. Nagy A, Berenyi A, Wypych M, Waleszczyk WJ, Benedek G (2010) Spectral receptive field properties of visually active neurons in the caudate nucleus. Neurosci Lett 480:148-153.
92. Nagy A, Paroczy Z, Markus Z, Berenyi A, Wypych M, Waleszczyk WJ, Benedek G (2008) Drifting grating stimulation reveals particular activation properties of visual neurons in the caudate nucleus. Eur J Neurosci 27:1801-1808.
93. Nagypal T, Gombkoto P, Utassy G, Averkin RG, Benedek G, Nagy A (2014) A new, behaving, head restrained, eye movement-controlled feline model for chronic visual electrophysiological recordings. J Neurosci Methods 221:1-7.
94. Newberg AB, Wintering NA, Morgan D, Waldman MR (2006) The measurement of regional cerebral blood flow during glossolalia: a preliminary SPECT study. Psychiatry Res 148:67-71.
95. Norita M, McHaffie JG, Shimizu H, Stein BE (1991) The corticostriatal and corticotectal projections of the feline lateral suprasylvian cortex demonstrated with anterograde biocytin and retrograde fluorescent techniques. Neurosci Res 10:149-155.
96. Obeso JA, Rodriguez-Oroz MC, Benitez-Temino B, Blesa FJ, Guridi J, Marin C, Rodriguez M (2008) Functional organization of the basal ganglia: therapeutic implications for Parkinson's disease. Mov Disord 23 Suppl 3:S548-559.
97. Phelps PE, Houser CR, Vaughn JE (1985) Immunocytochemical localization of choline acetyltransferase within the rat neostriatum: a correlated light and electron microscopic study of cholinergic neurons and synapses. J Comp Neurol 238:286-307.
98. Pigarev IN, Rodionova EI (1998) Two visual areas located in the middle suprasylvian gyrus (cytoarchitectonic field 7) of the cat's cortex. Neuroscience 85:717-732.

99. Pigarev IN, Levichkina EV (2011) Distance modulated neuronal activity in the cortical visual areas of cats. Exp Brain Res 214:105-111.

100. Pisani A, Bernardi G, Ding J, Surmeier DJ (2007) Re-emergence of striatal cholinergic interneurons in movement disorders. Trends Neurosci 30:545-553.

101. Plenz D, Kitai ST (1998) Up and down states in striatal medium spiny neurons simultaneously recorded with spontaneous activity in fast-spiking interneurons studied in cortex-striatum-substantia nigra organotypic cultures. J Neurosci 18:266-283.

102. Populin LC, Yin TC (1998) Behavioral studies of sound localization in the cat. J Neurosci 18:2147-2160.

103. Populin LC, Yin TC (2002) Bimodal interactions in the superior colliculus of the behaving cat. J Neurosci 22:2826-2834.

104. Pouderoux G, Freton E (1979) Patterns of unit responses to visual stimuli in the cat caudate nucleus under chloralose anesthesia. Neurosci Lett 11:53-58.

105. Robinson DA (1963) A Method of Measuring Eye Movement Using a Scleral Search Coil in a Magnetic Field. IEEE Trans Biomed Eng 10:137-145.

106. Rokszin A, Gombkoto P, Berenyi A, Markus Z, Braunitzer G, Benedek G, Nagy A (2011) Visual stimulation synchronizes or desynchronizes the activity of neuron pairs between the caudate nucleus and the posterior thalamus. Brain Res 1418:52-63.

107. Rolls ET, Thorpe SJ, Maddison SP (1983) Responses of striatal neurons in the behaving monkey. 1. Head of the caudate nucleus. Behav Brain Res 7:179-210.

108. Rymar VV, Sasseville R, Luk KC, Sadikot AF (2004) Neurogenesis and stereological morphometry of calretinin-immunoreactive GABAergic interneurons of the neostriatum. J Comp Neurol 469:325-339.

109. Schiffmann SN, Mailleux P, Przedborski S, Halleux P, Lotstra F, Vanderhaeghen JJ (1989) Cholecystokinin distribution in the human striatum and related subcortical structures. Neurochem Int 14:167-173.

110. Schmitzer-Torbert N, Redish AD (2004) Neuronal activity in the rodent dorsal striatum in sequential navigation: separation of spatial and reward responses on the multiple T task. J Neurophysiol 91:2259-2272.

111. Schmitzer-Torbert N, Jackson J, Henze D, Harris K, Redish AD (2005) Quantitative measures of cluster quality for use in extracellular recordings. Neuroscience 131:1-11.

112. Schmitzer-Torbert NC, Redish AD (2008) Task-dependent encoding of space and events by striatal neurons is dependent on neural subtype. Neuroscience 153:349-360.

113. Schultz W (1998) Predictive reward signal of dopamine neurons. J Neurophysiol 80:1-27.

114. Schultz W, Romo R (1988) Neuronal activity in the monkey striatum during the initiation of movements. Exp Brain Res 71:431-436.

115. Schulz JM, Reynolds JN (2013) Pause and rebound: sensory control of cholinergic signaling in the striatum. Trends Neurosci 36:41-50.

116. Schulz JM, Oswald MJ, Reynolds JN (2011) Visual-induced excitation leads to firing pauses in striatal cholinergic interneurons. J Neurosci 31:11133-11143.

117. Sedgwick EM, Williams TD (1967) The response of single units in the caudate nucleus to peripheral stimulation. J Physiol 189:281-298.

118. Seger CA, Cincotta CM (2005) The roles of the caudate nucleus in human classification learning. J Neurosci 25:2941-2951.

119. Smith Y, Parent A (1986) Neuropeptide Y-immunoreactive neurons in the striatum of cat and monkey: morphological characteristics, intrinsic organization and co-localization with somatostatin. Brain Res 372:241-252.

120. Stalnaker TA, Calhoon GG, Ogawa M, Roesch MR, Schoenbaum G (2012) Reward prediction error signaling in posterior dorsomedial striatum is action specific. J Neurosci 32:10296-10305.

121. Strecker RE, Steinfels GF, Abercrombie ED, Jacobs BL (1985) Caudate unit activity in freely moving cats: effects of phasic auditory and visual stimuli. Brain Res 329:350-353.

122. Stryker M, Blakemore C (1972) Saccadic and disjunctive eye movements in cats. Vision Res 12:2005-2013.

123. Takagi H, Somogyi P, Smith AD (1984) Aspiny neurons and their local axons in the neostriatum of the rat: a correlated light and electron microscopic study of Golgi-impregnated material. J Neurocytol 13:239-265.

124. Tang C, Pawlak AP, Prokopenko V, West MO (2007) Changes in activity of the striatum during formation of a motor habit. Eur J Neurosci 25:1212-1227.

125. Tepper JM, Bolam JP (2004) Functional diversity and specificity of neostriatal interneurons. Curr Opin Neurobiol 14:685-692.

126. Tepper JM, Koos T, Wilson CJ (2004) GABAergic microcircuits in the neostriatum. Trends Neurosci 27:662-669.

127. Tepper JM, Tecuapetla F, Koos T, Ibanez-Sandoval O (2010) Heterogeneity and diversity of striatal GABAergic interneurons. Front Neuroanat 4:150.

128. Theriault E, Landis DM (1987) Morphology of striatal neurons containing VIP-like immunoreactivity. J Comp Neurol 256:1-13.

129. Thorn CA, Atallah H, Howe M, Graybiel AM (2010) Differential dynamics of activity changes in dorsolateral and dorsomedial striatal loops during learning. Neuron 66:781-795.

130. Tollin DJ, Populin LC, Moore JM, Ruhland JL, Yin TC (2005) Sound-localization performance in the cat: the effect of restraining the head. J Neurophysiol 93:1223-1234.

131. Vicente AF, Bermudez MA, Romero Mdel C, Perez R, Gonzalez F (2012) Putamen neurons process both sensory and motor information during a complex task. Brain Res 1466:70-81.

132. Villablanca JR (2004) Counterpointing the functional role of the forebrain and of the brainstem in the control of the sleep-waking system. J Sleep Res 13:179-208.

133. Villablanca JR (2010) Why do we have a caudate nucleus? Acta Neurobiol Exp 70:95-105.

134. Villeneuve MY, Casanova C (2003) On the use of isoflurane versus halothane in the study of visual response properties of single cells in the primary visual cortex. J Neurosci Methods 129:19-31.

135. Vincent SR, Johansson O (1983) Striatal neurons containing both somatostatin- and avian pancreatic polypeptide (APP)-like immunoreactivities and NADPH-diaphorase activity: a light and electron microscopic study. J Comp Neurol 217:264-270.

136. Vincent SR, Staines WA, Fibiger HC (1983) Histochemical demonstration of separate populations of somatostatin and cholinergic neurons in the rat striatum. Neurosci Lett 35:111-114.

137. Webster KE (1965) The Cortico-Striatal Projection in the Cat. J Anat 99:329-337.

138. White NM (2009) Some highlights of research on the effects of caudate nucleus lesions over the past 200 years. Behav Brain Res 199:3-23.

139. Wilson CJ (1993) The generation of natural firing patterns in neostriatal neurons. Prog Brain Res 99:277-297.

140. Wilson CJ, Groves PM (1981) Spontaneous firing patterns of identified spiny neurons in the rat neostriatum. Brain Res 220:67-80.

141. Wilson CJ, Chang HT, Kitai ST (1990) Firing patterns and synaptic potentials of identified giant aspiny interneurons in the rat neostriatum. J Neurosci 10:508-519.

142. Wise SP, Murray EA, Gerfen CR (1996) The frontal cortex-basal ganglia system in primates. Crit Rev Neurobiol 10:317-356.

143. Wu Y, Parent A (2000) Striatal interneurons expressing calretinin, parvalbumin or NADPH-diaphorase: a comparative study in the rat, monkey and human. Brain Res 863:182-191.

144. Yarom O, Cohen D (2011) Putative cholinergic interneurons in the ventral and dorsal regions of the striatum have distinct roles in a two choice alternative association task. Front Syst Neurosci 5:36.

145. Yin HH, Mulcare SP, Hilario MR, Clouse E, Holloway T, Davis MI, Hansson AC, Lovinger DM, Costa RM (2009) Dynamic reorganization of striatal circuits during the acquisition and consolidation of a skill. Nat Neurosci 12:333-341.

146. Zhou FM, Wilson CJ, Dani JA (2002) Cholinergic interneuron characteristics and nicotinic properties in the striatum. J Neurobiol 53:590-605.

I.

Journal of Neuroscience Methods 221 (2014) 1–7

Contents lists available at ScienceDirect

Journal of Neuroscience Methods

journal homepage: www.elsevier.com/locate/jneumeth

Basic Neuroscience

A new, behaving, head restrained, eye movement-controlled feline model for chronic visual electrophysiological recordings

Tamás Nagypál[a], Péter Gombkötő[b], Györgyi Utassy[a], Robert G. Averkin[c], György Benedek[a], Attila Nagy[a,*]

[a] Department of Physiology, Faculty of Medicine, University of Szeged, Dóm tér 10, Szeged H-6720, Hungary
[b] Center for Molecular and Behavioral Neuroscience Rutgers University, 197 University Ave, Newark, NJ 07102, United States
[c] Research Group for Cortical Microcircuits of the Hungarian Academy of Sciences, Department of Physiology, Anatomy and Neuroscience, University of Szeged, Közép fasor 52, Szeged H-6726, Hungary

HIGHLIGHTS

- A new model for chronic visual electrophysiological recordings in behaving cat.
- A novel body position for recording (suspension).
- Rigorous control to avoid the confounding effects of eye movements.
- Stable recording for over two years.

ARTICLE INFO

Article history:
Received 24 July 2013
Received in revised form 9 September 2013
Accepted 10 September 2013

Keywords:
Suspended cat
Behavioral training
Fixation paradigm
Long-time recordings
Visual electrophysiology

ABSTRACT

Background: Anesthetized, paralyzed domestic cats are often used as model organisms in visual neurophysiology. However, in the last few decades, behaving animal models have gathered ground in neurophysiology, due to their advantages over anesthetized, paralyzed models.
New Method: In the present study a new, behaving, awake feline model is described, which is suitable for chronic visual electrophysiological recordings. Two trained, head- fixed cats were suspended in a canvas harness in a specially designed stand. The animals had been trained to fixate the center of a monitor during static and dynamic visual stimulation. Eye movements were monitored with implanted scleral coil in a magnetic field. Cell-level activity was recorded with eight electrodes implanted in the caudate nucleus.
Results: Our two trained cats could maintain accurate fixation, even during optic flow stimulation, in an acceptance window of ±2.5° and ±1.5°, respectively. The model has yielded accurate recordings for over two years.
Comparison with Existing Method(s): To our knowledge, this is the first awake, behaving feline model with rigorous eye movement control for chronic, cell-level visual electrophysiological recordings, which has actually proven to work during a longer period.
Conclusions: The new model is optimal for chronic visual electrophysiological recordings in the awake, behaving domestic cat.

1. Introduction

The domestic cat is a classical mammalian model organism in visual neurophysiology and neuroanatomy. Several high-impact discoveries have been based on the feline model, of which the most well-known may be those of the Nobel laureates Hubel and Wiesel (1961, 1962). In the last few decades, animal research has seen a clear tendency toward the use of awake, behaving animals, instead of the previously used anesthetized, paralyzed models.

In visual electrophysiology the anesthetized, paralyzed feline model was optimal for the analysis of visual receptive field properties of single neurons, as the confounding effect of eye movements was eliminated by the paralysis. However, the exclusion of the effects of the eye movements in awake, behaving experiments is not less necessary, as several visually active structures (e.g. the superior colliculus or the basal ganglia) show saccadic responses too (Hikosaka et al., 2000; Munoz and Fecteau, 2002). This necessitates

* Corresponding author at: Department of Physiology, University of Szeged, Dóm tér 10, H-6720 Szeged, POB 427, Hungary. Tel.: +36 62 545869; fax: +36 62 545842.
E-mail address: nagy.attila.1@med.u-szeged.hu (A. Nagy).

0165-0270/$ – see front matter © 2013 Elsevier B.V. All rights reserved.
http://dx.doi.org/10.1016/j.jneumeth.2013.09.004

a continuous monitoring of eye movements. For this purpose, implantation of scleral magnetic search coils was introduced (Fuchs and Robinson, 1966; Judge et al., 1980; Robinson, 1963). The model was developed for primate models, but it was successfully adapted to cats too. Awake, behaving animal models have two major advantages over anaesthetized ones: first, significantly fewer animals are required. Second, this way, the modulatory effects of anesthetics can be excluded. Such a modulatory effect was clearly demonstrated in the superior colliculus, a multisensory midbrain structure of the mammalian brain, where the large enhanced multisensory responses, which were described in anesthetized animals (Stein, 1998), could never be recorded from awake, behaving cats (Populin and Yin, 2002). Furthermore, different anesthetics have different effects on the visual sensitivity of the brain, which undermines the comparability of the results (Villeneuve and Casanova, 2003). Behaving animal models are often used in primate experiments, but they have rarely been utilized in cats, due to technical difficulties. In visual electrophysiology, only a few research groups are known that have performed visual experiments on eye-movement controlled, behaving cats. Pigarev and his colleagues investigated the visual cortical areas (Pigarev and Levichkina, 2011; Pigarev and Rodionova, 1998). Populin and Yin performed mainly auditory and auditory-visual experiments on the superior and inferior colliculi (Populin and Yin, 1998, 2002; Tollin et al., 2005). Huxlin and Pasternak (2004) investigated the training-induced recovery of visual motion perception after extrastriate cortical damage in adult cats. In each case, the head of the animal was fixed and its body was put either in a box or on a trolley, which could move along a 3-m long railway or in a canvas bag on a platform.

In our laboratory we investigate the sensory properties of the basal ganglia and the connected ascending tectofugal visual system. We have hitherto performed our experiments on anaesthetized and paralyzed cats (Gombkoto et al., 2013; Nagy et al., 2006, 2008). Our main goal was to introduce a feline model, which would be suitable for chronic visual and multisensory electrophysiological recordings in the awake, behaving cat. Here we present the entire experimental setup and demonstrate how eye-movements were monitored and controlled for. The applicability of the new model is demonstrated through recordings of neuronal responses from the caudate nucleus.

2. Materials and methods

Experiments were performed on one male (3.5 kg) and one female (2.5 kg) adult domestic cats. All experimental procedures were carried out to minimize the number and the discomfort of the animals involved, and followed the European Communities Council Directive of 24 November 1986 (86 609 EEC) and the National Institutes of Health guidelines for the care and use of animals for experimental procedures. The experimental protocol was accepted and approved by the Ethics Committee for Animal Research of the University of Szeged.

2.1. Animal preparation and surgery

The animals were initially anesthetized with ketamine hydrochloride (Calypsol (Gedeon Richter®), 30 mg/kg i.m). To reduce salivation and bronchial secretion, a subcutaneous injection of 0.2 ml 0.1% atropine sulphate was administered preoperatively. A cannula was inserted in the femoral vein and after intubation of the trachea the animals were placed in a stereotaxic headholder. All wounds and pressure points were treated regularly with local anesthetic (1%, procaine hydrochloride). Throughout the surgery, the anesthesia was maintained with 1.5% halothane in a 2:1 mixture of N_2O and oxygen. The depth of anesthesia was monitored by continuously checking the end-tidal halothane concentration and heart rate (electrocardiogram). The minimum alveolar anesthetic concentration (MAC) values calculated from the end-tidal halothane readings were kept in the range recommended by Villeneuve and Casanova (2003). The end-tidal halothane concentration, MAC values and the peak expired CO_2 concentrations were monitored with a capnometer (Capnomac Ultima, Datex-Ohmeda, ICN). The O_2 saturation of the capillary blood was monitored by pulse oxymetry. The peak expired CO_2 concentration was kept within the range 3.8–4.2% by adjustment of the respiratory rate or volume. The body temperature of the animal was maintained at 37 °C by a computer-controlled, warm-water heating blanket. Craniotomy was performed with a dental drill to allow a vertical approach to the target structures. The dura mater was preserved, and the skull hole was covered with a 4% solution of 38 °C agar dissolved in Ringer's solution. Then a reclosable plastic recording chamber (20 mm in diameter) was installed on the skull. Following this, the eight electrodes were implanted in the brain with the help of an adjustable microdrive system (a modified Harper-McGinty microdrive for the first animal, see McKown and Schadt (2006), and a modified Korshunov microdrive for the second animal, see Korshunov (1995)). The implanted chamber and microdriver system allowed a stable recording background for long-time (at least two years in the first cat). In order to monitor the eye movements of the animals, a scleral search coil was implanted into the eye. Although this method was originally developed for primates (Fuchs and Robinson, 1966; Judge et al., 1980; Robinson, 1963), **it was later adapted to cats, too** (Huxlin and Pasternak, 2004; Pigarev and Levichkina, 2011; Pigarev and Rodionova, 1998; Populin and Yin, 1998, 2002; Tollin et al., 2005). Additionally, a stainless steel headholder was cemented to the skull for head fixation purposes.

Surgical procedures were carried out under aseptic conditions. Before the surgical procedure, a preventive dose of antibiotic was given (1000 mg ceftriaxon, i.m., Rocephin 500 mg (Roche®)). The first five postoperative days 50 mg/kg antibiotic was provided intramuscularly. Nalbuphin and non-steroidal anti-inflammatory drugs were administered until the seventh postoperative day.

2.2. Behavioral training of the animals

The experimental animals were selected with distinguished care, in a one-year process, during which the animals were adapted to the laboratory environment and their temper was also observed. It was only after this selection and training process that the insertion of the recording electrodes took place. Water deprivation was not used. Cooperative behavior and adaptation to the laboratory environment was formed by a feeding routine. Independently of behavioral training or recording, the animals received food only in the laboratory (150–250 g/day). During the weekends, the animals had access to food in their cage ad libitum, without any weight control. Once the cat got accustomed to the laboratory environment, it was carefully clothed into the canvas harness. This harness leaves the head, tail and legs free. Initially, the cat spent only a few minutes in the harness, which was extended to two hours. It was also during this period that we gradually shifted to pulpy food provided trough a plastic tube. The next step in training, which is a novelty of our model, was the suspension of the animal. Cats, by nature, like to lie in a hammock; therefore, it is relatively easy to get them accustomed to the canvas harness in a suspended position. In this specific case, it was done as follows: First, we lifted the animal manually only a few centimeters from the floor in the canvas harness, while it was being fed. When the animal got used to being suspended this way, it was gradually introduced to the experimental stand (Fig. 1). The experimental stand is a cubical structure with each side open, in which the suspension harness is fastened at two points in by a rope pulley block. Before the implantation of the electrodes, it

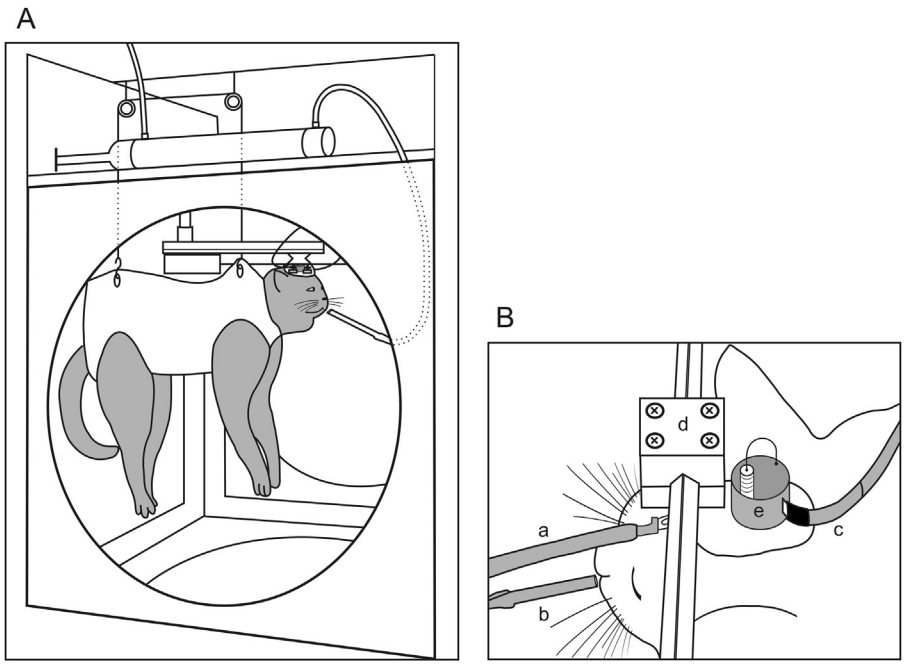

Fig. 1. Schematic drawing of the experimental setup. (A) the suspended cat in the canvas harness in the experimental stand. The head of the suspended cat is restrained in the stereotaxic frame. The cat is inside an electromagnetic field, generated by metal coils, installed in the four walls of the stand. Above (outside the magnetic field) is a hydraulic pump, which doses the food reward. (B) The schematic drawing of the head of the cat with the accessories for chronic recordings. The head of the cat is restrained via the implanted steel headholder (d) with two stainless steel bars, which are attached to the stereotaxic frame. The recording chamber with adjustable microdrive, which moves the eight recording wire-electrodes (e) and the recording cable with preamplifier (c) are placed behind the headholder. On the other side of the headholder, the adapter of the eye movements recording cable (a) can be seen. The cat receives the food reward through a plastic tube (b).

took approximately three months to adapt the cat to these circumstances. In the following step, the head of the suspended cat was fixed to the stereotaxic frame by the implanted steel headholder with two stainless steel bars (see Fig. 1**B**). In this paradigm, the stereotaxic device is placed within an electromagnetic field, which is generated by metal coils, installed into the wall of the stand. Once in the stereotaxic device, the animals were fed only with pulpy food (now as reward for successful trials, see below) through a plastic tube, dosed by a computer-driven hydraulic pump installed outside the magnetic field.

Having established the physical circumstances, the animals had to be taught the behavioral paradigm. A standard 17- inch CRT monitor (at 80 Hz refresh rate) was placed in front of the animal, at a distance of 57 cm. The initial part of behavioral training concentrates on fixation. The fixation point is projected on the center of the CRT monitor within an acceptance window of changeable size. The size of the fixation point is constant, 0.8° in diameter. If the cat holds fixation for a pre-set duration within the acceptance window, it receives food reward. During the fixation training, the fixation time was gradually increased from 100 ms to 1500 ms. Square fixation windows were used. The size of the initial fixation window was ±10° for both cats. During the training period, it was reduced to ±2.5° in ±2.5° steps, which took two months. This was the final size of the fixation window in the case of the first cat, but with the second animal we could further reduce the window to ±1.5° by three extra weeks of fixation training. After the fixation training, either random dot kinematogram (static) or optic flow (dynamic) stimuli were applied, while the animal maintained fixation. The size of the dots was 0.1° in diameter and their speed increased 0–7°/s toward the periphery. A trial consisted of the following stages: the cat first fixated on a central green fixation point ("Fixation"). During fixation, static random dots appeared in the visual field ("Random stationary dots") for 200 ms. After 200 ms, the static dots started moving radially as an optic flow for 1000 ms ("Optic flow"). A trial was considered successful if the cat managed to fixate during all phases of the trial. After each successful trial, the animal received reward. To minimize the influence of eye movements on neuronal activity, the trial was aborted immediately if the animal broke fixation. In such cases, no reward was given either. The intertrial interval was between 5000 and 10000 ms. Recording sessions began when the cats reached a stable 80% efficiency at the task.

Both the aforementioned training phases and the recordings took place in a dark laboratory room. Sessions (either training or recording) lasted 1–2 h a day, four to five times a week. The weight of the animals was checked regularly and was kept at least 90% of the initial value. The survival time of the implanted and trained cat appears to be long. In the first cat, the recordings have been going on for 2.5 years, while in the second cat, recordings began 3 months ago.

2.3. Recording and data analysis

Extracellular multielectrode recordings were made with eight implanted nichrome or platinum-iridium wire-electrodes (25 μm and 20 μm respectively, in formal insulation) in the caudate nucleus (CN). The implantation of the electrodes was made according to the Horsley–Clarke system (anterior 12–14 mm, lateral 5–6.5 mm at stereotaxic depths between 9 and 13.5 mm). Amplified neuronal activities were recorded without online filtering, at 20 kHz sampling rate. The signals were band-pass filtered offline (300–3000 Hz) to analyze multiunit activity in detail. Multiunit activity recorded by each electrode was first processed by NeuroScope, NDManager, KlustaKwik and then broken down into single unit signals by the use of Klusters (Harris et al., 2000; Hazan et al., 2006) under manual control. All statistical analyses were performed in Matlab® (MathWorks Inc., Natick, MA). Low frequency activities under 300 Hz (local field potentials) were also investigated.

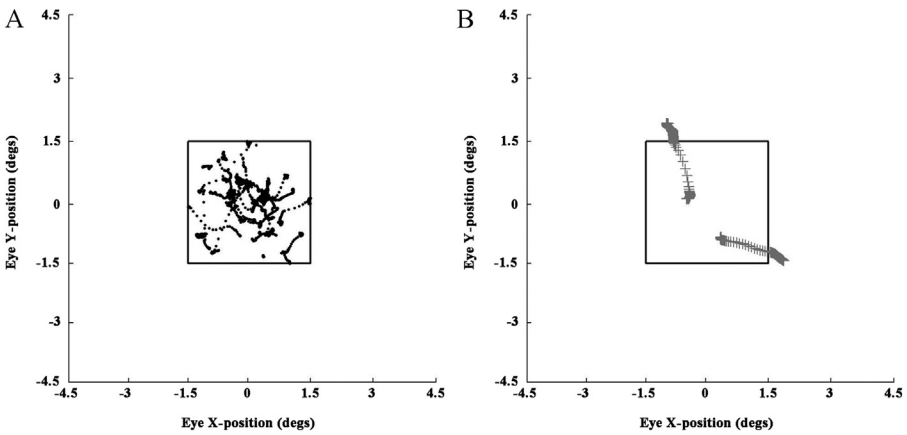

Fig. 2. Eye movement control during the experiments. (A) shows successful fixation as described in Section 2. (B) depicts failed fixation. During all phases of the task the cat was to maintain the fixation on a stationary fixation point, which was centered to the middle of the CRT monitor (0°, 0°). The black squares denote the fixation acceptance window (±1.5°). Each black dot and each gray cross shows a particular position of the eye during recording. Abscissa and ordinate denote the horizontal and vertical positions of the eye in degrees, respectively.

Eye movements were recorded via a search coil system (DNI Instruments, Newark, DE, USA) with a sampling rate of 1000 Hz, and these were also processed by Matlab®. The experiment was controlled by a custom-made software, including eye movement-recording, stimulus presentation, reward delivery and data collection via National Instruments DAQ®. The stimuli were generated by the Psychophysics Toolbox of Matlab®.

3. Results

In the present study we suggest a new chronic animal model, which is suitable for electrophysiological recordings from visual brain structures. The most straightforward points of the model are the daily at least two hours recording time, the several years recording period, the continuous eye control and the restrained head of the suspended animal during the experiments, which makes this model ideal for classic visual electrophysiological experiments.

3.1. Control of eye movements

In order to exclude the effect of eye movements on the recordings of neuronal activities the head restrained, cats had to be able to maintain their fixation. The final result of the training is that the head restrained, suspended animals can fixate quite accurately (within a ±2.5° fixation acceptance window for the first cat, and within a ±1.5° fixation acceptance window for the second cat), even during dynamic visual stimulation (Fig. 2).

A continuous control of eye movements was an essential part of our experiments. By the eye-tracker method (as described above), it became possible to follow and exactly reconstruct (visualize) the

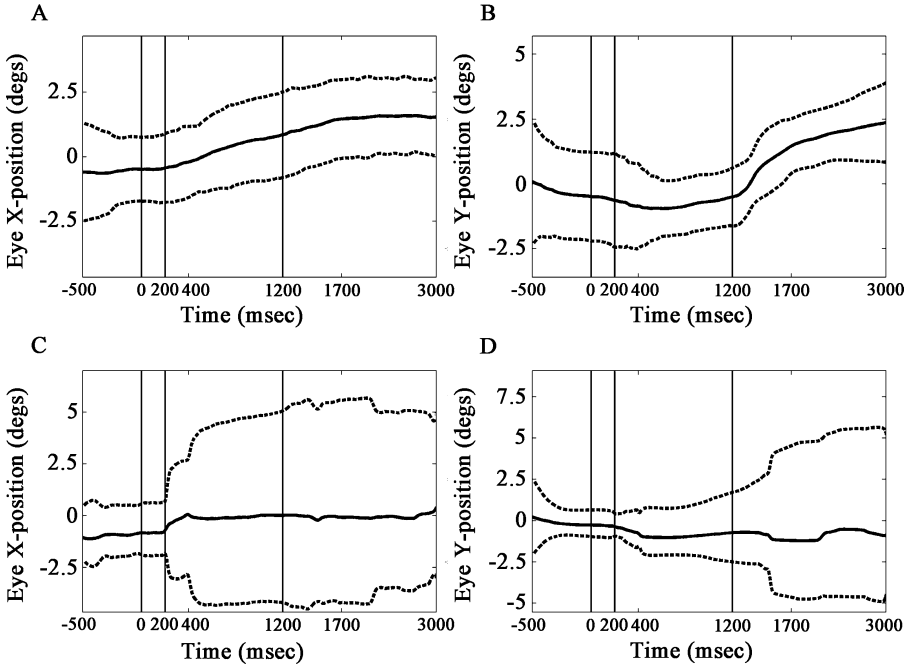

Fig. 3. Eye movements of the cat during the visual fixation paradigm. Top (A) and (B): successful fixation, bottom (C) and (D): failed fixation. (A) and (C) horizontal eye positions. (B) and (D) vertical eye positions (assuming a ±2.5° acceptance window). The bold black line shows the mean of eye movements, and the dotted lines denote standard deviations. Time is marked on the abscissa, and the ordinates show the horizontal (*X*) or the vertical (*Y*) positions of the eye. The vertical black lines separate the different epochs of the paradigm: fixation period (−500 to 0 ms), random static dot stimulation (0 to 200 ms), optic flow (200 to 1200 ms) and reward (1200 to 1700 ms). Fixation failure is demonstrated by the strong and suddenly increasing of the standard deviation in the horizontal plane (C) but not in the vertical one (D).

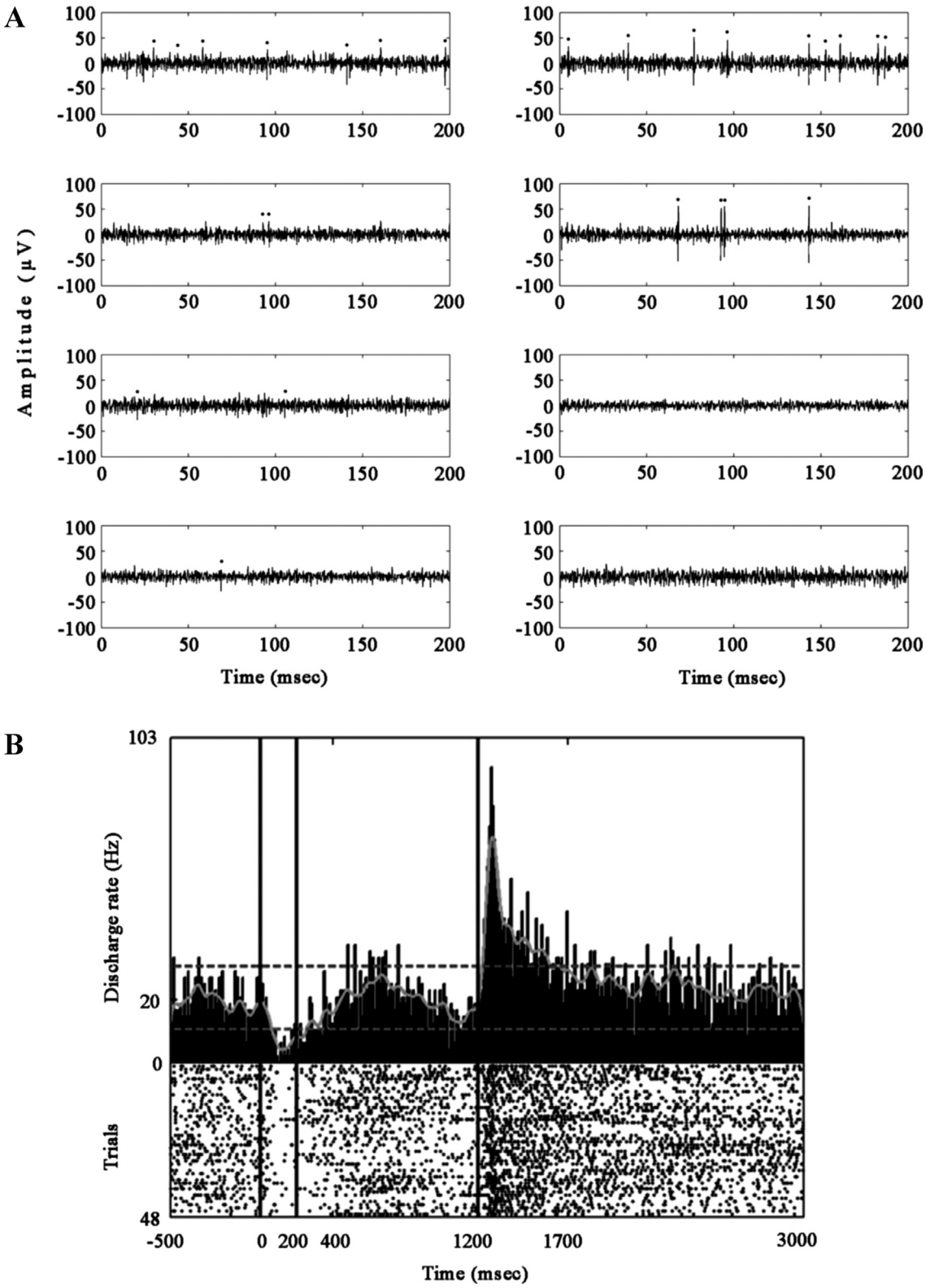

Fig. 4. Visual electrophysiological recordings. (A) shows the band pass filtered (from 300 Hz to 3000 Hz) neuronal activities from the eight electrodes implanted in the caudate nucleus. This recording was performed 433 days after the implantation of the wire-electrodes. The black points above the raw signals denote spikes (single cell activity). The abscissa denotes the time and the ordinate shows the amplitude of the electric signal. (B) depicts the peristimulus time histogram (top) and the raster plot (bottom) of the activity of a particular neuron, the spikes of which are marked on the right uppermost plot of (A). The vertical black lines separate the different epochs of the paradigm. Fixation period (−500 to 0 ms), random static dot stimulation (0 to 200 ms), optic flow (200 to 1200 ms) and reward (1200 to 1700 ms). The cat had to maintain fixation from the appearance of the fixation point (−500 ms) until the disappearance of the optic flow stimulation (1200 ms). Note the decreased activity during random static dots visual stimulation, and then the increased activity upon successful task completion (reward activity). The abscissa denotes time in milliseconds. The ordinate beside the raster plot denotes the number of the successful trials, while the ordinate beside the peristimulus time histogram shows the activity of the neuron (spikes/s, Hz). The continuous gray line is a smoothed curve of the activity, and the dashed gray lines show the ±2 SD of the average discharge rate.

eye movements of the animals. This also enabled us to detect failed fixation, in which cases the trial was rejected (Fig. 3).

3.2. Chronic visual electrophysiological recordings

Local field potentials and band pass filtered (300 Hz to 3000 Hz) neuronal activities from the CN to static as well as to dynamic visual stimulation were recorded and analyzed (Fig. 4).

4. Discussion

In the last few decades, behaving animal models have gradually gathered ground in neurophysiology, due to their advantages over anesthetized, paralyzed models. Behaving animals can be relatively easily used after brief behavioral training for several experimental purposes, but this is unfortunately not the case in visual and multisensory electrophysiological research. In sensory visual electrophysiology, the investigated structures often exhibit also visuomotor activity (e.g. saccades). This makes a continuous monitoring of eye movements indispensable. Furthermore, to minimize the visuomotor modulation of the recordings, teaching of the animal to fixate accurately is also essential. This is a relatively easy task for primates but requires a lengthy training in non- primate mammals.

Behaving feline models have gone through several stages of development. Since the beginning of the second half of the 20th century, mostly anesthetized, paralyzed cats were used in the investigation of the primary visual (striate) cortex, but in the first years some experiments were performed with behaving, unrestrained cats, too (Griffith and Horn, 1963; Hubel, 1959). In the next experiments, behaving cats were placed in a restraining box and they could put out their head through a small hole. The cats were in this position during the experiments. The head- and eye-movements were not controlled (Berkley, 1970; Blake et al., 1974; Franklin et al., 1975). Strecker et al. (1985) used freely moving cats, which were placed in a sound-attenuated behavioral chamber, however, also without eye control. Stryker and Blakemore (1972) took a step further, fixated the body and head of the cat with a canvas bag on a platform, and the eye movements were put under video surveillance. For some time, the scleral magnetic search coils developed for primates were utilized (Fuchs and Robinson, 1966; Judge et al., 1980; Robinson, 1963), but later they were adapted to cats (Huxlin and Pasternak, 2004; Pigarev and Levichkina, 2011; Pigarev and Rodionova, 1998; Populin and Yin, 1998, 2002; Tollin et al., 2005).

In the present study we give a detailed description a new feline model for chronic visual electrophysiology recordings. Our model apparently yields at least two hours recording time per day throughout several years from the same animal, with continuous eye movement control and stable head position. The head was restrained in some earlier used feline models, too (Hubel, 1959; Huxlin and Pasternak, 2004; Pigarev and Levichkina, 2011; Pigarev and Rodionova, 1998; Populin and Yin, 1998, 2002; Tollin et al., 2005), and some form of eye movement control was also present in other studies (e.g. Stryker and Blakemore, 1972), but to our knowledge we have been the first to utilize this whole range of methods at the same time. That is, in our model, the cats have to tolerate a canvas bag around their body, being in a suspended position, head restraint and also a scleral search coil. The suspended position is a further novelty as compared to earlier feline models where the cat was placed either in a box/on a trolley (Pigarev and Levichkina, 2011; Pigarev and Rodionova, 1998) or in a canvas bag on a platform (Huxlin and Pasternak, 2004; Populin and Yin, 1998, 2002; Tollin et al., 2005). It must be added that we experimented with the lying position too, but the animals either tolerated this poorly for longer periods, or simply fell asleep. We found the suspended position superior both in terms of its tolerability for the animals and handling.

Our fixation training method also proved to be successful. At the end of the training sessions, our first cat was able to keep fixation in a ±2.5°, square acceptance window, while the second one performed even better (±1.5°). This means a more rigorous control of eye movements, and possibly more accurate recordings than in some previous studies. Populin and Yin (1998, 2002) ±7.5° and ±5° square fixation acceptance windows for auditory, and for visual stimulation, respectively. Pigarev and Rodionova (1998) and Pigarev and Levichkina (2011) used a comparable, ±2° square acceptance window. It is true that Huxlin and Pasternak (2004) used a smaller, round fixation acceptance window of a diameter of 1.5°, but gave mainly the summarized and subjective account of the neuronal activities and not recorded the activity of the single cells from trial to trial. Our acceptance window was ±2.5° in the case of the first cat and ±1.5° in the case of the second cat. During these rigorous conditions the cats were able to hold the fixation in these small windows even during the optic flow dynamic visual stimulation. Optimal fixation, laborious behavioral training and the eight implanted wire-electrodes therefore made it possible to record visually evoked signals from the awake feline brain. Recordings in the two cats have been going on for over two years now, and stable signals of good quality are recorded. Thus we propose that the demonstrated model is an optimal behaving model for chronic, cell-level visual electrophysiological recordings.

Acknowledgements

We would like to thank Gabriella Dósai for her help in the training of the cats, to Alice Rokszin for her participation in the initial operative procedures, to Antal Berényi for his valuable help in data analyses and to Tamás Puskás for his participation in some experiments. The work was supported by OTKA/Hungary Grants: 83810, 75156 and TÁMOP/Hungary Grant 4.2.2.A-11/1/KONV-2012-0052. T. Nagypál is a fellow of Talentum Foundation of the Gedeon Richter Plc.

References

Berkley MA. Visual discrimination in the cat. In: Stebbins WC, editor. Animal Psychophysics the design and conduct of sensory experiments. New York: AppletonCentury-Crofts; 1970.
Blake R, Cool SJ, Crawford ML. Visual resolution in the cat. Vision Res 1974;14:1211–7.
Franklin KB, Jacobson SG, McDonald WI. Proceedings: The visual acuity of the cat. J Physiol 1975;252:49P–50P.
Fuchs AF, Robinson DA. A method for measuring horizontal and vertical eye movement chronically in the monkey. J Appl Physiol 1966;21:1068–70.
Gombkoto P, Berenyi A, Nagypal T, Benedek G, Braunitzer G, Nagy A. Co-oscillation and synchronization between the posterior thalamus and the caudate nucleus during visual stimulation. Neuroscience 2013;242:21–7.
Griffith JS, Horn G. Functional coupling between cells in the visual cortex of the unrestrained cat. Nature 1963;199:876–95, PASSIM.
Harris KD, Henze DA, Csicsvari J, Hirase H, Buzsaki G. Accuracy of tetrode spike separation as determined by simultaneous intracellular and extracellular measurements. J Neurophysiol 2000;84:401–14.
Hazan L, Zugaro M, Buzsaki G. Klusters, NeuroScope, NDManager: a free software suite for neurophysiological data processing and visualization. J Neurosci Methods 2006;155:207–16.
Hikosaka O, Takikawa Y, Kawagoe R. Role of the basal ganglia in the control of purposive saccadic eye movements. Physiol Rev 2000;80:953–78.
Hubel DH. Single unit activity in striate cortex of unrestrained cats. J Physiol 1959;147:226–38.
Hubel DH, Wiesel TN. Integrative action in the cat's lateral geniculate body. J Physiol 1961;155:385–98.
Hubel DH, Wiesel TN. Receptive fields, binocular interaction and functional architecture in the cat's visual cortex. J Physiol 1962;160:106–54.
Huxlin KR, Pasternak T. Training-induced recovery of visual motion perception after extrastriate cortical damage in the adult cat. Cereb Cortex 2004;14:81–90.
Judge SJ, Richmond BJ, Chu FC. Implantation of magnetic search coils for measurement of eye position: an improved method. Vision Res 1980;20:535–8.

Korshunov VA. Miniature microdrive for extracellular recording of neuronal activity in freely moving animals. J Neurosci Methods 1995;57:77–80.
McKown MD, Schadt JC. A modification of the Harper-McGinty microdrive for use in chronically prepared rabbits. J Neurosci Methods 2006;153:239–42.
Munoz DP, Fecteau JH. Vying for dominance: dynamic interactions control visual fixation and saccadic initiation in the superior colliculus. Prog Brain Res 2002;140:3–19.
Nagy A, Eordegh G, Paroczy Z, Markus Z, Benedek G. Multisensory integration in the basal ganglia. Eur J Neurosci 2006;24:917–24.
Nagy A, Paroczy Z, Markus Z, Berenyi A, Wypych M, Waleszczyk WJ, Benedek G. Drifting grating stimulation reveals particular activation properties of visual neurons in the caudate nucleus. Eur J Neurosci 2008;27:1801–8.
Pigarev IN, Levichkina EV. Distance modulated neuronal activity in the cortical visual areas of cats. Exp Brain Res 2011;214:105–11.
Pigarev IN, Rodionova EI. Two visual areas located in the middle suprasylvian gyrus (cytoarchitectonic field 7) of the cat's cortex. Neuroscience 1998;85:717–32.
Populin LC, Yin TC. Behavioral studies of sound localization in the cat. J Neurosci 1998;18:2147–60.
Populin LC, Yin TC. Bimodal interactions in the superior colliculus of the behaving cat. J Neurosci 2002;22:2826–34.
Robinson DA. A method of measuring eye movement using a scleral search coil in a magnetic field. IEEE Trans Biomed Eng 1963;10:137–45.
Stein BE. Neural mechanisms for synthesizing sensory information and producing adaptive behaviors. Exp Brain Res 1998;123:124–35.
Strecker RE, Steinfels GF, Abercrombie ED, Jacobs BL. Caudate unit activity in freely moving cats: effects of phasic auditory and visual stimuli. Brain Res 1985;329:350–3.
Stryker M, Blakemore C. Saccadic and disjunctive eye movements in cats. Vision Res 1972;12:2005–13.
Tollin DJ, Populin LC, Moore JM, Ruhland JL, Yin TC. Sound-localization performance in the cat: the effect of restraining the head. J Neurophysiol 2005;93:1223–34.
Villeneuve MY, Casanova C. On the use of isoflurane versus halothane in the study of visual response properties of single cells in the primary visual cortex. J Neurosci Methods 2003;129:19–31.

II.

PLOS ONE

RESEARCH ARTICLE

Activity of Caudate Nucleus Neurons in a Visual Fixation Paradigm in Behaving Cats

Tamás Nagypál[1], Péter Gombkötő[2], Balázs Barkóczi[1], György Benedek[1], Attila Nagy[1]*

1 Department of Physiology, Faculty of Medicine, University of Szeged, Szeged, Hungary, **2** Center for Molecular and Behavioral Neuroscience Rutgers University, Newark, New Jersey, United States of America

* nagy.attila.1@med.u-szeged.hu

Citation: Nagypál T, Gombkötő P, Barkóczi B, Benedek G, Nagy A (2015) Activity of Caudate Nucleus Neurons in a Visual Fixation Paradigm in Behaving Cats. PLoS ONE 10(11): e0142526. doi:10.1371/journal.pone.0142526

Editor: Maurice J. Chacron, McGill University, CANADA

Received: September 17, 2015

Accepted: October 22, 2015

Published: November 6, 2015

Data Availability Statement: All relevant data are within the paper and its Supporting Information files.

Funding: Funded by Hungarian Brain Research Program Grant KTIA_13_NAP-A-I/15 (AN) (http://www.agykutatas.com/); OTKA/Hungary Grant 83810. (http://www.otka.hu/) (GB). T. Nagypál was a fellow of Talentum Foundation of the Gedeon Richter Plc. (https://www.richter.hu/hu-HU/felelossegvallalas/alapitvanyok/Pages/Richter-Gedeon-Talentum-Alapitvany.aspx). The funders had no role in study design, data collection and analysis, decision to publish, or preparation of the manuscript.

Abstract

Beside its motor functions, the caudate nucleus (CN), the main input structure of the basal ganglia, is also sensitive to various sensory modalities. The goal of the present study was to investigate the effects of visual stimulation on the CN by using a behaving, head-restrained, eye movement-controlled feline model developed recently for this purpose. Extracellular multielectrode recordings were made from the CN of two cats in a visual fixation paradigm applying static and dynamic stimuli. The recorded neurons were classified in three groups according to their electrophysiological properties: phasically active (PAN), tonically active (TAN) and high-firing (HFN) neurons. The response characteristics were investigated according to this classification. The PAN and TAN neurons were sensitive primarily to static stimuli, while the HFN neurons responded primarily to changes in the visual environment i.e. to optic flow and the offset of the stimuli. The HFNs were the most sensitive to visual stimulation; their responses were stronger than those of the PANs and TANs. The majority of the recorded units were insensitive to the direction of the optic flow, regardless of group, but a small number of direction-sensitive neurons were also found. Our results demonstrate that both the static and the dynamic components of the visual information are represented in the CN. Furthermore, these results provide the first piece of evidence on optic flow processing in the CN, which, in more general terms, indicates the possible role of this structure in dynamic visual information processing.

Introduction

The basal ganglia, which are components of cortical and subcortical loops in the mammalian brain [1] are strongly involved in sensorimotor functions. It is assumed that for the eliciting of the normal motor behavior in response to sensory information from the environment the basal ganglia are essential. Thus it comes as no surprise that the CN neurons are sensitive to various modalities of visual stimulation [2–9]. Beside the characterization of classical visual receptive field properties of the CN neurons [5, 10] their responsiveness to extended visual stimuli was also investigated [11, 12]. They were markedly sensitive to very low spatial and high temporal frequencies and exhibited narrow temporal and spatial frequency tuning. These characteristics suggest that these neurons can be involved in the processing of dynamic visual information

Competing Interests: The authors have declared that no competing interests exist.

[12–14]. An especially relevant dynamic aspect of the incoming visual information is the apparent motion of the environment during self-motions, that is, optic flow. Logical as this question might be, so far it has not been investigated if it is possible to activate CN neurons directly by an optic flow stimulus, while a positive answer could throw new light on the CN as an important structure of dynamic visual processing during self-motion. For that reason, the first question we ask in this study is whether such a direct activation is possible.

Neuroanatomical studies revealed several distinct neuron groups in the CN. Of these, medium spiny neurons, GABAergic interneurons and cholinergic interneurons are the most often observed [15]. Similarly, electrophysiological studies in rodents and primates described three large groups based on the recorded neurons' electrophysiological properties: phasically active (PAN), high-firing (HFN) and tonically-firing (TFN) neurons [16–20]. It is known from these studies that there is a strong correspondence between the anatomical and electrophysiological clusters. PANs correspond to the medium spiny projection neurons, HFNs to the GABAergic interneurons and the TFNs to the cholinergic interneurons [21–28]. The second question raised by the present study is whether the same or a similar classification is possible in the feline brain.

To answer the questions raised above, we used behaving, head-restrained eye movement-controlled cats trained for chronic visual electrophysiological recordings [29] in a behavioral paradigm. We categorized the neurons of the feline CN according their electrophysiological properties in different functional clusters and analyzed their responsiveness to static as well optic flow visual stimuli.

Materials and Methods

Experiments were carried out on two adult feline domestic cats (2.6 kg and 3.25 kg). Cats were trained for the applied visual fixation task. All experimental procedures were carried out to minimize the number and the discomfort of the animals involved and followed the European Communities Council Directive of 24 November 1986 (86 609 EEC) and the National Institutes of Health guidelines for the care and use of animals for experimental procedures. The experimental protocol was accepted and approved by the Ethics Committee for Animal Research of the University of Szeged (No: I-74-24/2012).

Animal Preparation and Surgery

The animals were initially anesthetized with ketamine hydrochloride (Calypsol (Gedeon Richter®), 30 mg/kg i.m). To reduce salivation and bronchial secretion, a subcutaneous injection of 0.2 ml 0.1% atropine sulphate was administered preoperatively. A cannula was inserted in the femoral vein and after intubation of the trachea the animals were placed in a stereotaxic headholder. All wounds and pressure points were treated regularly with local anesthetic (1%, procaine hydrochloride). Throughout the surgery the anesthesia was maintained with 1.5% halothane in a 2:1 mixture of N_2O and oxygen. The depth of anesthesia during the surgery was monitored by continuously checking the end-tidal halothane concentration and heart rate (electrocardiogram). The end-tidal halothane concentration, MAC values and the peak expired CO_2 concentrations were monitored with a capnometer (CapnomacUltima, Datex-Ohmeda, ICN). The O_2 saturation of the capillary blood was monitored by pulse oxymetry. The minimum alveolar anesthetic concentration (MAC) values calculated from the end-tidal halothane readings were kept in the range recommended by Villeneuve and Casanova [30]. The peak expired CO_2 concentration was kept within the range 3.8–4.2% by adjusting the respiratory rate or volume. The body temperature of the animal was maintained at 37°C by a computer-controlled, warm-water heating blanket. Craniotomy was performed with a dental drill to

allow a vertical approach to the target structures. The dura mater was preserved, and the skull hole was covered with a 4% solution of 37°C agar dissolved in Ringer's solution. Then a reclosable plastic recording chamber (Ultem 1000, internal diameter = 22.5mm) was mounted on the skull. Following this, the eight electrodes were implanted in the brain with the help of an adjustable microdrive system (a modified Harper-McGinty microdrive for the first animal (see McKown and Schadt, [31]) and a modified Korshunov microdrive for the second animal [32]). In order to control the eye movements, a scleral search coil was implanted into the right eye [33]. To restrain the head of the animal during the experiments, a stainless steel headholder was cemented on the skull. All surgical procedures were carried out under aseptic conditions. Before the surgical procedure, antibiotic prophylaxis was applied (1000 mg ceftriaxon, i.m., Rocephin 500 mg (Roche®)). The first five postoperative days, 50 mg/kg i.m. antibiotic was provided. Nalbuphin and non-steroidal anti-inflammatory drugs were administered until the seventh postoperative day.

Brief Description of the Behavioral Training of the Animals

When the cat got accustomed to the laboratory environment, it was carefully clothed into a canvas harness. First, we lifted the animal manually only a few centimeters from the floor. When the clothed animal got used to being suspended, it was gradually introduced to the experimental stand. The experimental stand is a cubical structure with each side open, in which the suspension harness is fastened at two points in by a rope pulley block. The head of the suspended cat was fixed to the stereotaxic frame by the implanted steel headholder with two stainless steel bars. The stereotaxic frame was placed within an electromagnetic field, which is generated by metal coils, installed into the wall of the stand. The animal was trained to perform fixation during recordings of neuronal activities to different kind of visual stimulation. If a trial of the task was completed without the breaking the fixation the animal received mashed food reward through a plastic tube, dosed by a computer-driven hydraulic pump installed outside the magnetic field. The behavioral training and later the recording sessions lasted approximately 2 hours per a day, four to five times during a week. The weight of the animals was checked regularly and was kept at least 90% of the initial value. The detailed description of the implantation and the behavioral training of the animal can be found in our recent methodological paper [29].

Behavioral Paradigm and Visual Stimulation

For visual stimulation and the projection of the fixation point a standard 17- inch CRT monitor (refresh rate: 100 Hz) was placed in front of the animal, at a distance of 57 cm. During the recordings the effect of the eye movements on the neuronal activity has to be controlled for, so the cats were trained to perform visual fixation during the visual stimulation. For this, a fixation point was projected on the center of the CRT monitor. The size of the fixation point was 0.8° in diameter. The animal had to look at the fixation point and keep its gaze within a square fixation acceptance window during the trials of the visual fixation task. The size of the acceptance window was 5°. The stimulation task was initiated by the animal, by keeping fixation in the acceptance window for 500 ms. Two sorts of stimuli were applied: first a static random dot pattern, which was followed by an optic flow stimulus. The size of the stimulation screen was 40.5 ° by 30.5 °. The size of each dot in both the static and the dynamic stimulus was 0.1° in diameter. The speed of dot movement in the optic flow increased from 0 to 7°/sec toward the periphery of the stimulation screen. The stimuli were generated using a custom made script prepared in the Psychtoolbox of Matlab®.

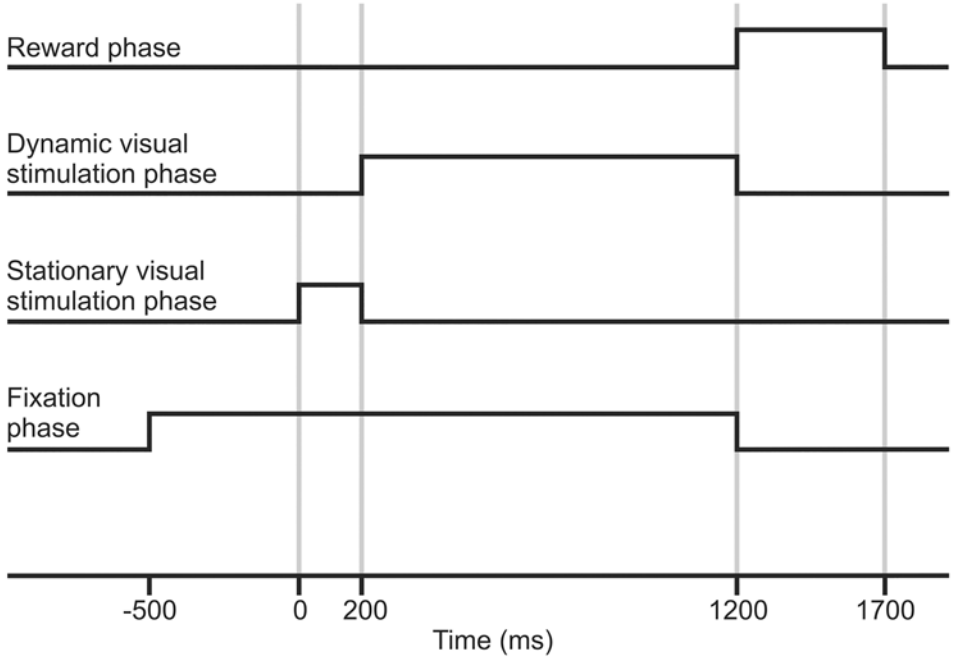

Fig 1. Schematic representation of the phases of the behavioral paradigm. At the beginning of the trial the cat has to direct its gaze to a green fixation point projected in the center of a CRT monitor (refresh rate 100 Hz). Then, the animal has to maintain fixation within an acceptance window for 500 ms (fixation phase). If the fixation phase is successfully accomplished, a static random dot pattern appears (at 0 ms), and it remains on the screen for 200–500 ms (static stimulation phase). After this, the dots of same static pattern start to move coherently in a radial center-in or center-out direction (optic flow, dynamic stimulation phase, 1000 ms). As can be seen in the figure, the animal has to hold fixation throughout the stimulation phases. If it manages to do so, the trial is accepted, and the animal is rewarded with a few drops of mashed cat food (reward phase, 500 ms).

doi:10.1371/journal.pone.0142526.g001

Fig 1 is a schematic representation of a single trial of the applied behavioral visual fixation paradigm. To minimize the influence of eye movements on the neuronal activity, the animal had to hold fixation during the trials. A trial was immediately aborted if the animal broke fixation, and in this case no reward was given. Any single trial consisted of the following phases:

1. Fixation phase: a green fixation point appeared in the center of the stimulation screen. In this phase the cat had to direct its gaze to the fixation point and keep fixation in a pre-determined fixation window (see above) for 500 ms. The accomplishment of this initiated the next phase.
2. Static stimulation phase (200–500 ms): immediately after the successful completion of the fixation phase, a static random dot pattern appeared in the visual field.
3. Dynamic stimulation phase (1000 ms): the dots of the static pattern began to move radially (optic flow). The dots moved either toward the periphery of the screen (center-out optic flow) or toward the center of the screen (center-in optic flow).
4. Reward phase (500 ms post stimulation) and intertrial interval (4000–10000 ms): If the cat managed to maintain fixation throughout all the stimulation phases of a single trial, a few drops of pulpy food reward was given and we considered the trial as a correct one. This phase was longer, so that the cat could eat the reward without muscle activity interfering with the recordings of the next trial. The actual recordings started when the cats reached a

stable 80% efficiency in fixation maintenance in the training sessions. The recordings took place in a dark laboratory room (background luminance: 0.5 cd/m^2). The luminance of the stimulus was 5 cd/m^2 (Mavolux 5032C, GOSSEN Foto- und Lichtmesstechnik GmbH, Germany). The computer-controlled trials (either with center-out or center-in optic flow) were presented in a random order. A recording session was considered successful (and the data included in the analysis) if the cat performed at least 30 correct trials to center-out and also to center-in optic flow stimuli.

Recording and Data Analysis

Extracellular multielectrode recordings were carried out with eight implanted parylene isolated platinum-iridium wire-electrodes (diameter: 25 μm) from the first cat and with eight implanted formvar insulated Nickel-Chrome wire-electrodes (diameter: 50 μm) from the CN of the second cat. The position of the guiding tube (diameter = 0.65 mm), which contained the wire-electrodes during implantation, was anterior 13 and lateral 5.5 mm according to the Horsley-Clarke coordinates. The position of the single wire-electrodes ranged between anterior 12.5–14 mm, lateral 4.5–6 mm at stereotaxic depths between 9 and 13.5 mm. At the end of the experiments, the first animal was deeply anesthetized with pentobarbital (200 mg/kg i.v.) and perfused transcardially with 4% paraformaldehyde solution. The brain was removed and cut into coronal sections of 40 μm, and the sections were stained with DAPI (4',6-diamidino-2-phenylindole, Sigma-Aldrich Co., USA). Recording sites were localized on the basis of the marks of the electrode penetrations.

Amplified neuronal activities were band-pass filtered (300 to 5000 Hz). The raw data were first processed by NeuroScope, NDManager, KlustaKwik and then broken down into single unit signals by the use of Klusters [34, 35] under manual control.

We intended to classify the CN neurons in functional groups by their electrophysiological properties. It is known from rat and primate studies that spontaneous activity, the proportion of the summed values over 2 seconds divided by the total session time in the interspike intervals ($propISI_{>2sec}$), and the shape of the autocorrelogram at different time resolutions (100ms, 1000 ms) can be used to classify the CN neurons in different groups [16, 18]. The above mentioned electrophysiological parameters were calculated for each recorded CN unit. The spontaneous discharge rate of each neuron was calculated based on the last 3000 ms period of the intertrial intervals. In this way, the recorded neurons could be classified in three groups (Fig 2): PANs are characterized by peaky autocorrelogram and ISI values over 2 seconds. The $propISI_{>2sec}$ was usually higher than 0.5, and the spontaneous discharge rate was low, in most cases under 3 spikes/sec. The HFNs have autocorrelograms with a blunt peak, the $propISI_{>2sec}$ is lower than 0.5, and the spontaneous discharge rate is higher than 5 spikes/sec. Finally, TANs are characterized by a deep gap in the autocorrelogram, the $propISI_{>2sec}$ is lower than 0.5, and the spontaneous discharge rate is between 2 and 12 spikes/sec.

Firing rates during the different phases of the behavioral paradigm (static, dynamic, reward) were compared to the background activity, which was measured in the last 3000 ms period of the intertrial interval, with the Mann-Whitney rank-sum test. We considered the neuronal activity as response if the stimulated activity in a particular phase or phases of the paradigm was significantly different ($p<0.05$) from the background activity. Similarly, the comparison between discharge rate of each optic-flow sensitive single neuron in response to center-in and center-out optic flow stimuli was performed using Mann-Whitney test. The neuron was considered to be direction sensitive if the difference between the responses to center-in and center-out stimulation was significant ($p<0.05$). We also calculated the net firing rate of each unit by subtracting their background activity from the summed firing of the neurons. The background

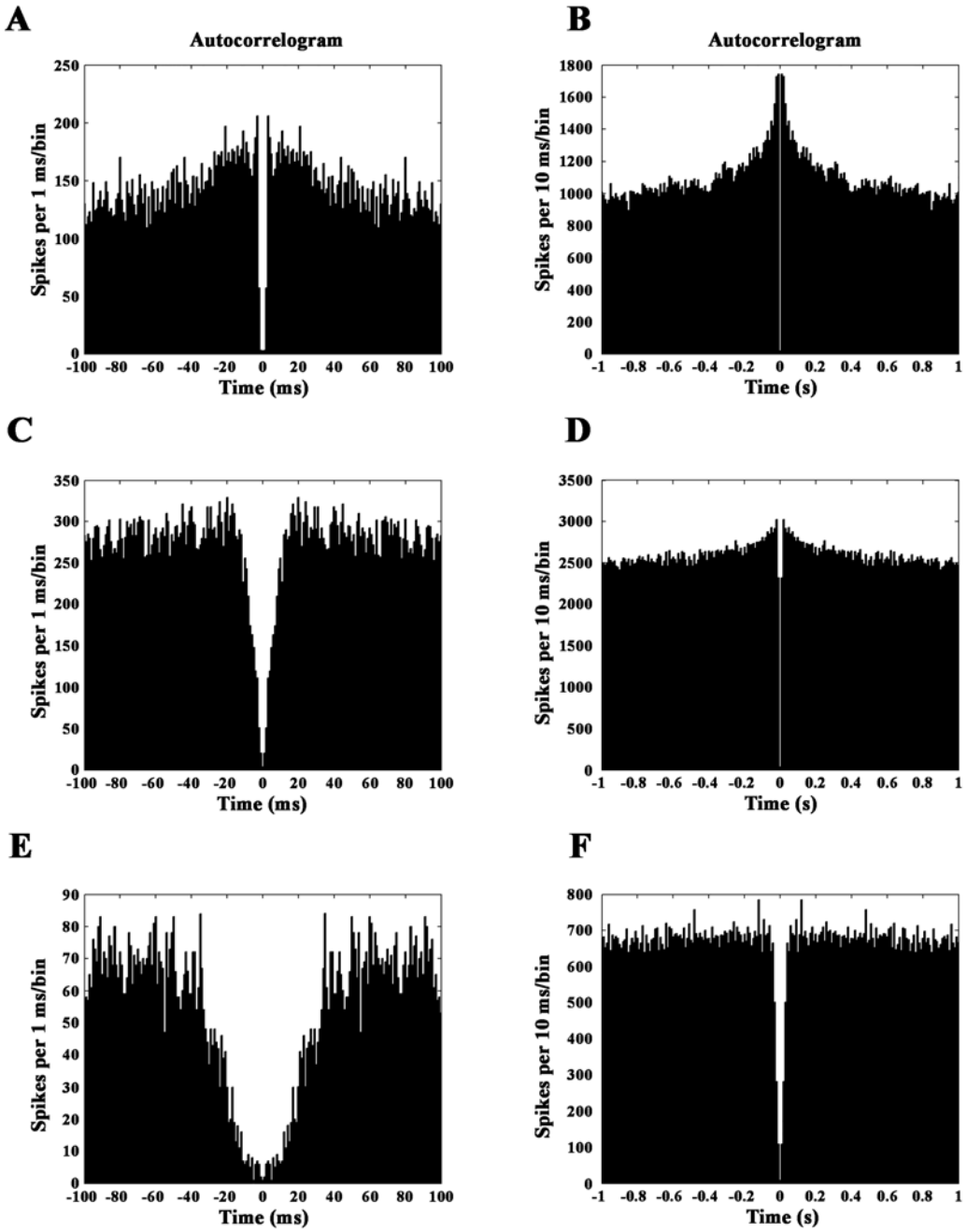

Fig 2. Autocorrelograms of the CN neurons. Neurons were classified on the basis of the shape of their autocorrelograms (at 100 ms and 1000 ms time resolutions), prop$ISI_{>2sec}$ and the background discharge rate in three big groups (PAN, HFN, TAN). Neurons belonging to each group have characteristic autocorrelogram. PANs are usually characterized by peaky autocorrelogram (A,B). HFNs have autocorrelograms with a blunt peak (C,D) and TANs are characterized by a deep gap in the autocorrelogram (E,F).

doi:10.1371/journal.pone.0142526.g002

activities and the net firing rates of different CN neuron subpopulations (PAN, HFN and TFN) in different epochs of the paradigm were compared by one-way analysis of variance (ANOVA). In the case of significant variance ($p<0.05$) Tukey's HSD analysis was performed to find the significantly different CN neuron subpopulation. All statistical analyses were performed in Matlab® (MathWorks Inc., Natick, MA).

Table 1. The number of responsive CN neurons by the different phases of the applied paradigm.

	Static	Optic flow		Stimulus off	Reward
		center-out	center-in		
Phasically active neurons					
increased activity	26	17	16	1	27
decreased activity	24	2	6	0	6
High-firing neurons					
increased activity	18	16	20	7	30
decreased activity	18	9	8	1	0
Tonically active neurons					
increased activity	11	3	5	0	6
decreased activity	2	1	1	1	0

doi:10.1371/journal.pone.0142526.t001

Eye movements were monitored and recorded with a search coil system (DNI Instruments, Newark, DE, USA) at a sampling rate of 250 Hz, and these were processed by a custom software written under Matlab®.

The recording of the eye movements, stimulus presentation, reward delivery, and data collection were also coordinated by a custom software via 16 channels National Instrument Card DAQ®.

Results

Altogether 346 units were recorded from the CN. The primary aim of the present study was to describe the visual response characteristics of the CN neurons. Based on their electrophysiological properties (see in methods), we could group the recorded CN neurons in three major clusters: PANs (221 neurons), HFNs (88 neurons) and TANs (28 neurons). Our secondary aim was to compare the response characteristics of these neuronal functional groups. Table 1 summarizes the responsivenes of the different CN neuron clusters. Because of the very low spontaneous discharge rate (below 1 spike/second), we excluded 135 PANs from the further analysis. Further nine CN neurons were excluded from the analysis, because it was not possible to classify them as belonging to any of the three major clusters. After all the exclusions, responses from 202 neurons were analyzed. The responsive CN neurons showed mainly increased firing rate, while decreased activity was also found during the different phases of the visual behavioral paradigm. Significant changes in the activity of the CN neurons were recorded not only during the actual visual stimulation. In line with earlier studies [36], reward-related neuronal responses were also recorded shortly before and during the reward period (provided that the task was successfully completed).

In the following we are describing the stimulus-related response characteristics of the functional clusters.

Response Characteristics of the Phasically Active Neurons

After the exclusion of the neurons that exhibited spontaneous activity lower than 1 spike/s, the response characteristics of 86 PANs were analyzed. The mean spontaneous discharge rate was 2.93 spikes/sec (SD: ±2.18). Overall, the visual responses of the PANs were moderate or weak (Table 2). During static visual stimulation, significant activity change was observed in 50

Table 2. The net discharge rates (spikes/sec) of the PANs, HFNs and TANs by the different phases of the applied paradigm.

	Phasically active neurons					
	N	Mean	Median	SD	Min	Max
Background activity	86	2.93	2.34	2.18	0.97	8.88
Static						
increased activity	26	1.91	0.72	3.34	0.23	16.51
decreased activity	24	0.55	0.44	0.52	0.06	1.43
Optic flow:center-out						
increased activity	17	0.94	0.87	0.48	0.38	1.92
decreased activity	2	0.37	0.37	0.13	0.28	0.46
Optic flow:center-in						
increased activity	16	1.34	1.04	0.90	0.41	3.60
decreased activity	6	0.88	0.88	0.33	0.50	1.32
Reward						
increased activity	27	3.11	2.14	2.65	0.53	10.09
decreased activity	6	0.38	0.18	0.47	0.12	1.32
	High-firing neurons					
	N	Mean	Median	SD	Min	Max
Background activity	88	14.45	12.85	6.81	4.67	37.91
Static						
increased activity	18	8.51	7.92	4.51	1.80	19.52
decreased activity	18	3.18	1.88	3.75	0.45	15.91
Optic flow:center-out						
increased activity	16	5.34	4.47	3.80	0.99	14.48
decreased activity	9	1.13	1.12	0.57	0.29	1.77
Optic flow:center-in						
increased activity	20	4.56	3.51	3.63	0.30	12.84
decreased activity	8	0.79	0.85	0.38	0.24	1.33
Reward						
increased activity	30	9.57	7.06	7.05	1.82	32.65
decreased activity	0	-	-	-	-	-
	Tonically active neurons					
	N	Mean	Median	SD	Min	Max
Background activity	28	5.24	5.81	2.37	1.26	10.11
Static						
increased activity	11	1.69	1.20	1.49	0.43	4.83
decreased activity	2	0.23	0.23	0.23	0.06	0.39
Optic flow:center-out						
increased activity	3	1.24	1.36	0.23	0.98	1.38
decreased activity	1	0.21	-	-	-	-
Optic flow:center-in						
increased activity	5	0.97	0.98	0.59	0.32	1.85
decreased activity	1	0.81	-	-	-	-
Reward						
increased activity	6	2.89	1.86	3.79	0.24	9.91
decreased activity	0	-	-	-	-	-

Increased activities are given as net values after the subtraction of the background activity from the gross activity. Decreased activities are given as absolute values of the net changes.

doi:10.1371/journal.pone.0142526.t002

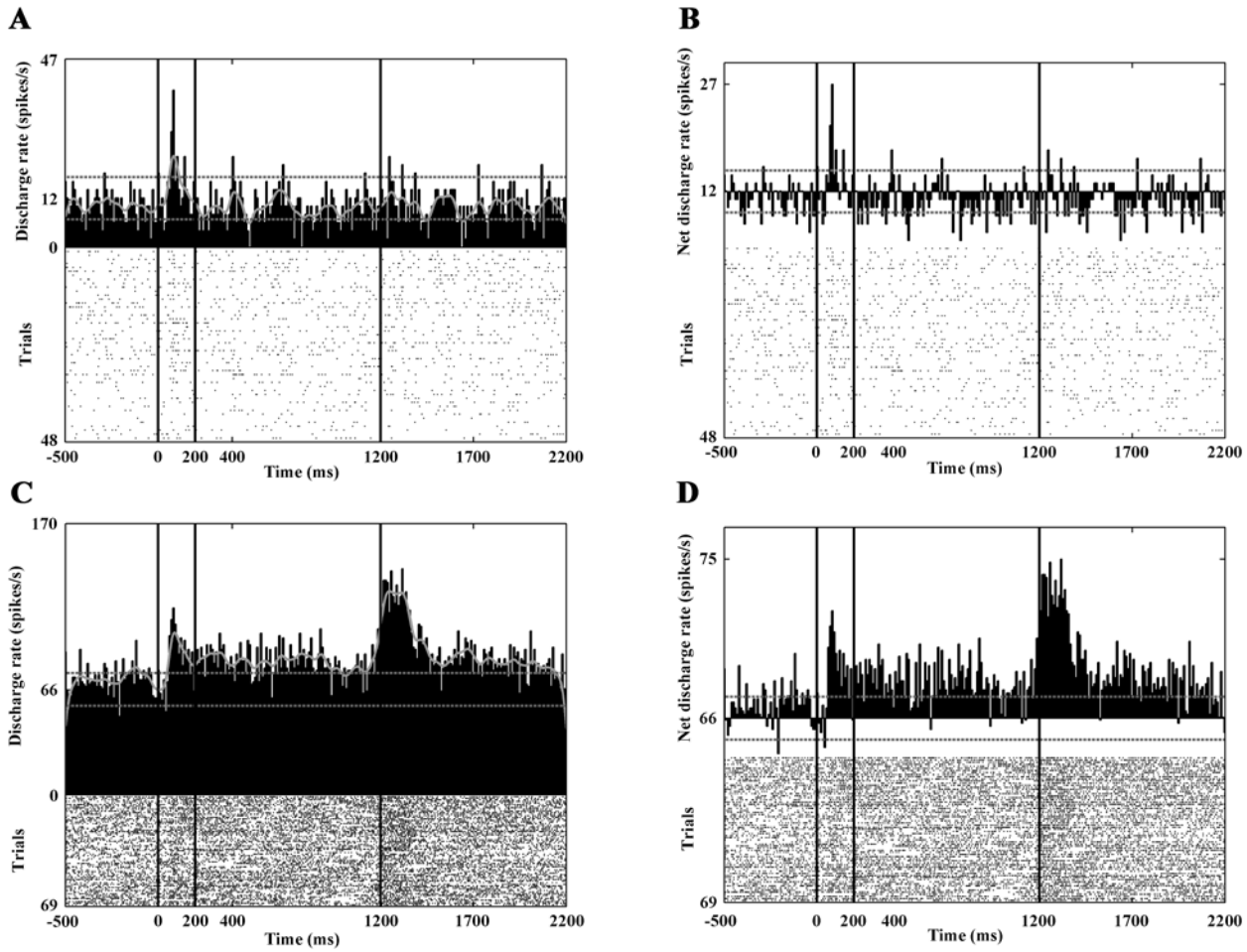

Fig 3. Response characteristics of the CN neurons to static visual stimulation. Each panel of the figure contains a PSTH (top) and a raster plot (bottom) to represent the activity of a neuron. Panels A and B show the activity of a PAN, panels C and D show the firing pattern of a HFN. A and C show the gross activities, B and D show the net activity change after the subtraction of the background activity. The vertical black lines denote the boundaries between the different phases of the paradigm: fixation phase (-500 to 0 ms), static visual stimulation (0 to 200 ms), dynamic visual stimulation (200 to 1200 ms), reward phase (1200 to 1700 ms). Note the phasic response of the PAN to static stimulation (A,B). The activity pattern of the presented HFN (C,D) is more complex: increased activity can be observed not only to random dot patterns, but also to optic flow and during the reward phase. The abscissa denotes the time in milliseconds. The ordinate denotes the number of successful trials and the activity of the neuron. The lowest number is the number of the successful trials, the next is the average discharge during the whole recording and the highest number is the stimulated activity (Hz). The continuous grey curve is a smoothed curve of the activity, and the dashed grey lines indicate ± 2 SD of the average background discharge rate in the whole recording.

doi:10.1371/journal.pone.0142526.g003

neurons. In 26 cases this meant a significant increase, and in 24 cases a significant decrease was seen. Fig 3A and 3B show the responses of a PAN CN neuron to static visual stimulation.

Twenty-nine neurons showed activity change during dynamic visual stimulation. During the center-out optic flow 17 of them, while during the center-in optic flow 16 of them showed increased activity. In eight cases decreased activity was seen in response to this type of stimulation. The peristimulus time histograms (PSTHs) in Fig 4A and 4B show such a response.

In the reward phase 27 neurons showed significantly increased activity and six of them decreased their discharge rate. The question arises whether this activity is purely reward-related and/or related to the offset of the stimulus. In order to check this, we analyzed the aborted trials too, where the animal had broken the fixation. In this case the stimulus disappeared immediately and the animal got no reward. While the animal has broken the fixation the appearing eye movements

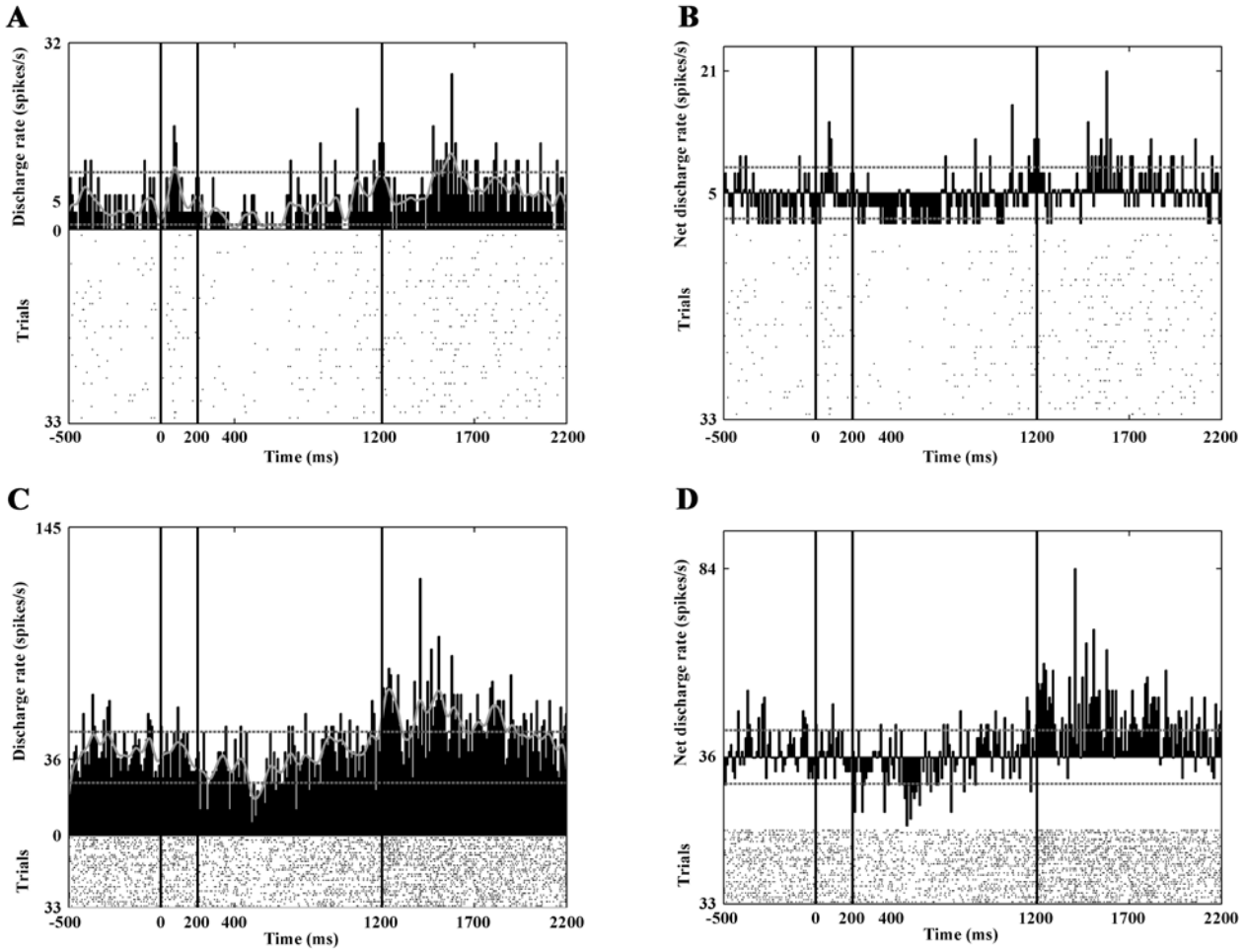

Fig 4. Decreased responses to optic flow stimulation. Panels A and B show the activity of a PAN, panels C and D show the firing pattern of a HFN. Note the marked activity decrement during optic flow stimulation. The conventions are the same as in Fig 3.

doi:10.1371/journal.pone.0142526.g004

could also elicit changes in the neuronal activity. In order to exclude the effects of eye movement-related activity in this case, the correlation between the interspike intervals and the normalized amplitude of the eye movements recorded during the experiment was computed. Fig 5D denotes the result of the linear regression analysis. This clearly shows the lack of connection (ρ^2: 0.02, $p>0.05$) and in this way the absence of eye movement- related activity. Whether the change in activity is reward-related can be told by a simple examination of the PSTHs in relation to the offset of the stimulus: if the response is reward-related, no peak in the PSTH can be observed. If there is a peak in these histograms, the activity is likely to be related to the stimulus offset. Fig 5 shows the activity of a PAN, which responded with increased discharges to the offset of the stimulus.

Response Characteristics of the High-Firing Neurons

Eighty-eight high-firing neurons were analyzed. The mean spontaneous discharge rate was 14.45 spikes/sec (SD: ±6.81). During the static phase 18 neurons increased and 18 neurons decreased their activity significantly (Fig 3C and 3D). Thirty-seven high-firing CN neurons responded to the optic flow stimulus. During the center-out optic flow 16 neurons and during center-in optic flow 20 neurons exhibited increased activity. The visual responses of this group

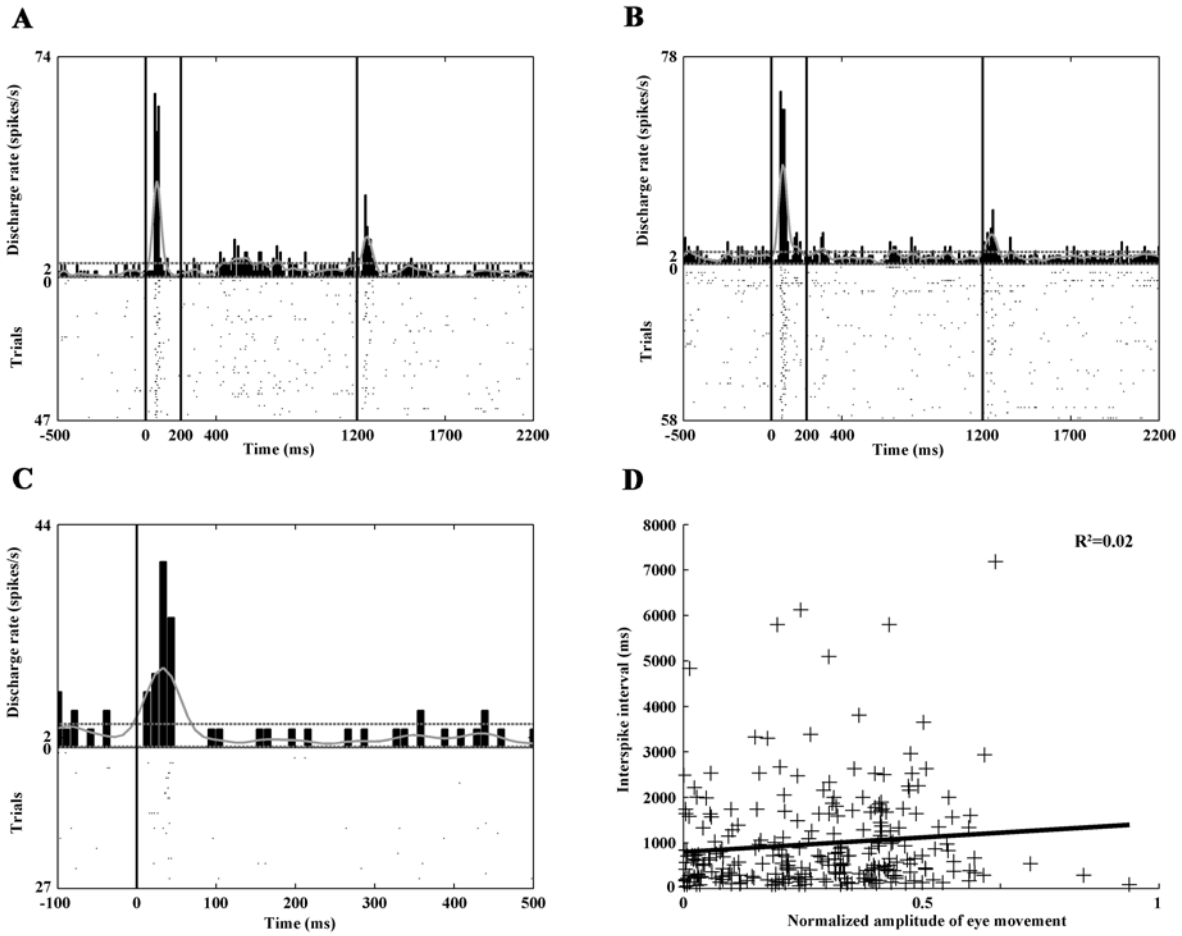

Fig 5. Stimulation-related response of a PAN. The PSTHs in panels A and B show the activity of the neuron in response to stimulation. A: response to center-out optic flow. B: response to center-in optic flow. The response to random dot patterns (A,B), to center-out optic flow (A) but not to center-in (B) and the beginning of the reward phase are readily observable (A,B). The conventions are the same as in Fig 3. In order to decide whether the increased activity at the beginning of the reward phase is purely reward-related or related to stimulus offset, the aborted trials (where the cat had broken the fixation during visual stimulation and therefore got no reward) were also analyzed (C). Panel C is aligned to the time of the breaking of the fixation, which corresponded to the offset of the stimulus because the trial was immediately aborted upon fixation breaking. Note the PSTH peak, which indicates responsiveness to the offset of the stimulus. Furthermore, in order to control for the effects of saccadic activity, the correlation between the interspike intervals and the normalized amplitude of the eye movements recorded during the experiment was computed (D). The linear regression analysis clearly shows the lack of connection (ρ^2: 0.02, $p>0.05$). This means the activity is of no saccadic origin.

doi:10.1371/journal.pone.0142526.g005

are much clearer and stronger than those of the PANs and TANs (Table 2). Fig 4C and 4D and Fig 6 show the responses of three HFNs to optic flow (one cell with decreased and two cells with increased activity).

During the reward phase, 30 neurons increased their activity and none of the high-firing neurons showed significantly decreased activity (Fig 3C and 3D and Fig 7). It was also found that altogether eight of the analyzed HFNs were active (seven of them with increased activity) during the offset of the stimulus. Similarly to the PAN, which was sensitive to the offset of the stimulus the HFNs with offset-related responses showed no eye movement connected activity.

Response Characteristics of the Tonically Firing Neurons

Beside the PANs and HFNs a small number of CN neurons (28) were classified as tonically firing (TAN). The mean spontaneous discharge rate was 5.24 spikes/sec (SD: ± 2.37). During the

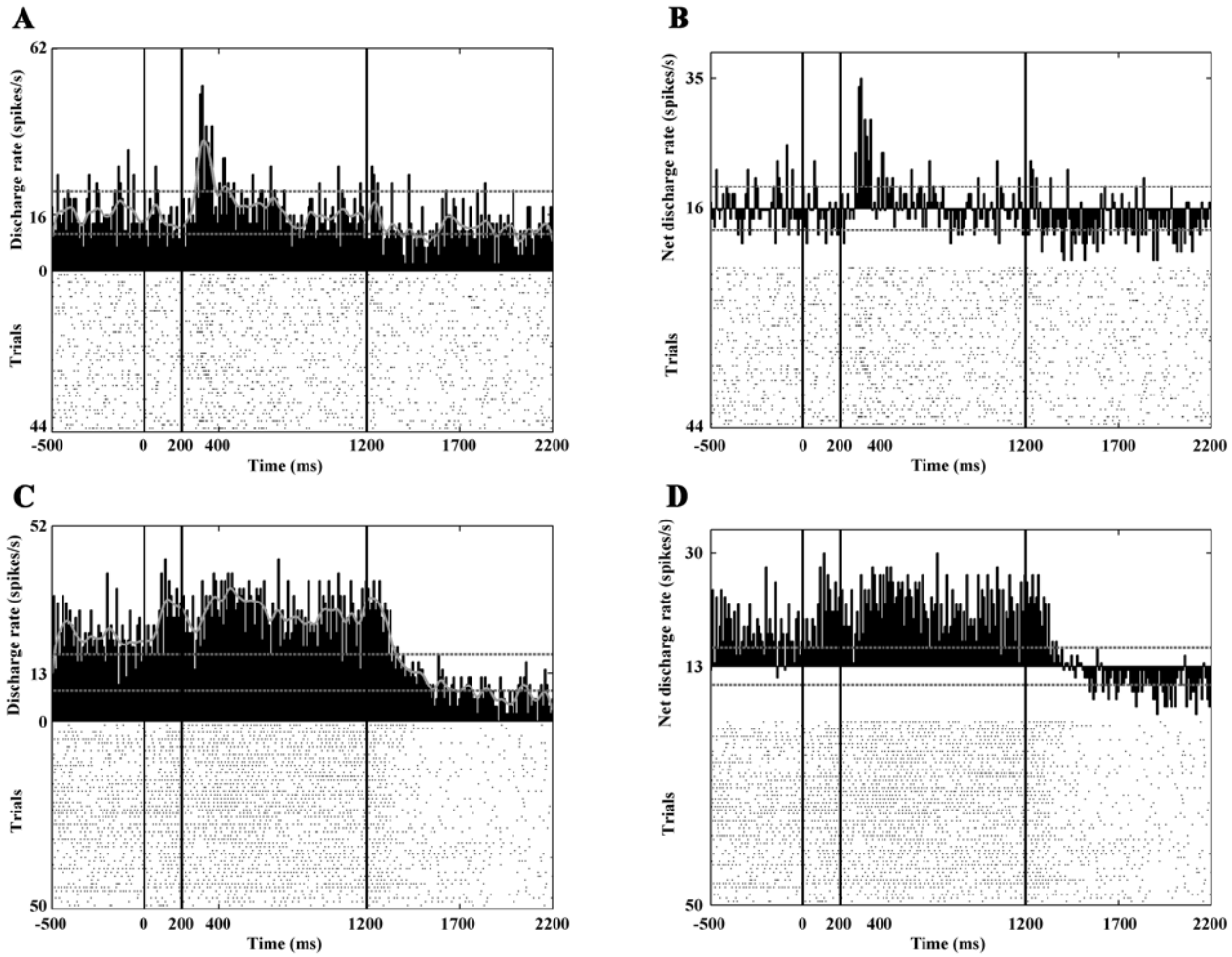

Fig 6. Marked responses to optic flow stimulation. Panels A and B show the activity of a HFN with a characteristic phasic response to the onset of the optic flow. Panels C and D show the responses of another HFN to static as well as to optic flow stimulation. Note the marked responses of these units to optic flow stimulation. The conventions are the same as in Fig 3.

doi:10.1371/journal.pone.0142526.g006

static stimulation phase 11 neurons showed significantly increased and only 2 decreased activity. Seven of them responded by increasing their discharge rate to the optic flow stimulus (3 to the center-out and 5 to the center-in stimulus). The visual responses of the TANs were moderate or weak (Table 2). During the reward phase 6 neurons increased their activity. The offset of the stimulus influenced the activity of only one TAN. Similarly to the PAN and the HFNs, which were sensitive to the offset of the stimulus the TAN with offset-related response showed no eye movement connected activity.

Sensitivity to the Direction of the Optic Flow

Altogether 74 (30 PANs, 36 HFNs and 8 TAN) of the 346 analyzed CN neurons showed significant activity change upon optic flow stimulation. In the majority of the analyzed neurons this change was not direction-dependent. Direction-dependent activity change was observed in twenty neurons (9 PAN, 8 HFN, 3 TAN). About half of the selective neurons (11 neurons) responded stronger to center-in stimulus while the second half of them (9 neurons) responded stronger to the center out optic flow. Fig 7 shows the PSTHs of a direction sensitive HFN.

At the population level there was no significant difference between the proportions of direction preferences within PANs, HFNs and TANs (χ-square test; $\chi^2(2) = 1.001$, df = 2, level of significance: 0.05). Thus, the PANs, the HFNs and the TANs of the CN appear to code the direction of the optic flow to a similar extent.

Activity of the Neuron Groups during the Different Phases of the Behavioral Paradigm

Similarly to other studies [37, 38], we found using one-way ANOVA and the following post hoc analysis that the background activity of the HFNs was significantly higher ($p<0.001$) than that of the PANs and the TANs (Table 2). To exclude the effect of the background activities, we subtracted these from the gross activities and so calculated the net firing rates. For the further analyses, the absolute values of the net discharge rates were applied. Table 2 provides detailed information about the net discharge rates of the PANs, HFNs and TANs by phase (i.e. static, dynamic, reward). A one-way ANOVA indicated significant variance ($p<0.01$). The subsequent post-hoc analysis (Tukey's HSD) revealed that the HFNs were both the most sensitive

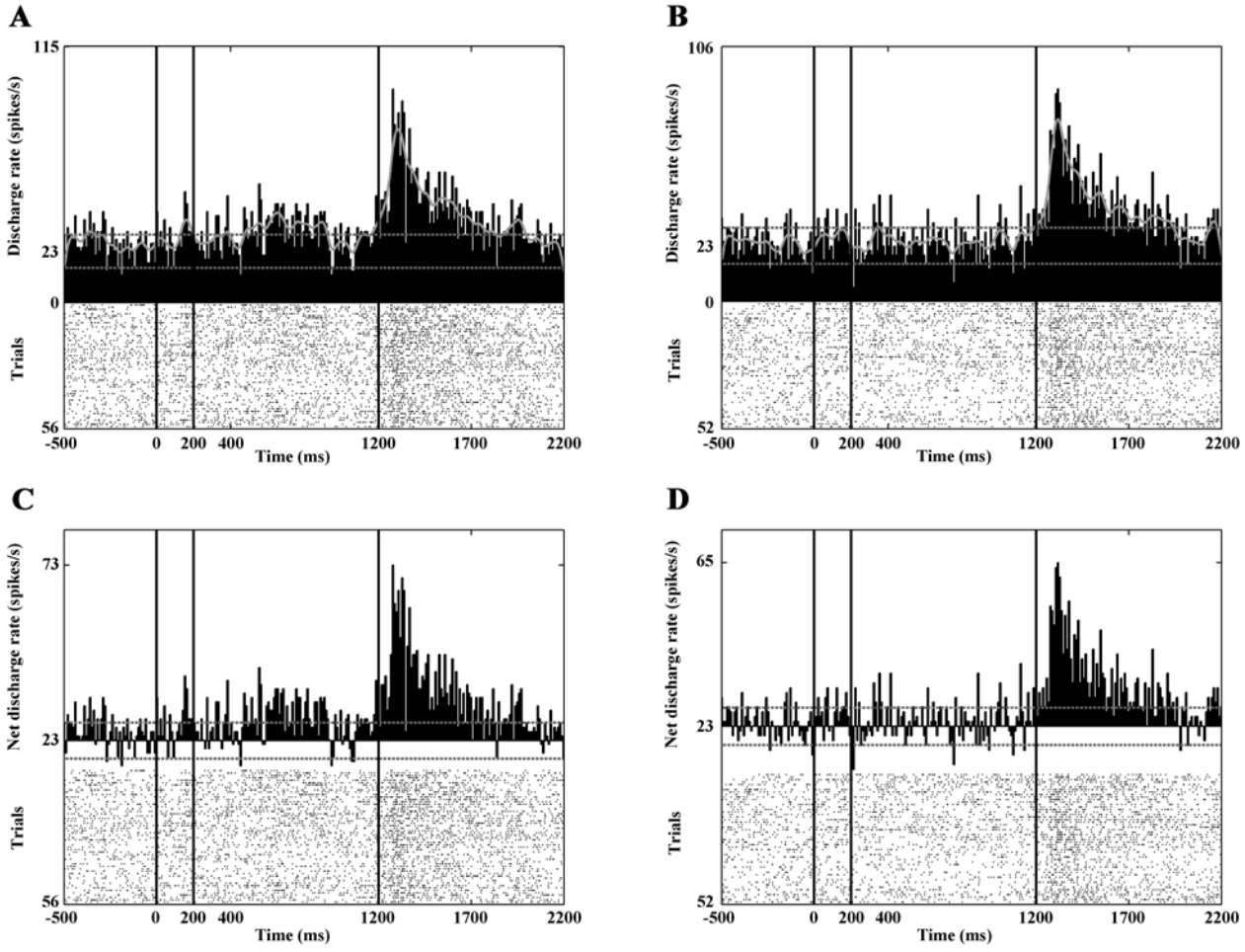

Fig 7. Selective responses to the direction of the optic flow. This figure demonstrates the activity of a HFN. Panels A (gross activity) and C (net activity) show the activities in response to center-out optic flow. Panels B (gross activity) and D (net activity) show the activities in response to center-in optic flow. Note that this neuron exhibits increased activity to center-out optic flow but no response to center-in optic flow. In other words, the neuron is selectively sensitive to the center-out direction. A strong reward-related activity can also be observed. The conventions are the same as in Fig 3.

doi:10.1371/journal.pone.0142526.g007

and exhibited the most vigorous responses throughout all the phases of the fixation paradigm. In summary, the activity of the HFNs differed significantly from the activity of both PANs and TANs, while the activities of the latter two did not differ significantly.

Discussion

In the present study we managed to provide a detailed description of the visual response profile of different CN neurons in the brain of behaving cats, after having classified them according to their electrophysiological characteristics. To our knowledge, such observations have not been made before.

In the last few decades, behaving animal models have gradually gathered ground in neurophysiology, due to their advantages over anesthetized, paralyzed models. Behaving animals can be relatively easily used after brief behavioral training for several experimental purposes, but this is unfortunately not the case in visual and multisensory electrophysiological research. In visual electrophysiology, the investigated neurons often exhibit visuomotor activity (e.g. activity changes during saccades). This makes a continuous monitoring of eye movements indispensable. To minimize the influence of eye movements on the neuronal activities, the animal had to maintain fixation during the whole length of the trials. In this way the eye movement-related components of the activity can be excluded. During the analysis of neuronal responses, which were correlated to stimulus offset (see in Results) the aborted trials were also analyzed where the animal has broken the fixation. In these cases because of the lack of fixation the effects of eye movements on the neuronal activities were also investigated. The correlation between the interspike intervals and the normalized amplitude of the eye movements recorded during the experiments revealed no eye movement- correlated activity among the CN neurons, which were sensitive to the offset of the visual stimuli.

In a recent study we gave a detailed description a new feline model for chronic visual electrophysiological recordings [29]. This model yielded a relatively long recording time per day throughout several years from the same animal, with continuous eye movement control and stable head position. This model was also the basis of the present study.

Turning now to the discussion of the results, the most important achievement of this study may be the electrophysiological categorization of neurons in the feline CN. Similarly to earlier findings in rodents and primates [18, 19, 39–43] PANs, TANs and HFNs were found. The validity and applicability of this classification is signified by the fact that over 97% of the recorded CN units fell into one of the three major categories, and it was only 3% that did not fit any of them. Earlier studies suggested a strong correspondence between the three biggest anatomical (medium spiny, cholinergic and parvalbumin immunpositive GABAergic interneurons) and electrophysiological (PAN, TAN, HFN) groups of the CN neurons. A growing body of evidence suggests that PAN neurons correspond to the medium spiny projection neurons, HFNs to the parvalbumin immunpositive GABAergic interneurons and the TFNs to the cholinergic interneurons [21–28]. As for the uncategorizable neurons (three percent in this study), these can belong to one of the numerous interneuron types of the caudate nucleus, such as the neuropeptide Y-, nitric oxide synthase- and somatostatin- containing [44, 45], calretinin immunpositive [46], tyrosine hydroxylase immunpositive [26, 47], cholecystokinin immunpositive [48] and vasoactive intestinal polypeptide immunpositive [49–51] interneurons—with no claim to being exhaustive. The low prevalence of these interneurons in the feline brain is in line with earlier findings in rodents and primates where the prevalence of each group of these interneurons is under 1%.

A further finding that fits with earlier studies in other species is that the majority of the CN units in the feline brain appear to be PAN (64% in our sample). In other species 77–97% of the

striatal projection neurons belong to this most probably GABAergic cluster. Striatal projection neurons comprise up to 97% of the rodent striatum, while this proportion is significantly lower in higher vertebrates, especially in primates [20, 46, 52–55]. It must be noted that PANs are often difficult to detect because of their extremely low background activity [21, 56], which means that the sixty-four percent finding may be an underestimation due to undersampling, which, in turn, can also have an effect on the estimations of the two other groups.

As for the two other major groups, our results suggest that they are much less prevalent than PAN (HFN 25% and TAN 8%). This is also in line with the results of earlier rodent and primate studies. The parvalbumin immunpositive GABAergic interneurons comprise roughly 1–20% of the striatal neurons of rats and primates [54], while the cholinergic group adds up to only about 10 percent of the CN neurons (up to 10% in primates [57], an 2% in cats [58]).

Beyond the electrophysiological classification of the neurons in the feline CN, we also determined the visual response characteristics of the neurons belonging to the three major classes. The applied dynamic stimulus was quite new in this context, as hitherto optic flow has not been applied to investigate CN neurons. In our earlier studies we demonstrated that the CN neurons are strongly sensitive to very low spatial and high temporal frequency sinewave gratings and exhibit narrow temporal and spatial frequency tuning [11, 12]. It has been hypothesized for some time that neurons with such spatio-temporal visual response characteristics could have a role in the processing of optic flow [13, 14]. In the present study we revisited this hypothesis and provided the first piece of direct evidence on the processing of optic flow in the feline CN.

After the categorization of the CN units based on their electrophysiological properties, it was possible to investigate their visual response characteristics by group. Our results demonstrate that both the static and the dynamic components of the visual information are represented in the CN. The PANs and TANs were more sensitive to static than to dynamic visual stimulation, that is, they responded to the random dot patterns, but not to the optic flow. On the other hand, HFNs were almost equally sensitive to both static and dynamic stimulation (i.e. approximately the same proportion of these neurons responded to random dot pattern and to optic flow stimulation). The stimulus offset modulated the activity of a significant proportion of HFNs, which was not observed with PANs and TANs. This suggests that the PANs and TANs are primarily sensitive to static, continuous, unchanging visual stimuli. As mentioned before, the response characteristics of the HFNs are different: these neurons seem to be equally responsive to both static and dynamic stimulation (including stimulus offset). Furthermore, the net activity changes of the HFNs were significantly stronger than what was observed in PANs and TANs, regardless of the actual phase of the behavioral paradigm. These suggest that HFNs are the most sensitive units in the CN to visual stimuli.

We have also investigated whether the direction of the optic flow (center-in or center-out) is reflected in the activity of the CN neurons. The majority of the CN units showed no such sensitivity. Of the other hand a smaller population of the CN neurons were sensitive to this aspect of the stimulation. About half of the direction sensitive units responded stronger to center in stimuli and the second half of them were more sensitive to center out flow field. The sensitivity of the CN neurons to optic flow gives further support to the hypothesis that the CN neurons participate in motion perception, most probably in the perception of changes in the visual environment during self-motion [12–14].

In summary, we consider the following as the most important achievements of this study:

First, we managed to utilize our head- restrained, eye movement- controlled behaving feline model [29] in a visual electrophysiological study aimed at the analysis and classification of CN neurons in terms of their visual responsiveness.

Second, we described that different CN neuronal groups (PAN, TAN, HFN) are differently sensitive to static and dynamic visual stimulation. PAN and TAN neurons are primarily sensitive to static stimuli, while HFNs are primarily sensitive to changes in the visual environment of the animal. By this we also showed that visually sensitive neurons in the feline CN can be classified similarly to what had previously been found in other species.

Third, we managed to demonstrate optic flow processing in the feline CN, which emphasizes the role of this structure in the detection and processing of visual information related to motion.

Acknowledgments

The authors thank to Siposné Gabriella Dósai-Molnár and László Rácz for the technical assistance, to Robert Averkin for the microdrives and the wire electrodes and to Gábor Braunitzer for his contribution to the preparation of the manuscript. The authors declare no competing financial interests.

Author Contributions

Conceived and designed the experiments: TN PG GB AN. Performed the experiments: TN BB AN. Analyzed the data: TN PG BB AN. Wrote the paper: TN GB AN.

References

1. McHaffie JG, Stanford TR, Stein BE, Coizet V, Redgrave P. Subcortical loops through the basal ganglia. Trends Neurosci. 2005; 28(8):401–7. doi: 10.1016/j.tins.2005.06.006 PMID: 15982753
2. Chudler EH, Sugiyama K, Dong WK. Multisensory convergence and integration in the neostriatum and globus pallidus of the rat. Brain Res. 1995; 674(1):33–45. PMID: 7773693
3. Gombkoto P, Rokszin A, Berenyi A, Braunitzer G, Utassy G, Benedek G, et al. Neuronal code of spatial visual information in the caudate nucleus. Neuroscience. 2011; 182:225–31. doi: 10.1016/j.neuroscience.2011.02.048 PMID: 21376107
4. Hikosaka O, Sakamoto M, Usui S. Functional properties of monkey caudate neurons. II. Visual and auditory responses. J Neurophysiol. 1989; 61(4):799–813. PMID: 2723721
5. Nagy A, Eordegh G, Norita M, Benedek G. Visual receptive field properties of neurons in the caudate nucleus. Eur J Neurosci. 2003; 18(2):449–52. PMID: 12887427
6. Rokszin A, Gombkoto P, Berenyi A, Markus Z, Braunitzer G, Benedek G, et al. Visual stimulation synchronizes or desynchronizes the activity of neuron pairs between the caudate nucleus and the posterior thalamus. Brain Res. 2011; 1418:52–63. doi: 10.1016/j.brainres.2011.08.015 PMID: 21924706
7. Rolls ET, Thorpe SJ, Maddison SP. Responses of striatal neurons in the behaving monkey. 1. Head of the caudate nucleus. Behav Brain Res. 1983; 7(2):179–210. PMID: 6830651
8. Strecker RE, Steinfels GF, Abercrombie ED, Jacobs BL. Caudate unit activity in freely moving cats: effects of phasic auditory and visual stimuli. Brain Res. 1985; 329(1–2):350–3. PMID: 3978457
9. Vicente AF, Bermudez MA, Romero Mdel C, Perez R, Gonzalez F. Putamen neurons process both sensory and motor information during a complex task. Brain Res. 2012; 1466:70–81. doi: 10.1016/j.brainres.2012.05.037 PMID: 22640776
10. Pouderoux G, Freton E. Patterns of unit responses to visual stimuli in the cat caudate nucleus under chloralose anesthesia. Neurosci Lett. 1979; 11(1):53–8. PMID: 431886
11. Nagy A, Berenyi A, Wypych M, Waleszczyk WJ, Benedek G. Spectral receptive field properties of visually active neurons in the caudate nucleus. Neurosci Lett. 2010; 480(2):148–53. doi: 10.1016/j.neulet.2010.06.030 PMID: 20561561
12. Nagy A, Paroczy Z, Markus Z, Berenyi A, Wypych M, Waleszczyk WJ, et al. Drifting grating stimulation reveals particular activation properties of visual neurons in the caudate nucleus. Eur J Neurosci. 2008; 27(7):1801–8. doi: 10.1111/j.1460-9568.2008.06137.x PMID: 18371085
13. Brosseau-Lachaine O, Faubert J, Casanova C. Functional sub-regions for optic flow processing in the posteromedial lateral suprasylvian cortex of the cat. Cereb Cortex. 2001; 11(10):989–1001. PMID: 11549621

14. Morrone MC, Di Stefano M, Burr DC. Spatial and temporal properties of neurons of the lateral suprasylvian cortex of the cat. J Neurophysiol. 1986; 56(4):969–86. PMID: 3783239
15. Steiner H, Tseng KY. Handbook of Basal Ganglia Structure and Function: Academic Press; 2010.
16. Barnes TD, Kubota Y, Hu D, Jin DZ, Graybiel AM. Activity of striatal neurons reflects dynamic encoding and recoding of procedural memories. Nature. 2005; 437(7062):1158–61. doi: 10.1038/nature04053 PMID: 16237445
17. Galvan A, Hu X, Smith Y, Wichmann T. In vivo optogenetic control of striatal and thalamic neurons in non-human primates. PloS One. 2012; 7(11):e50808. doi: 10.1371/journal.pone.0050808 PMID: 23226390
18. Schmitzer-Torbert N, Redish AD. Neuronal activity in the rodent dorsal striatum in sequential navigation: separation of spatial and reward responses on the multiple T task. J Neurophysiol. 2004; 91 (5):2259–72. doi: 10.1152/jn.00687.2003 PMID: 14736863
19. Schmitzer-Torbert NC, Redish AD. Task-dependent encoding of space and events by striatal neurons is dependent on neural subtype. Neuroscience. 2008; 153(2):349–60. doi: 10.1016/j.neuroscience.2008.01.081 PMID: 18406064
20. Yarom O, Cohen D. Putative cholinergic interneurons in the ventral and dorsal regions of the striatum have distinct roles in a two choice alternative association task. Front Syst Neurosci. 2011; 5:36. doi: 10.3389/fnsys.2011.00036 PMID: 21660109
21. Apicella P. Tonically active neurons in the primate striatum and their role in the processing of information about motivationally relevant events. Eur J Neurosci. 2002; 16(11):2017–26. PMID: 12473069
22. Berke JD. Uncoordinated firing rate changes of striatal fast-spiking interneurons during behavioral task performance. J Neurosci. 2008; 28(40):10075–80. doi: 10.1523/JNEUROSCI.2192-08.2008 PMID: 18829965
23. Kawaguchi Y. Physiological, morphological, and histochemical characterization of three classes of interneurons in rat neostriatum. J Neurosci. 1993; 13(11):4908–23. PMID: 7693897
24. Kawaguchi Y, Wilson CJ, Augood SJ, Emson PC. Striatal interneurones: chemical, physiological and morphological characterization. Trends Neurosci. 1995; 18(12):527–35. PMID: 8638293
25. Mallet N, Le Moine C, Charpier S, Gonon F. Feedforward inhibition of projection neurons by fast-spiking GABA interneurons in the rat striatum in vivo. J Neurosci. 2005; 25(15):3857–69. doi: 10.1523/JNEUROSCI.5027-04.2005 PMID: 15829638
26. Tepper JM, Tecuapetla F, Koos T, Ibanez-Sandoval O. Heterogeneity and diversity of striatal GABAergic interneurons. Front Neuroanat. 2010; 4:150. doi: 10.3389/fnana.2010.00150 PMID: 21228905
27. Wilson CJ. The generation of natural firing patterns in neostriatal neurons. Prog Brain Res. 1993; 99:277–97. PMID: 8108553
28. Wilson CJ, Chang HT, Kitai ST. Firing patterns and synaptic potentials of identified giant aspiny interneurons in the rat neostriatum. J Neurosci. 1990; 10(2):508–19. PMID: 2303856
29. Nagypal T, Gombkoto P, Utassy G, Averkin RG, Benedek G, Nagy A. A new, behaving, head restrained, eye movement-controlled feline model for chronic visual electrophysiological recordings. J Neurosci Methods. 2014; 221:1–7. doi: 10.1016/j.jneumeth.2013.09.004 PMID: 24056229
30. Villeneuve MY, Casanova C. On the use of isoflurane versus halothane in the study of visual response properties of single cells in the primary visual cortex. J Neurosci Methods. 2003; 129(1):19–31. PMID: 12951229
31. McKown MD, Schadt JC. A modification of the Harper-McGinty microdrive for use in chronically prepared rabbits. J Neurosci Methods. 2006; 153(2):239–42. doi: 10.1016/j.jneumeth.2005.10.020 PMID: 16406040
32. Averkin R, Korshunov V, Benedek G. A microdrive assembly for chronic neuronal recording. 12th Meeting of the Hungarian Neuroscience Society; Budapest, Hungary: Front Syst Neurosci; 2009.
33. Judge SJ, Richmond BJ, Chu FC. Implantation of magnetic search coils for measurement of eye position: an improved method. Vision Res. 1980; 20(6):535–8. PMID: 6776685
34. Harris KD, Henze DA, Csicsvari J, Hirase H, Buzsaki G. Accuracy of tetrode spike separation as determined by simultaneous intracellular and extracellular measurements. J Neurophysiol. 2000; 84(1):401–14. PMID: 10899214
35. Hazan L, Zugaro M, Buzsaki G. Klusters, NeuroScope, NDManager: a free software suite for neurophysiological data processing and visualization. J Neurosci Methods. 2006; 155(2):207–16. doi: 10.1016/j.jneumeth.2006.01.017 PMID: 16580733
36. Schultz W. Predictive reward signal of dopamine neurons. J Neurophysiol. 1998; 80(1):1–27. PMID: 9658025

37. Berke JD, Okatan M, Skurski J, Eichenbaum HB. Oscillatory entrainment of striatal neurons in freely moving rats. Neuron. 2004; 43(6):883–96. doi: 10.1016/j.neuron.2004.08.035 PMID: 15363398

38. Plenz D, Kitai ST. Up and down states in striatal medium spiny neurons simultaneously recorded with spontaneous activity in fast-spiking interneurons studied in cortex-striatum-substantia nigra organotypic cultures. J Neurosci. 1998; 18(1):266–83. PMID: 9412506

39. Barnes TD, Mao JB, Hu D, Kubota Y, Dreyer AA, Stamoulis C, et al. Advance cueing produces enhanced action-boundary patterns of spike activity in the sensorimotor striatum. J Neurophysiol. 2011; 105(4):1861–78. doi: 10.1152/jn.00871.2010 PMID: 21307317

40. Gage GJ, Stoetzner CR, Wiltschko AB, Berke JD. Selective activation of striatal fast-spiking interneurons during choice execution. Neuron. 2010; 67(3):466–79. doi: 10.1016/j.neuron.2010.06.034 PMID: 20696383

41. Kubota Y, Liu J, Hu D, DeCoteau WE, Eden UT, Smith AC, et al. Stable encoding of task structure coexists with flexible coding of task events in sensorimotor striatum. J Neurophysiol. 2009; 102(4):2142–60. doi: 10.1152/jn.00522.2009 PMID: 19625536

42. Stalnaker TA, Calhoon GG, Ogawa M, Roesch MR, Schoenbaum G. Reward prediction error signaling in posterior dorsomedial striatum is action specific. J Neurosci. 2012; 32(30):10296–305. doi: 10.1523/JNEUROSCI.0832-12.2012 PMID: 22836263

43. Thorn CA, Atallah H, Howe M, Graybiel AM. Differential dynamics of activity changes in dorsolateral and dorsomedial striatal loops during learning. Neuron. 2010; 66(5):781–95. doi: 10.1016/j.neuron.2010.04.036 PMID: 20547134

44. Smith Y, Parent A. Neuropeptide Y-immunoreactive neurons in the striatum of cat and monkey: morphological characteristics, intrinsic organization and co-localization with somatostatin. Brain Res. 1986; 372(2):241–52. PMID: 2871900

45. Vincent SR, Staines WA, Fibiger HC. Histochemical demonstration of separate populations of somatostatin and cholinergic neurons in the rat striatum. Neurosci Lett. 1983; 35(2):111–4. PMID: 6134260

46. Rymar VV, Sasseville R, Luk KC, Sadikot AF. Neurogenesis and stereological morphometry of calretinin-immunoreactive GABAergic interneurons of the neostriatum. J Comp Neurol. 2004; 469(3):325–39. doi: 10.1002/cne.11008 PMID: 14730585

47. Dubach M, Schmidt R, Kunkel D, Bowden DM, Martin R, German DC. Primate neostriatal neurons containing tyrosine hydroxylase: immunohistochemical evidence. Neurosci Lett. 1987; 75(2):205–10. PMID: 2883616

48. Adams CE, Fisher RS. Sources of neostriatal cholecystokinin in the cat. J Comp Neurol. 1990; 292 (4):563–74. doi: 10.1002/cne.902920406 PMID: 1691213

49. Hokfelt T, Herrera-Marschitz M, Seroogy K, Ju G, Staines WA, Holets V, et al. Immunohistochemical studies on cholecystokinin (CCK)-immunoreactive neurons in the rat using sequence specific antisera and with special reference to the caudate nucleus and primary sensory neurons. J Chem Neuroanat. 1988; 1(1):11–51. PMID: 3077312

50. Takagi H, Somogyi P, Smith AD. Aspiny neurons and their local axons in the neostriatum of the rat: a correlated light and electron microscopic study of Golgi-impregnated material. J Neurocytol. 1984; 13 (2):239–65. PMID: 6726290

51. Theriault E, Landis DM. Morphology of striatal neurons containing VIP-like immunoreactivity. J Comp Neurol. 1987; 256(1):1–13. doi: 10.1002/cne.902560102 PMID: 2434535

52. Graveland GA, Williams RS, DiFiglia M. A Golgi study of the human neostriatum: neurons and afferent fibers. J Comp Neurol. 1985; 234(3):317–33. doi: 10.1002/cne.902340304 PMID: 3988987

53. Kemp JM, Powell TP. The structure of the caudate nucleus of the cat: light and electron microscopy. Philos Trans R Soc Lond B Biol Sci. 1971; 262(845):383–401. PMID: 4107495

54. Luk KC, Sadikot AF. GABA promotes survival but not proliferation of parvalbumin-immunoreactive interneurons in rodent neostriatum: an in vivo study with stereology. Neuroscience. 2001; 104(1):93–103. PMID: 11311534

55. Wise SP, Murray EA, Gerfen CR. The frontal cortex-basal ganglia system in primates. Crit Rev Neurobiol. 1996; 10(3–4):317–56. PMID: 8978985

56. Lau B, Glimcher PW. Action and outcome encoding in the primate caudate nucleus. J Neurosci. 2007; 27(52):14502–14. doi: 10.1523/JNEUROSCI.3060-07.2007 PMID: 18160658

57. Fino E, Venance L. Spike-timing dependent plasticity in striatal interneurons. Neuropharmacology. 2011; 60(5):780–8. doi: 10.1016/j.neuropharm.2011.01.023 PMID: 21262240

58. Phelps PE, Houser CR, Vaughn JE. Immunocytochemical localization of choline acetyltransferase within the rat neostriatum: a correlated light and electron microscopic study of cholinergic neurons and synapses. J Comp Neurol. 1985; 238(3):286–307. doi: 10.1002/cne.902380305 PMID: 4044917